

**Journal of Experimental Biology**  
**Colonial Architecture Modulates the Speed and Efficiency of Multi-Jet Swimming in Salp Colonies**  
--Manuscript Draft--

<b>Manuscript Number:</b>	jeb.249465R1
<b>Article Type:</b>	Research Article
<b>Full Title:</b>	Colonial Architecture Modulates the Speed and Efficiency of Multi-Jet Swimming in Salp Colonies
<b>Abstract:</b>	<p>Salps are marine pelagic tunicates with a complex life cycle including a solitary and colonial stage. Salp colonies are composed of asexually budded individuals that coordinate their swimming by multi-jet propulsion. Colonies develop into species-specific architectures with distinct zooid orientations. These distinct colonial architectures vary in how frontal area scales with the number of zooids in the colony. Here, we address how differences in frontal area drive differences in swimming speed and the relationship between swimming speed and cost of transport in salps. We (1) compare swimming speed across salp species and architectures, (2) evaluate how swimming speed scales with the number of zooids across colony in architectures, and (3) compare the metabolic cost of transport across species and how it scales with swimming speed. To measure swimming speeds, we recorded swimming salp colonies using in situ videography while SCUBA diving in the open ocean. To estimate the cost of transport, we measured the respiration rates of swimming and anesthetized salps collected in situ using jars equipped with non-invasive oxygen sensors. We found that linear colonies swim faster, which supports idea that their differential advantage in frontal area scales with an increasing number of zooids. We also found that higher swimming speeds predict lower costs of transport in salps. These findings underscore the importance of considering propeller arrangement to optimize speed and energy efficiency in bioinspired underwater vehicle design, leveraging lessons learned from the diverse natural laboratory provided by salp diversity.</p>
<b>Corresponding Author:</b>	Alejandro Damian-Serrano, Ph.D. University of Oregon Oregon Institute of Marine Biology Eugene, OR UNITED STATES
<b>Other Authors:</b>	<p>Kaiden A. Walton, B.S.  Anneliese Bishop-Perdue, B.S.  Sophie Bagoye  Kevin T. Du Clos, Ph.D.  Bradford J. Gemmell, Ph.D.  Sean P. Colin, Ph.D.  John H. Costello, Ph.D.  Kelly R. Sutherland, Ph.D.</p>
<b>Keywords:</b>	salps; colonial architecture; multi-jet propulsion; swimming; cost of transport
<b>Additional Information:</b>	
<b>Question</b>	<b>Response</b>
<b>Editor Suggestions</b>  You may request that your submission is assigned to a specific <a href="#">editor</a> . Please suggest no more than three editor names in order of preference. Although you may suggest an editor for your submission, the journal will make the final assignment. If you do not request an editor, your	Sheila Patek (previous editor for first submission)

submission will be assigned to the most appropriate editor as determined by the editorial staff.	
<b>Companion Paper</b>	No
Is your paper a companion paper (part of a group of papers being submitted)?	
<b>Special Issue</b>	No, this article is not part of a special themed issue
<b>Open Access</b>	<b>Green Open Access</b>
Please check your funder requirements carefully and select the appropriate Open Access publication route below. A quote for your Open Access publication charges will be available to view on the final submission page, revealing any institutional discounts and providing you with another chance to select Open Access. See <b>Instructions</b> for further information.	
<b>Word Count</b>	8041
<b>Number of Figures</b>	7
<b>Number of Tables</b>	0

Dear Dr Damian-Serrano,

...

As you will see, the reviewers gave favourable reports but raised some critical points that will require amendments to your manuscript. Both reviewers (and I) appreciate the extensive revisions based on the first round of reviews. However, there still remain a considerable number of areas needed revision. The reviewers provide clear and constructive feedback about which areas need additional work.

>We thank the Editor for her generous feedback.

I also emphasize the need to be clear about sample sizes (N, n, df, test statistics) when reporting the statistical results.

>We added details on sample sizes everywhere where p-values are reported across the results.

Also, there appears to be a misconception by the authors about why phylogenetic comparative methods are used. The most crucial reason is to address the non-independence of data points when species are more or less closely related (independence of data points is required of all the statistics used in this manuscript). Please fix that section of the manuscript and clearly state how violating the rule of non-independence of data points may have influenced your statistics-based findings. Or, include a phylogeny and perform the statistics correctly using appropriate statistical methods.

>Please see response to the last point raised by Reviewer 1.

Please make sure to plot all data points on the box plots (data transparency requirement of JEB).

>We added jittered data points to the boxplots in Figs. 3 and 7 and now all data points are plotted in all plots.

Lastly, I encourage the authors to upload their R code to accompany the data spreadsheet. The code would further enhance the replicability of the study.

>We have now included the R code in the resubmission.

Provided you are able to fully address the reviewers' comments, we hope you won't mind the extra work involved in revising your manuscript and adhering to our formatting instructions below. Please ensure that you clearly highlight all changes made in the revised manuscript. Please avoid using 'Track changes' in Word files as these are lost in PDF conversion.

I would be grateful if you would also list how you have dealt with the points raised by the editor and reviewers in the 'Response to Reviewers' box. Please attend to all of the editor's and

reviewers' comments. If you do not agree with any of their criticisms or suggestions please explain clearly why this is so.

In order to promote timely publication, we generally ask that the revision be completed within 90 days from the date of this letter. However, we recognise that this may not always be possible so we will be happy to grant an extension where this is needed: please just contact the Editorial Office.

I look forward to receiving your revised manuscript.

With best wishes,

S. Patek

Handling Editor

---

#### Comments from the Reviewers:

Reviewer 1: Damian-Serrano et al have considered a comparison of swimming and metabolic-rate measurements across numerous species of salp to address a hypothesis that differences in swimming speed are driven by frontal area differences between different colony formations. I reviewed an earlier version of this manuscript and find this version to be a great improvement. However, I still have number of suggestions for improving the presentation of this work. Most importantly, the statistical analysis requires greater transparency in its presentation in the methods and through reporting of sample size in the Results.

>We thank Reviewer 1 for their generous feedback and for their willingness to re-review our manuscript.

#### SPECIFIC COMMENTS

(Line numbers are the ones on the right)

L45 - Given the hypothesis, seems like you'd want to see how COT scales with frontal area too.

>Since COT was only different in a few of the architectures based on Tukey's posthoc pairwise comparisons and was mostly unrelated to frontal area (Table S2B), we chose to focus on the more robust relationship between swimming speed and COT.

L49 - The statement about "due to their differential advantage in frontal area scaling" is in interpretation is written in the tone of an observation. Given the evidence, I think it would be more appropriate to say sometime like "We found that linear colonies generally swim faster, which supports the idea that . . ."

>We rephrased the statement to "We found that linear colonies swim faster, which supports idea that their differential advantage in frontal area scales with an increasing number of zooids."

L63 - Maybe "drawing" and "ejecting" instead of "inhaling" and "exhaling"?

>We modified the statement to "Zooids in the colony feed and propel themselves by drawing water in through the oral siphon, using muscle contraction to compress their pharyngeal chamber, and ejecting a jet of water from their atrial siphon (Bone & Trueman 1983)."

L91 - I think Alexander and Vogel only makes sense as a citations if they offered a unique statement about drag in salps, which may be the case. They are not really strong sources on the origins of drag.

>We chose to omit this statement all together when we streamlined the Introduction in response to Reviewer 2's comments.

L139 - Nothing against Vogel, but there many options in the primary literature, and reviews, to support this statement, which would more directly point to the source of the information.

>We replaced this citation with Andersen et al 2016.

Andersen, K. H., Berge, T., Gonçalves, R. J., Hartvig, M., Heuschele, J., Hylander, S., ... & Kiørboe, T. (2016). Characteristic sizes of life in the oceans, from bacteria to whales. Annual review of marine science, 8(1), 217-241.

L168 - The statement about "scaling drive disparities between colonial architectures" is important because it articulates a major aim of the study. So, I recommend using more precise language: disparities in what respect?

>We rewrote this statement to be more precise and concise: "...we investigate how swimming speed varies with the number of propeller zooids and differences in frontal area scaling between colonial architectures."

I believe JEB requires that you provide the location of manufacturers.

>We added the locations of manufacturers to the products throughout the Methods wherever possible.

I do not think Eqns. 1 and 2 are necessary, but fine to include.

>We kept the equations for completeness.

L288 - Readers may wonder why dried mass was not selected as the means of normalizing the metabolic measurements by animal size, given the presumably large volume of these gelatinous organisms that is not comprised of living tissue. Isn't it possible that differences in the measurements could be due to differences in the proportion of metabolically-active tissue. A concise mention of these considerations would be helpful.

>We added the following explanation: "Biovolume was used instead of dry mass to normalize measurements due to the inherent difficulties of accurately measuring dry mass of these fragile gelatinous organisms in the field. Biovolume provides a consistent and reliable measure of the

live size of the colony, which is directly relevant to the volume of water being displaced during swimming."

L323 - This section requires a more expansive description of the statistical analysis. What particular linear models? Which continuous variables, in particular? How are repeated measures taken into account? I'm not sure if testing relative to a zero slope makes sense (vs. comparing regressions between species), but I am not sure what variables are being referenced here.

>We added the following text in the Methods to state more precisely how we used statistical methods.

Linear model: "To test the relationships between pairs of continuous variables across architectures (e.g. swimming speed vs. number of zooids), we used linear regressions."

Testing against zero slope: "We evaluated the significance of the slope parameter when compared against a flat slope (one-tailed t-test) to test whether changes in the independent variable (e.g. number of zooids) were associated with changes in the dependent variable (e.g. swimming speed)."

Repeated measures: "Owing to the patchiness of some species despite 80+ hours spent underwater (Table S1), we used replicate measurements ( $n$ ) from each specimen ( $N$ ) in swimming speed ANOVAs and regressions. We used an exponential regression to test the relationship between speed and COT. Specimen means ( $N$ ) were used for all COT comparisons and regressions. Individual measurements ( $n$ ) were used up to determine oxygen consumption rates. To evaluate the relative contribution of zooid size, pulsation rate, zooid number, and architecture type on swimming speed, we fitted a generalized linear model and evaluated the significance and proportion of variance explained by each factor using their partial  $R^2$ ."

Sample sizes should be reported in the Results. It should be made clear when p-values are reported what the sample sizes are. Supplemental tables and mention in the methods is insufficient.

>We added sample sizes everywhere where p-values were reported throughout the ms, including in the figure legends.

Fig. 5 - zooids/pulse — Does this mean zooid length/pulse? Perhaps this could be phrased more specifically?

>We updated the y-axis label to read "zooid lengths per pulsation".

L408-415 - These details should be offered in the Methods.

>We briefly describe the generalized linear model (GLM) in the Methods and then name the model variables again in Results-- salp swimming speed (U) from zooid length (L), pulsation

rate (P), number of zooids (Z), and colonial architecture represented as frontal area scaling mode (A) -- so that the reader won't have to backtrack to the Methods.

L439 - Paragraphs should be 3 or more sentences.

>We adjoined this paragraph to the next one, which is also about energetic investment.

L442-446 - Run on sentence.

>We split the sentence into three sentences. The new wording reads: "We then compared the proportion of energetic investment in swimming to the COT values across species (Fig. S3A,B). We found no relationship with absolute COT (N = 74, 14 species, p = 0.24). We found a positive relationship with zooid-length scaled COT (N = 74, 14 species, Swimming % = 0.11\*COT per zooid length + 34.4, adjusted R<sup>2</sup> = 0.22, p < 0.001), indicating that species with more costly locomotion per zooid length invest a larger proportion of their energy budget in swimming."

L479 - size, by what metric?

>We rephrased the wording to be more precise "...suggesting an underlying relationship between pulsation rate and zooid length..."

Please cite the results supporting all of the statements of findings in the Discussion. This appears more towards the end of the Discussion than at the beginning.

>We added relevant figure and table citations throughout the Discussion.

L497 - There is no such thing as a "less hydrodynamic configuration." L603 Says "highly hydrodynamic forms". These are misuses of the term "hydrodynamic". By analogy, one would not say that one animal is more mechanical than another.

>We removed these mentions of "more/less hydrodynamic" and replaced them with the term "streamlined".

L631-634 - I do not follow the logic of the co-evolution of traits as reason for a phylogenetic analysis as being inappropriate. This merits a more clear explanation or perhaps it is a non-essential point that could be avoided.

>We thank the Reviewer for raising this important point. We understand the importance of addressing the non-independence of data points when dealing with species that are related to varying degrees and acknowledge that our statement was not sufficiently clear. We have revised the text to clarify our reasoning and acknowledge the potential influence of phylogenetic history on residual variation as follows: "In the current study we did not use phylogenetic comparative methods in our analysis because like other investigators comparing biomechanical properties across species (e.g. Dabiri et al. 2010, Di Santo et al. 2021) we were

interested in inherent mechanical relationships dictated by the colony architectures. For instance, a linear arrangement of zooids inherently reduces drag compared to a cluster arrangement, leading to faster swimming speeds and potentially higher efficiency regardless of phylogenetic history. In other words, any phylogenetic inertia is irrelevant in instantaneous relationships between traits (Felsenstein 1985). Moreover, independence of data is often incorrectly assumed to be an assumption of standard (nonphylogenetic) regressions (Uyeda et al. 2018), when in reality the assumptions relate to the independence and distribution of the error terms. Thus, when all the phylogenetic signal is present in the predictor, as it is in the case with colonial architecture (Damian-Serrano et al. 2022) and its associated characteristics, there is no need for any “phylogenetic correction” (Uyeda et al. 2018). However, there may be unaccounted factors explaining the residual variation in our analyses that may bear phylogenetic signal. For example, tunic stiffness, tunic smoothness, muscle band number, muscle fiber density, swimming behavior, as well as metabolic and physiological baselines may be more similar between more closely related species, potentially erasing some of the architecture-specific signal. Future studies could address the role of phylogeny and heritable factors in salp swimming speed and cost of transport using phylogenetic comparative methods. These analyses could reveal whether these factors have co-evolved with each other and/or with respiration rate or colonial architecture.”

Dabiri, J. O., Colin, S. P., Katija, K., & Costello, J. H. (2010). A wake-based correlate of swimming performance and foraging behavior in seven co-occurring jellyfish species. *Journal of experimental biology*, 213(8), 1217-1225.

Di Santo, V., Goerig, E., Wainwright, D. K., Akanyeti, O., Liao, J. C., Castro-Santos, T., & Lauder, G. V. (2021). Convergence of undulatory swimming kinematics across a diversity of fishes. *Proceedings of the National Academy of Sciences*, 118(49), e2113206118.

Felsenstein, J. (1985). Phylogenies and the comparative method. *The American Naturalist*, 125(1), 1-15.

Uyeda, J. C., Zenil-Ferguson, R., & Pennell, M. W. (2018). Rethinking phylogenetic comparative methods. *Systematic Biology*, 67(6), 1091-1109.

Damian-Serrano, A., Hughes, M., & Sutherland, K. R. (2023). A new molecular phylogeny of salps (Tunicata: thalicea: salpida) and the evolutionary history of their colonial architecture. *Integrative Organismal Biology*, 5(1), obad037.

Reviewer 2: The primary aim of the paper is to determine what effect, if any, the architectures of salps colonies have on the swimming speed and metabolic costs of the organisms. The stated motivation for the work is to provide insight into bio-inspired designs, such as for underwater vehicles.

The authors' experimental measurements of difficult-to-obtain quantities and their contribution to the body of knowledge regarding salps are impressive. They have also made a conscious effort to clarify and strengthen many points, which indicates a desire to be clear, open, and honest in their reporting. Below I have tried to balance recognition of the enormous challenges involved in

obtaining the data and the limited number of available data points for analysis with gauging the appropriateness of the strength of the claims.

>We thank Reviewer 2 for their generous feedback.

There are two main outstanding issues of the paper as I read it. First is the number of predictions and expectations in the introductory part of the paper, which tend to take away from rather than strengthen the main hypotheses.

>We have eliminated the predictions and expectations in the Introduction and now focus on a single expectation based on frontal area (p. 3): "Salp colonial architectures differ in how the number of zooids in the colony scales with their frontal area relative to motion (Madin 1990). Some architectures (linear, bipinnate, and helical) have a constant frontal area, regardless of zooid number. These architectures may benefit from increased thrust delivered by larger numbers of zooids while maintaining a constant frontal area. However, the rest of the architectures (oblique, transversal, whorl, and cluster) have an increasing (directly proportional) frontal area as the number of zooids increases (Fig. 1). Therefore, we expect the latter architectures to not only obtain more thrust, but to also experience more frontal water resistance as zooid number increases. As a result, we anticipate that swimming speed will be greater in colonies that bear a larger number of zooids, but only (or more so) for species with architectures that have a constant frontal area."

The second is a claim of a causal relationship based on indirect rather than direct evidence. It's possible these questions/issues could be addressed within the current architecture of the paper. Statement of hypotheses. The introduction contains at least 12 expectations/predictions (Lines 84, 85, 90, 91, 98, 102, 106, 129, 137, 142, 146, 158, 162.)

> Instead of stating expectations based on previous literature in the Introduction, we now discuss the Results in light of previous literature in the Discussion. The paper reads more smoothly.

The last paragraph (Lines 309-318) of the introduction states that the following will be studied: how swimming speed varies with the number of propellers and whether there are differences in frontal scaling drive [which?] disparities between architectures, assessing how cost of transport varies, and how COT varies with swimming speed and pulsation effort.

We have edited the last paragraph in the Introduction to say: "In addition, we investigate how swimming speed varies with the number of propeller zooids and differences in frontal area scaling between colonial architectures. Finally, we compare cost of transport (COT) across salp species and assess how COT scales with swimming speed and pulsation effort."

Is one or more of these the main hypothesis of the paper? Many measurements are made and many tests run, but they don't seem to address a single (or maybe two) clearly stated question or line of inquiry. This may be in part due to the fact that there is limited data in some cases, so

there may be a desire to present the case from many different angles. And I think the paper does have an intention (see below), but the number of side predictions obscures it. I suggest moving the predictions/expectations to the discussion as part of the analysis if they support the central thesis while leaving the introduction clear to lay the groundwork for the primary aim. If the authors feel the predictions lay this ground work, they may have a different notion of how to tighten the focus.

>We have streamlined the Introduction and now have a single prediction regarding scaling of frontal area. After re-visiting the literature, we determined that there are not enough data on the relationship between swimming speed and COT to have an a priori hypothesis. We therefore have re-worded the Introduction such that studying COT is a research objective rather than addressing a specific hypothesis. The end of the Introduction now reads: "we compare cost of transport (COT) across salp species and assess how COT scales with swimming speed and pulsation effort."

Statement of causal relationships. If a clear purpose were to be identified, it appears to be the main result from the abstract which reads (Lines 49-53): "We found that linear colonies generally swim faster due to their differential advantage in frontal area scaling with an increasing number of zooids." I agree with the findings to an extent, but the cause is less clear. The qualifier on lines 525-542 acknowledges that there may be confounding factors, but the strength of the statement in the abstract belies that notion.

>We rephrased this to: "We found that linear colonies generally swim faster, which is consistent with the hypothesis that their differential advantage in frontal area scaling contributes to their increased speed."

Focusing on Figure 5 A for example, I agree that this shows linear colonies tend to swim faster as the number of zooids increases when only considering linear colonies. However, it would be a strong statement to state that linear colonies swim faster than bipinnate and helical as number of zooids grow (line 503) based on these data because 1) there is only one helical specimen and 2) that pattern is not necessarily clear in the range where you have data for all three types of specimens, and you only have linear specimens in the region where you see a clear increase in speed on the right.

In figure 5 B, there is a similar concern with the oblique data point, but also the gap in colony numbers for the cluster data is concerning. Ignoring the point on the right, there appears to be an upward trend in swimming speed, even if more slight than the left. This could indicate the right-hand point is an outlier, or there is likely a non-monotonic relationship between swimming speed and a number of colonies in some of the architectures. This means there is possibly a region where larger frontal areas swim as fast or faster than architectures with lower frontal areas. The data presented here neither confirm nor deny this.

>We agree with the reviewer that there is patchiness in sample sizes and gaps in zooid numbers. And, we originally had a figure showing number of zooids vs. swimming speed for each individual species in the Supplemental section but we removed it to comply with JEB's

figure limits (the raw data are still available in Dataset S1). We added a sentence to the Results associated with Fig. 5 to acknowledge the uncertainties associated with low specimen numbers: "However, the limited sample sizes for helical and oblique chains prevent us from drawing firm conclusions about these architectures."

Questions about data comparison:

\*In table S1, there is a lot of variation in the mean length of zooids between species. Is there a lot of variation within a species? It might be appropriate to report the standard deviation.

>The raw data including all of the zooid lengths and showing the full variability is available now in Dataset S1A and S1B.

\*I couldn't open/find the Dataset S1, so this might have been addressed already. There is some discussion about the 2D versus stereo measurements and that the 2D measurements gave slower speeds. I didn't see that it was specified which species were measured with which apparatus. Using obtainable footage is reasonable, especially when the specimens are hard to collect/track/find. But if speed is a primary part of the argument, it should be obvious where the differences in speed measurements lie.

>We were sorry to hear that the reviewer couldn't access Dataset 1; please do let us know of there are any challenges with access this time. Dataset S1A specifies each video file analyzed, species and camera system (3D or 2D). Both measurement types were used for *S. zonaria* and *S. maxima*. However, *Brookssia*, *Ritteriella* spp., *Pegea*, *I. cylindrica*, *M. hexagona*, *S. fusiformis*, *S. aspera*, *C. bakeri*, *C. polae*, and *C. sewelli* were 3D-only; whereas *Helicosalpa*, *Thalia*, *C. affinis*, and *C. quadriluminis* were 2D-only.

Minor things:

\*It might be more appropriate to refer to these as all of the known architectures throughout rather than all of the architectures unless it is definitively known that no other configurations are possible.

>We modified the wording in the Introduction to: "In this study, we compare swimming speeds across 17 salp species and energetic costs of swimming across 15 species, encompassing all seven known salp colony architectures"

\*Different marker point shapes would make the graphs more color-/resource accessibility friendly. The results would be hard to discern for someone with a different color perception or who can only access a black-and-white copy. Similarly, using different striping patterns on bar charts would make the graphs more accessible. This might be something for the publisher to address.

>We appreciate this point and agree that the different markers might be hard to distinguish in a greyscale print version of Figs. 4, 5 and 7. On the other hand, since electronic versions are more accessible and widely read, we will leave the plotting requirements up to the publisher.

1   **Title: Colonial Architecture Modulates the Speed and  
2   Efficiency of Multi-Jet Swimming in Salp Colonies**

3  
4   **Authors:** Alejandro Damian-Serrano<sup>1</sup>, Kai A. Walton<sup>1</sup>, Anneliese Bishop-Perdue<sup>1</sup>, Sophie  
5   Bagoye<sup>1</sup>, Kevin T. Du Clos<sup>2</sup>, Bradford J. Gemmell<sup>3</sup>, Sean P. Colin<sup>4,5</sup>, John H. Costello<sup>6</sup>, Kelly R.  
6   Sutherland<sup>1</sup>

7  
8   **Author Affiliations:**  
9

- 10   (1) Institute of Ecology and Evolution, Department of Biology, University of Oregon. 473 Onyx  
11   Bridge, 5289 University of Oregon, Eugene, OR 97403-5289, USA.  
12   (2) Louisiana Universities Marine Consortium, 8124 Highway 56, Chauvin, LA 70344, USA.  
13   (3) Department of Integrative Biology, University of South Florida, 4202 East Fowler Avenue,  
14   Tampa, FL 33620, USA.  
15   (4) Marine Biology and Environmental Science, Roger Williams University, Bristol, RI 02809, USA.  
16   (5) Whitman Center, Marine Biological Laboratory, Woods Hole, MA 02543, USA.  
17   (6) Biology Department, Providence College, Providence, RI 02918, USA.

18  
19   **Running title:** Architecture Modulates Salp Swimming

20  
21   **Summary Statement (30 words)**

22  
23   Linear arrangements in multi-jet propelled marine colonial invertebrates are faster than less  
24   streamlined architectures without incurring in higher costs of transport, offering insights for  
25   bioinspired underwater vehicle design.

26  
27  
28  
29  
30  
31  
32  
33

34     **Abstract**

35  
36     Salps are marine pelagic tunicates with a complex life cycle including a solitary and colonial stage.  
37     Salp colonies are composed of asexually budded individuals that coordinate their swimming by  
38     multi-jet propulsion. Colonies develop into species-specific architectures with distinct zooid  
39     orientations. These distinct colonial architectures vary in how frontal area scales with the number  
40     of zooids in the colony. **Here, we address how** differences in frontal area drive differences in  
41     swimming speed and **the relationship between** swimming speed **and** cost of transport in salps.  
42     We (1) compare swimming speed across salp species and architectures, (2) evaluate how  
43     swimming speed scales with the number of zooids across colony in architectures, and (3)  
44     compare the metabolic cost of transport across species and how it scales with swimming speed.  
45     To measure swimming speeds, we recorded swimming salp colonies using in situ videography  
46     while SCUBA diving in the open ocean. To estimate the cost of transport, we measured the  
47     respiration rates of swimming and anesthetized salps collected in situ using jars equipped with  
48     non-invasive oxygen sensors. We found that linear colonies swim faster, **which supports idea that**  
49     **their** differential advantage in frontal area **scales** with an increasing number of zooids. We also  
50     found that higher swimming speeds predict lower costs of transport in salps. These findings  
51     underscore the importance of considering propeller arrangement to optimize speed and energy  
52     efficiency in bioinspired underwater vehicle design, leveraging lessons learned from the diverse  
53     natural laboratory provided by salp diversity.

54

55     **Keywords:** salps, colonial architecture, multi-jet propulsion, swimming, cost of transport

56

57     **Introduction**

58         Salps (Tunicata: Thaliacea: Salpida) are planktonic invertebrates that have a two-phase  
59     life cycle comprised of a solitary oozooid that asexually buds colonies of sexually reproducing  
60     blastozooids. Salp colonies are composed of up to hundreds of genetically identical, physically  
61     and neurophysiologically integrated pulsatile zooids (Bone et al. 1980, Mackie 1986). Zooids in  
62     the colony feed and propel themselves by **drawing** water **in** through the oral siphon, using muscle  
63     contraction to compress their pharyngeal chamber, and **ejecting** a jet of water from their atrial  
64     siphon (Bone & Trueman 1983). While solitary oozooids move using single-jet propulsion, salp  
65     blastozooid colonies integrate multiple propelling jets, which increases their thrust and reduces  
66     the drag that results from periodical acceleration and deceleration via asynchronous swimming  
67     (Sutherland & Weihs 2017).

68       Currently, there are 48 described species of salps (WoRMS, 2024) and while salps are  
69 widely distributed, most species are restricted to open ocean environments, far from the coast,  
70 which poses unique challenges to accessing them for direct study in their environment (Hamner  
71 et al 1975, Haddock 2004). Moreover, salps cannot be maintained alive in containers beyond a  
72 few hours since they are extremely fragile and sensitive to the presence of solid walls. Therefore,  
73 many morphological, ecological, and functional aspects of salp diversity, such as swimming  
74 speeds and metabolic demands, have remained unexplored. One such aspect is colonial  
75 architecture or the way that the zooids are arranged relative to each other in the colony. Salp  
76 colonies develop into species-specific architectures with distinct zooid orientations, including  
77 transversal, oblique, linear, helical, and bipinnate chains; as well as whorls, and clusters (Damian-  
78 Serrano & Sutherland, 2023). These architectures **likely drive aspects of** swimming performance  
79 (Madin 1990, Damian-Serrano et al. 2023).

80       Linear salp chains have been **described as** more efficient swimmers due to the reduction  
81 of drag associated with a more streamlined form (Bone & Trueman 1983). In a multi-jet system,  
82 having a larger number of propellers **can** improve the hydrodynamic and inertial benefits granted  
83 by asynchronous multijet propulsion, in addition to providing additional thrust to the colony (Madin  
84 1990, Sutherland & Weihs 2017). The effect of varying numbers of propeller zooids on swimming  
85 speed has never been investigated in salps, nor how this relationship may vary across their  
86 diverse colonial architectures. Salp colonial architectures differ in how the number of zooids in  
87 the colony scales with their frontal area relative to motion (Madin 1990). Some architectures  
88 (linear, bipinnate, and helical) have a constant frontal area, regardless of zooid number. These  
89 architectures **may** benefit from increased thrust delivered by larger numbers of zooids while  
90 maintaining a constant frontal area. However, the rest of the architectures (oblique, transversal,  
91 whorl, and cluster) have an increasing (directly proportional) frontal area as the number of zooids  
92 increases (Fig. 1). Therefore, we expect the latter architectures to not only obtain more thrust, but  
93 to also experience more frontal water resistance **as zooid number increases**. As a result, we  
94 **anticipate** that swimming speed will be greater in colonies that bear a larger number of zooids,  
95 but only (or more so) for species with architectures that have a constant frontal area.

96

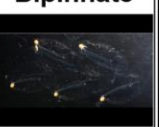
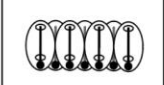
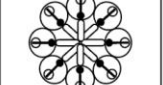
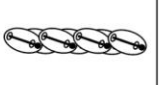
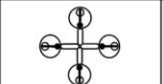
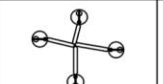
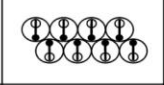
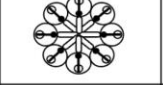
	Transversal	Whorl	Cluster	Helical	Oblique	Linear	Bipinnate
Architecture							
							
Frontal area 4 zooids							
Frontal area 8 zooids							
Scaling	2	2	2	1	$1 \times 2$	1	1

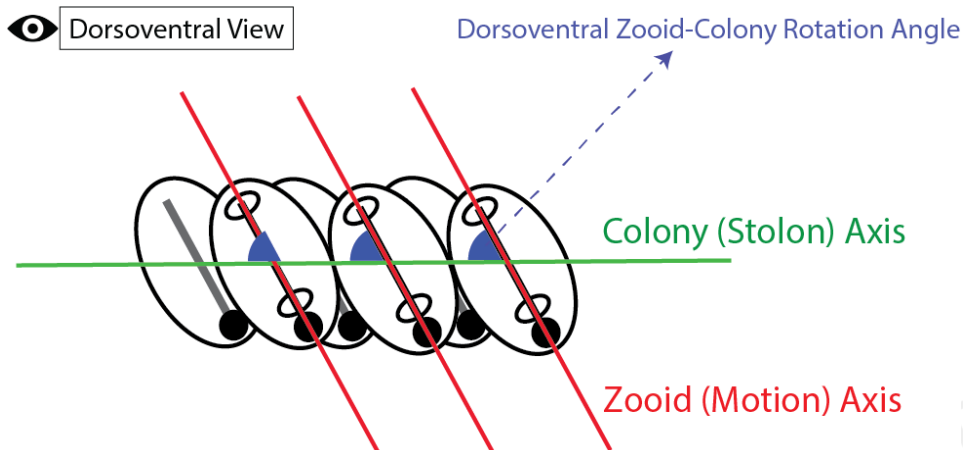
Figure 1. Salp colonial architectures with representative species photos (*Pegea* sp. for transversal, *Cyclosalpa affinis* for whorl, *Cyclosalpa sewelli* for cluster, *Helicosalpa virgula* for helical, *Thalia cicatricosa* for oblique, *Soestia zonaria* for linear, and *Ritteriella retracta* for bipinnate) and diagrams showing the distinct zooid orientations. The subsequent rows show the frontal view of colonies with four and eight zooids, with the final row indicating the expected frontal area increase factor between the four and the eight zooid colonies. Full black circles in the diagrams represent viscerae (guts) while the open circle represent siphons. Black straight lines inside the zooids indicate gill bars while gray straight lines represent endostyles.

Linearity of colonies, as well as zooid size and pulsation rates, are additional factors that could influence swimming performance. The degree of linearity in a colony can be expressed as the degree of parallelism between the zooids and the elongation axis of the colony (Fig. 2). This angle is determined by the degree of developmental dorsoventral zooid rotation, which can span from 90°, in transversal chains with no rotation, to 0° (perfect linearity), in some linear chains such as those from the species *Soestia zonaria* (Damian-Serrano & Sutherland, 2023). Strong reductions in the dorsoventral zooid rotation angle toward linear forms have evolved multiple times independently (Damian-Serrano et al. 2023), possibly due to adaptive advantages related to their swimming efficiency. Body size predicts swimming velocity in many animals (Andersen et al. 2016), however colonies with multiple swimming units may circumvent this size-speed relationship by having multiple propellers. Pulsation rates may also influence swimming speed as has been shown in solitary salps (Madin 1990). Pulsation by salps serves the dual role of locomotion and filter feeding. The relationship between pulsation and speed might therefore be particularly relevant for species that undergo diel vertical migration (Madin et al. 1996) and in other species pulsation may serve to maximize filtration rates. Considering the tradeoffs between

121 swimming and filtering, the eco-evolutionary relevance of swimming speed, and the hydrodynamic  
122 efficiency likely varies between species (Damian-Serrano et al. 2023).

123

124



125  
126 Figure 2. Schematic of an oblique chain from the dorsoventral perspective showing the zooid and  
127 stolon axes and the zooid rotation angle (degree of linearity) relative to those axes. Black lines  
128 indicate gill bars (mostly occluded by zooid axis) while gray lines represent endostyles.

129 The energetic costs of salp locomotion from mechanically estimated propulsive efficiency  
130 suggest that like other jet-propelled swimmers, salps are hydrodynamically efficient (Sutherland  
131 & Madin 2010, Gemmell et al. 2021, Trueman et al. 1984). The few metabolic measurements of  
132 swimming salps show that more active species-- in terms of swimming speed and pulsation rates--  
133 have the highest respiration rates (Cetta et al. 1986) and that salps have higher respiration rates  
134 than other gelatinous taxa (Biggs 1977, Schneider 1992, Mayzaud et al. 2005, Trueblood 2019).  
135 However, the specific costs incurred by their swimming activity and their relationship to swimming  
136 speed have never been examined across the diversity of salp species.

137 In this study, we compare swimming speeds across 17 salp species and energetic costs  
138 of swimming across 15 species, encompassing all seven known salp colony architectures (Fig. 1,  
139 Table S1). In addition, we investigate how swimming speed varies with the number of propeller  
140 zooids and differences in frontal area scaling between colonial architectures. Finally, we compare  
141 cost of transport (COT) across salp species and assess how COT scales with swimming speed  
142 and pulsation effort.

143

## 144 Materials and Methods

145         *Fieldwork* – We observed salps via 48 bluewater SCUBA dives (Haddock & Heine, 2005)  
146 from a small vessel off the coast of Kailua-Kona (Hawai'i Big Island, 19°42'38.7" N 156°06'15.8"  
147 W), over 2000 m of offshore water during September 2021, April 2022, September 2022 and May  
148 2023. We spent a total of 42.2 hours (84.4 person hours: ADS & KRS) collecting and imaging  
149 salp colonies. Some dives were diurnal, where we collected most of the specimens of *Iasis*  
150 *cylindrica*, *Cyclosalpa affinis*, *Cyclosalpa sewelli*, and *Brooksia rostrata*. We observed and  
151 collected most specimens of other species during night dives (blackwater diving). We recorded in  
152 situ underwater videos of salp colonies swimming using a variety of cameras including primarily  
153 a dark field stereovideography system (Sutherland et al. 2024), as well as a lightweight dual  
154 GoPro stereo system, a brightfield single-camera system (Colin et al. 2022), and a darkfield  
155 single-camera system. The primary stereovideography system was comprised of two  
156 synchronized high-resolution cameras (Z Cam E2, Nan Shan, Shenzhen, China and Sync Cable;  
157 4K at 60 or 120 fps) with 17mm f/1.8 lenses (Olympus M.Zuiko Digital) housed in custom  
158 aluminum housings (Sexton Company, Salem, OR, USA). Each field of view was 23 x 42 mm and  
159 in-focus depth was 20-25 mm. The image from the right-hand camera was viewed using an  
160 external monitor (Aquatica Digital, Montreal, Quebec, Canada), and illumination was provided  
161 with two 10,000-lumen lights (Keldan, Bruegg, Switzerland). An L-shaped plastic framer helped  
162 the videographer position colonies in the field of view of both cameras. Before diving, the stereo  
163 system was calibrated in a swimming pool using a cube with reflective landmarks. Calibration  
164 images were processed using the CAL software package (SeaGIS measurement science,  
165 Bacchus Marsh, Victoria, Australia). Over the course of the study, we observed 241 salp colonies  
166 (N) from 18 species and recorded 1,946 measurements (n) (Dataset1A, Table S1). Throughout  
167 the manuscript, we refer to the number of specimens as N and the number of measurements as  
168 n.

169         *Measuring salp colony swimming speed* – For most species, we collected and analyzed  
170 footage from multiple specimens (Dataset1A, Table S1). We analyzed the swimming behavior of  
171 salp colonies arranged in linear (six species, 64 specimens), bipinnate (three species, 17  
172 specimens), whorl (three species, 10 specimens), cluster (two species, eight specimens), and  
173 transversal (one species, two specimens) architectures, with oblique and helical architectures  
174 represented by a single specimen. We used a combination of spatially calibrated stereo video  
175 and 2D videos with a reference scale in the frame. From the stereo videos, we manually selected  
176 and measured the relative XYZ positions of salp colony zooids in EventMeasure (SeaGIS). We  
177 implemented a cutoff in the RMS (root mean squared) point error estimate of < 2 mm.

178 We complemented gaps in taxon sampling with archived 2D videos in the lab from  
179 previous expeditions to West Palm Beach (FL, USA) and the Pacific coast of Panama. These two-  
180 dimensional single-camera videos were collected using a Sony FDR-AX700 4K Camcorder  
181 (3840x2160 pixels, 60-120 fps) with a Gates Underwater Housing (**Poway, CA, USA**) using  
182 brightfield illumination (Colin et al 2022) or darkfield illumination. For these 2D videos, we used  
183 the FFmpeg plugin in ImageJ to manually select and measure the relative XY positions of salp  
184 zooids in sequences where the colony was swimming horizontally within the focal plane. The  
185 colonies were assumed to be in the same plane as the scale bar so at same distance from the  
186 camera. However, in videos with a broad focal depth, this may not always had been the case,  
187 thus potentially introducing some measurement error.

188 We tracked and manually selected the position of the first zooid's viscera (using a contrast-  
189 based centering macro to mark the center point) as well as the position of a reference particle in  
190 the water (methods described in Sutherland et al. 2024) in 10-30 frames across 50-500 frame  
191 windows spanning 2-4s of swimming on the synchronized left and right videos in EventMeasure.  
192 The reference particle was a non-swimming organism (such as a foraminiferan or radiolarian) or  
193 a non-living particle. In addition, we recorded the pulsation rates of the specimens measured by  
194 counting the number of times the atrial siphon contracted in a known period. For each analyzed  
195 frame, we calculated the horizontal x, vertical y, and depth z (in the case of the stereo video  
196 measurement files) components of the relative positions of the frontal zooid to the reference  
197 particle as shown in Eq. 1.

$$\begin{aligned} x &= n_{animal} - n_{particle} \\ y &= n_{animal} - n_{particle} \quad \text{Eq. 1} \\ z &= n_{animal} - n_{particle} \end{aligned}$$

203 Then we calculated the instantaneous relative speeds of the frontal zooid using Eq. 2  
204 (without the z component in the case of the 2D videos) given the known frame rate of each video.  
205

$$U = \frac{\sqrt{(x_2-x_1)^2 + (y_2-y_1)^2 + (z_2-z_1)^2}}{t_2-t_1} \quad \text{Eq. 2}$$

207  
208 *Salp colonial architecture* – To examine the relationships between locomotory variables  
209 and colonial architecture, we adopted the species-specific architecture characterizations and  
210 dorsoventral zooid rotation angle measurements for each species from Damian-Serrano et al.

211 (2023). Using stills from the underwater videos, we measured zooid length, zooid width, and  
212 number of zooids in ImageJ manually selecting the point coordinates. These measurements were  
213 repeated in at least three locations from each colony. When a distinct zooid size gradient was  
214 observed, we measured zooids in locations from the proximal, middle, and distal regions to  
215 capture the full range of variation in the specimen.

216 *Respiration measurements* – We collected healthy, adult blastozooid (aggregate stage)  
217 colonies across 18 salp species (Dataset S1B) during blue- and black-water SCUBA dives off the  
218 coast of Kona (Hawaii, USA) between September 2021 and May 2023. We analyzed the  
219 respiration rates of salp colonies arranged in linear (seven species, N = 46), bipinnate (three  
220 species, N = 29), whorl (three species, N = 23), cluster (two species, N = 18), and transversal  
221 (one species, N = 13) architectures, oblique chains (*Thalia* sp., N = 7), and helical architectures  
222 represented by *Helicosalpa virgula* (N = 2). Specimens were sealed *in situ* with their surrounding  
223 water in plastic jars equipped with a PreSens oxygen sensor spot (Regensburg, Germany) and a  
224 self-healing rubber port to allow for the injection of solutions without the introduction of air bubbles.  
225 We removed as many symbiotic animals from the salps as possible before closing the lid without  
226 damaging the colony. The same method was applied to one or more seawater controls to account  
227 for the oxygen demand of the local seawater's microbiome. Several collection events occurred  
228 during each 20-60 min long SCUBA dive. Jars with larger animals were opened during the safety  
229 stop to allow them to re-oxygenate. Upon the divers' return to the boat, we measured the initial  
230 oxygen concentration (mg/l) and temperature, and then repeated the measurements at intervals  
231 between 15min and 3h, for total periods ranging between 2h and 5h, depending on logistic  
232 constraints in the field and the rate of oxygen depletion. The exact interval time for each  
233 measurement was variable but recorded (Dataset S1B).

234 To estimate the energetic expenditure of different salp species while actively swimming,  
235 we recorded the oxygen consumption of intact specimens while swimming inside the jar. To obtain  
236 a baseline of basal respiration rate (while not swimming), we anesthetized some specimens  
237 before the start of the first oxygen measurement time. A few specimens were used for paired  
238 experiments, where their swimming respiration was recorded for a few hours, then inoculated with  
239 the anesthetic, and recorded anesthetized for another set of hours. To anesthetize salps, we  
240 injected their jars with small volumes of concentrated (50 g/l) bicarbonate-buffered MS-222  
241 through the rubber ports on the lids. We tailored the injection volume to the jar size aiming for a  
242 final concentration of 0.2g/l, following the methods in Trueman et al. (1984). We also injected  
243 some seawater control jars to evaluate the effect of MS-222 on oxygen concentration in seawater  
244 and found no effect.

When multiple seawater controls were collected using jars of different sizes, we paired each jar with the control that had the most similar volume. If among multiple controls only some were jars injected with anesthetic, we paired the anesthetized specimen jars with the injected controls and the intact specimen jars with the intact controls. In experiment 26 (see Dataset S1B for experiment numbers), the control jar was lost due to an encounter with an oceanic white tip shark, thus we paired those measurements with the nearest relative time points from the control jar in experiment 25, collected the same day hours earlier. At the end of each experiment, we identified the salp specimens used in the experiments to the species level, counted the number of zooids, measured the zooid length (total length including projections), and measured the biovolume of the colony using a graduated cylinder. For those specimens where colony or zooid volume was not measured directly, we estimated the colony volume from their zooid length and the number of zooids using a Generalized Additive Model with the measured specimens.

We estimated the oxygen consumption rate for each specimen by fitting a linear regression of consumed oxygen mass (concentration by container volume) against the duration of the measurement series. We subtracted the slope calculated for the relevant control jar to the estimated slope of the animal jar. Since our seawater controls were not filtered, some experiments had abnormally high estimated background respiration rates, leading to negative values. We removed these data points before the analysis. To estimate biovolume-specific rates, we divided the rates by the colony volumes. We then compared the biovolume-specific respiration rates of active (swimming) and anesthetized specimens within each species, calculating the difference as a measure of biovolume-specific swimming cost respiration rate. Biovolume was used instead of dry mass to normalize measurements due to the inherent difficulties of accurately measuring dry mass of these fragile gelatinous organisms in the field. Biovolume provides a consistent and reliable measure of the live size of the colony, which is directly relevant to the volume of water being displaced during swimming. We also calculated the relative investment in swimming as the proportion of biovolume-specific respiration rate comprised by the swimming-specific rate. To capture variability within species, we calculated the mean respiration rate of anesthetized specimens for each species and subtracted it from each intact specimen's total respiration rate to get multiple swimming-specific rate values within each species. We noticed that some species had higher average respiration rates among the anesthetized specimens than among the swimming specimens, leading to negative swimming-specific respiration estimates. We interpreted this anomaly as a systematic error due to the extremely low respiration rates of some species that fall within the effective detection limit of our experimental setup given the random variation range of respiration rates in seawater both in experimental jars and in control jars. Small

279 absolute negative values get amplified into large relative values, especially in small animals with  
280 a minuscule biovolume denominator. Therefore, we removed the swimming specimens that had  
281 lower respiration rates than the mean anesthetized respiration rate for their species. We also  
282 removed two respirometry outliers of *Thalia* sp. which had extremely high swimming respiration  
283 rates (>7500 pgO<sub>2</sub>/ml/min, whereas all other measurements across species including other  
284 *Thalia* sp. were limited to 0-1700 pgO<sub>2</sub>/ml/min), which were likely due to amplification of  
285 experimental error (presence of organic matter or symbionts, underestimation of colony volume  
286 due to loss of tiny zooids in the sieves) with the small biovolume denominators in this species.

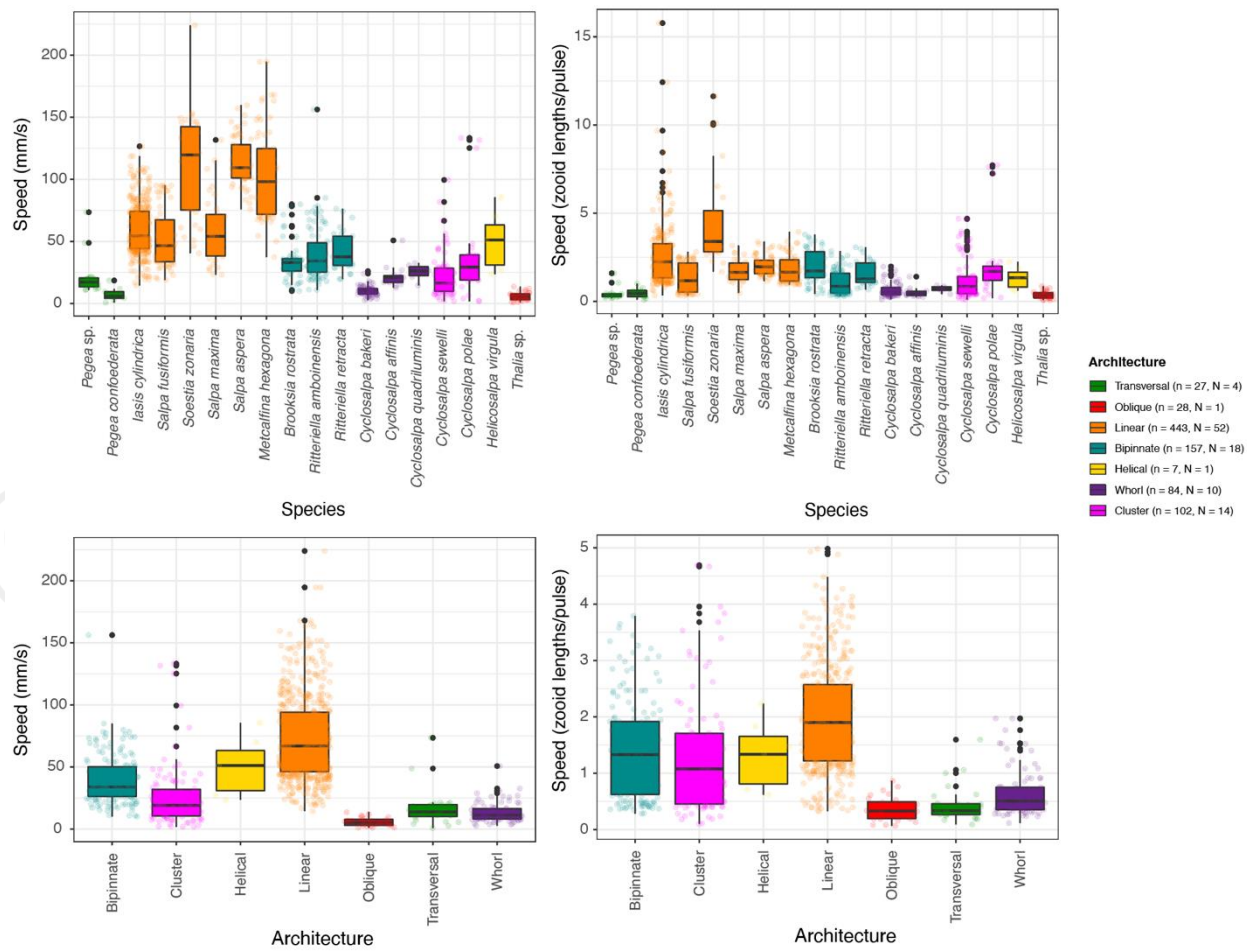
287 *Estimating costs of transport* – We define the cost of transport (COT) as the amount of  
288 oxygen consumed per tissue volume per distance traveled by the colony. To estimate the COT,  
289 we divided the swimming-specific respiration rates by the mean swimming speed for each species  
290 measured from the stereo and 2D video data. Since the specimens used for speed measurements  
291 in the videos and those used in the respirometry experiments had different zooid sizes, we used  
292 the mean zooid-lengths per second speeds from the video measurements and then multiplied  
293 them by the actual zooid lengths of the respirometry specimens to estimate their absolute (mm/s)  
294 speeds. Pulsation rate estimates were taken from species averages from the video specimens.  
295 We also calculated the size-specific COT by transforming the swimming distances into zooid  
296 lengths measured from the respirometry specimens.

297 *Statistical Analyses* – All data wrangling and statistics were carried out in R 3.6.3 (R Core  
298 Team 2021). To test for differences between architectures, we used ANOVAs with Tukey's post-  
299 hoc pairwise contrasts, reporting the difference magnitude and the adjusted p-value in  
300 supplementary tables S2A and S2B. To test the relationships between pairs of continuous  
301 variables **across architectures** (e.g. swimming speed vs. number of zooids), we used **linear**  
302 **regressions**. We evaluated the significance of the slope parameter when compared against a flat  
303 slope (one-tailed t-test) **to test whether changes in the independent variable** (e.g. number of  
304 zooids) **were associated with changes in the dependent variable** (e.g. swimming speed). Owing  
305 to the patchiness of some species despite 80+ hours spent underwater (Table S1), we used  
306 replicate measurements (n) from each specimen (N) in swimming speed ANOVAs and  
307 regressions. We used an exponential regression to test the relationship between speed and COT.  
308 Specimen means (N) were used for all COT comparisons and regressions. Individual  
309 measurements (n) were used up to determine oxygen consumption rates. To evaluate the relative  
310 contribution of zooid size, pulsation rate, zooid number, and architecture type on swimming  
311 speed, we fitted a generalized linear model and evaluated the significance and proportion of  
312 variance explained by each factor using their partial R<sup>2</sup>.

313

314 **Results**

315 Salp colony swimming speeds, pulsation rates, and respiration rates varied within and  
 316 across species and colony architectures. When considering speed in terms of mm/s, we found  
 317 a relationship between pulsation rate (effort) and absolute speed ( $n = 947$ ,  $N = 111$ , 18  
 318 species, Speed mm/s =  $0.41 * \text{Pulsation rate} + 52.14$ ,  $p < 0.0001$ , Fig. S1A), as well as with  
 319 zoid-size corrected swimming speed ( $n = 848$ ,  $N = 100$ , 18 species, Speed zoid lengths/s  
 320 =  $0.96 * \text{Pulsation rate} + 1.73$ , adjusted  $R^2 = 0.18$ ,  $p < 0.0001$ , Fig. S1B). Normalized swimming  
 321 speeds (zoid lengths per pulse) allow for a more direct comparison of swimming speed across  
 322 colonial architectures.



323

324 Figure 3. Boxplots showing the absolute (A) and corrected for body size and pulsation rate (B)  
 325 swimming speeds recorded for each salp species and architecture (C, D) respectively. Colors  
 326 correspond to colonial architecture types. Sample sizes are included in the legend and Tukey's

327 post-hoc pairwise comparisons across architecture types are listed in Dataset 1A and Table S2A,  
328 respectively.

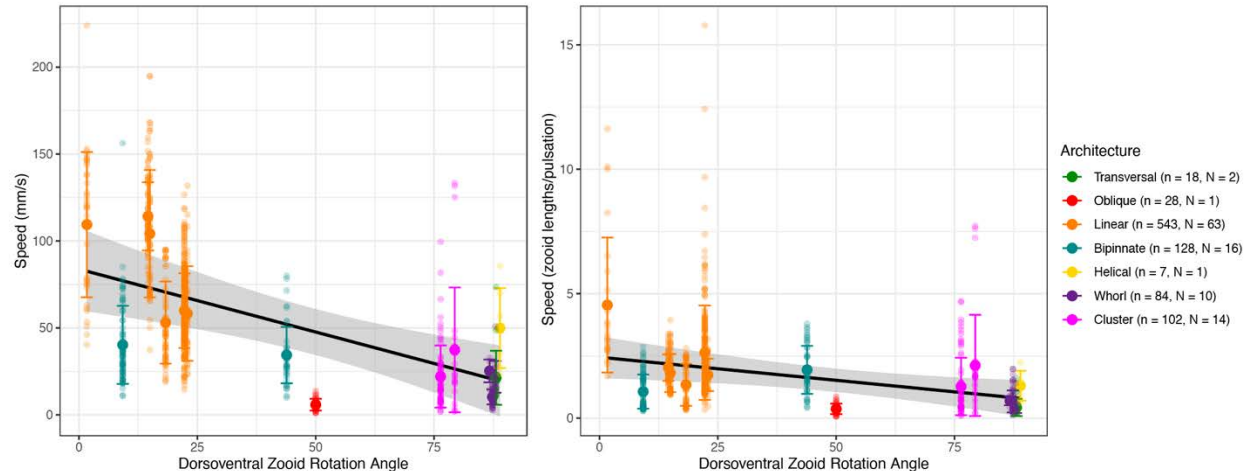
329

330 *Swimming speeds across salp architectures*

331 Swimming speed varied significantly (5 architectures, 16 species, N = 109, n = 913,  
332 ANOVA F > 38, p < 0.001) between colonial architecture types (Fig. 3C, D, Table S2A). Speeds  
333 measured with 2D methods were slightly slower than those measured with 3D methods within the  
334 species in which they overlapped. This is to be expected since 2D methods cannot account for  
335 the z (depth) component of the speed vector. Measurements of helical and oblique chains were  
336 limited to a single specimen, so they were excluded from the analysis. In terms of absolute speed  
337 (mm/s), linear architectures were significantly faster than every other architecture (Tukey's p <  
338 0.001). While bipinnate chains were significantly slower than linear chains, they were significantly  
339 faster than transversal chains, clusters, and whorls (Tukey's p < 0.002). Clusters were not  
340 significantly faster than transversal chains nor whorls. Transversal chains were on par to whorls,  
341 with no significant differences between them.

342 In terms of relative speed (zooid lengths/pulse), linear architectures were significantly  
343 faster than every other architecture (Tukey's p < 0.001). Bipinnate chains were significantly faster  
344 than whorls and transversal chains (Tukey's p < 0.01), but not significantly different from clusters.  
345 Clusters were significantly faster than whorls (Tukey's p < 0.001) in relative speed. Whorls and  
346 transversal chains presented similar relative swimming speeds with no significant differences.

347 Since linear architectures had the fastest mean swimming speeds (Fig. 3C, D), we  
348 investigated the relationship between swimming speeds with the dorsoventral zooid rotation  
349 angle, which represents the degree of linearity of the colony (Fig. 4). Species with more parallel  
350 (lower angles) dorsoventral zooid rotation presented faster absolute speeds (n = 910, N = 107,  
351 16 species, Speed mm/s = -0.78\*DV Zoid angle + 81.25, adjusted R<sup>2</sup> = 0.33, p < 0.0001) and  
352 faster size-and-effort corrected swimming speeds (n = 810, N = 96, 16 species, Speed  
353 zooids/pulse = -0.016\*DV Zoid angle + 2.37, adjusted R<sup>2</sup> = 0.09, p < 0.0001).

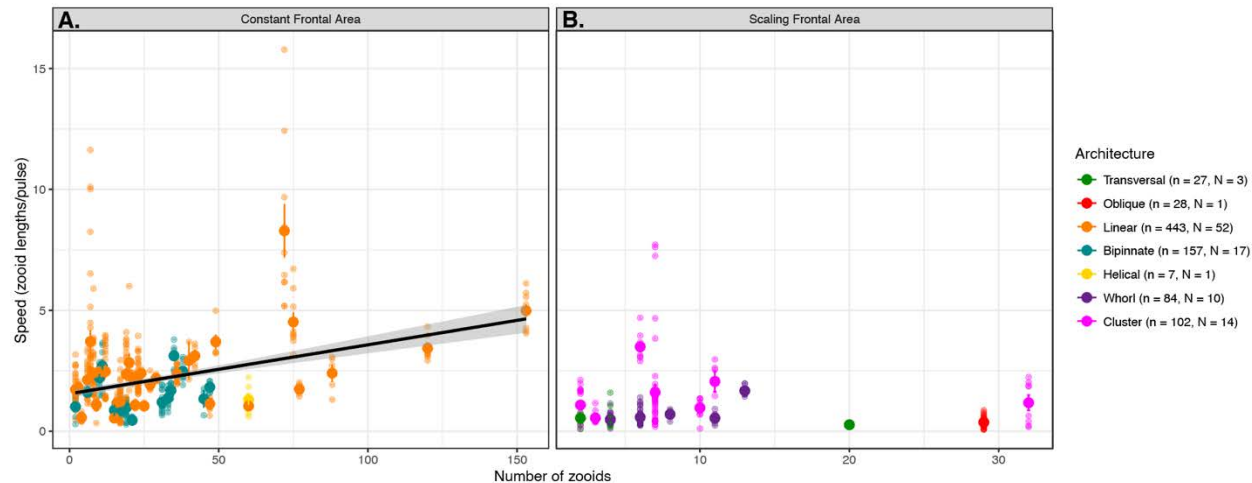


354  
355 Figure 4. Absolute (A) and relative (B) colony swimming speed (specimen mean with standard  
356 errors, total n=103) for each salp species across their degree of dorsoventral zooid rotation. Error  
357 bars indicate standard error. The color indicates colonial architecture. Gray areas indicate the  
358 95% confidence interval of the linear regression (black line).

359  
360 We compared how swimming speeds scale with the number of zooids in the colony and  
361 found differences between colonial architectures. Swimming speed in whorls increased with  
362 number of zooids ( $n = 84$ ,  $N = 10$ , 3 species, Speed mm/s =  $0.08 \times \text{Number of zooids} + 0.12$ ,  
363 adjusted  $R^2 = 0.3$ ,  $p < 0.0001$ ), though the data for this architecture was limited to small numbers  
364 of zooids (4 to 13) and relatively slow speeds (under 51 mm/s). Linear chain architectures did  
365 increase in relative speed with the number of zooids ( $n = 443$ ,  $N = 52$ , 6 species, Speed mm/s =  
366  $0.02 \times \text{Number of zooids} + 1.77$ , adjusted  $R^2 = 0.14$ ,  $p < 0.001$ ), as did bipinnate chains ( $n = 157$ ,  
367  $N = 18$ , 3 species, Speed mm/s =  $0.015 \times \text{Number of zooids} + 1.05$ , adjusted  $R^2 = 0.04$ ,  $p < 0.02$ ).  
368 This relationship was not significant for any of the other architectures.

369 We pooled the data from multiple architectures into scaling modes to evaluate the overall  
370 relationship in colonies with a constant frontal area (linear, bipinnate, and helical species) and in  
371 colonies with scaling frontal area (transversal, whorl, cluster, and oblique species) with linear  
372 regressions (Fig. 1). This aggregation allowed the inclusion of data from architectures for which  
373 we only have one specimen (helical and oblique). When pooled by scaling mode (Fig. 5), the  
374 regression on colonies with a constant frontal area had a higher intercept on the swimming speed  
375 axis than in those with a scaling frontal area (1.54 and 1.09 zoid lengths/pulse, respectively),  
376 reflecting the generally higher swimming speed of the former. Moreover, the regression on  
377 colonies with constant frontal area had a significant positive slope ( $n = 607$ ,  $N = 71$ , 10 species,  
378 Speed mm/s =  $0.02 \times \text{Number of zooids} + 1.55$ , adjusted  $R^2 = 0.12$ ,  $p < 0.001$ ), while the regression

379 on those with scaling frontal area was not significant ( $n = 241$ ,  $N = 29$ , 8 species,  $p = 0.073$ ).  
 380 However, the limited sample sizes for helical and oblique chains prevent us from drawing firm  
 381 conclusions about these architectures.



382  
 383 Figure 5. Linear relationships between relative swimming speed (zoid lengths per pulsation,  
 384 specimen mean with standard errors) and number of zooids in the colony for constant (A) and  
 385 scaling (N=71) (B) frontal motion-orthogonal frontal area (N=29) scaling modes. Gray areas  
 386 represent the 95% confidence intervals of the regressions.

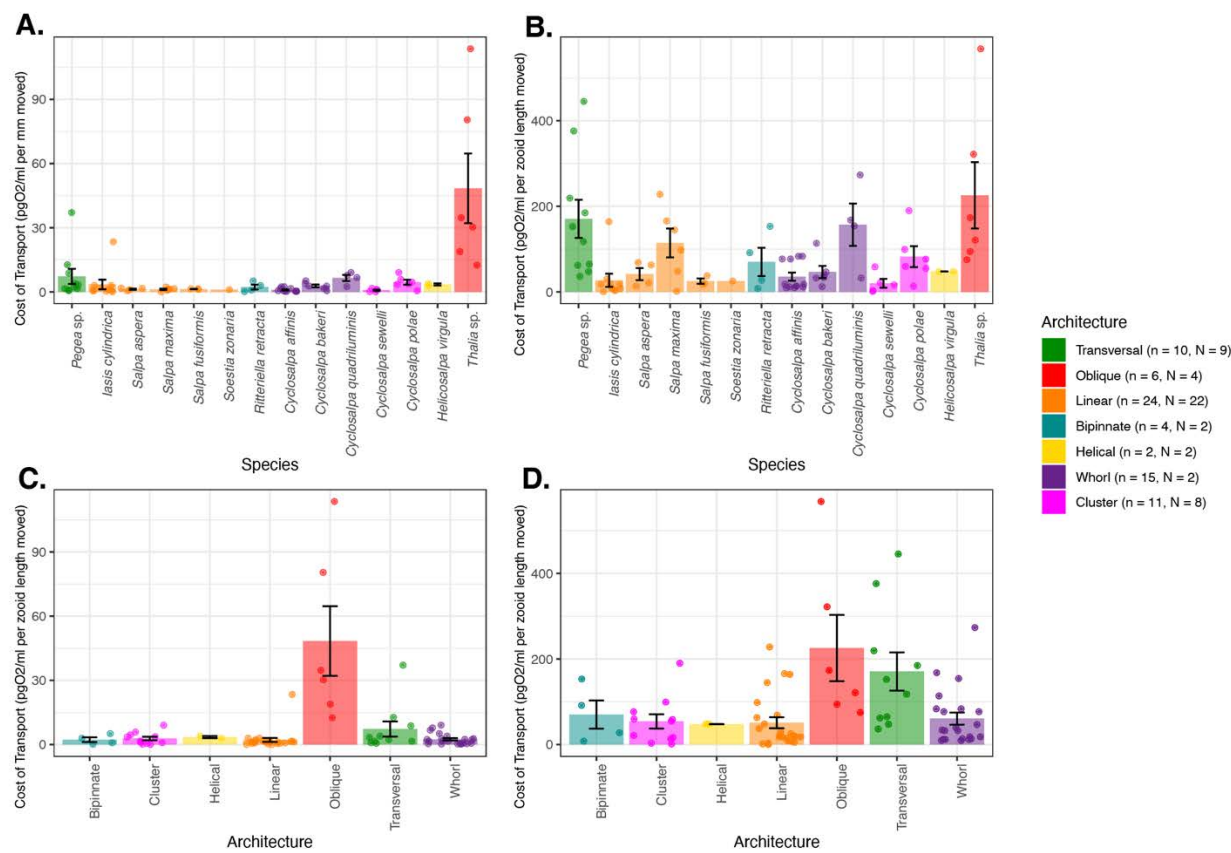
387  
 388 Putting together all the different organismal factors that we analyzed in this study, we  
 389 calculated a generalized linear regression model to predict absolute salp swimming speed ( $U$ )  
 390 from zooid length ( $L$ ), pulsation rate ( $P$ ), number of zooids ( $Z$ ), and colonial architecture  
 391 represented as frontal area scaling mode ( $A$ ) as expressed in Eq. 3. While our results suggest  
 392 that the effect of  $Z$  depends on  $A$ , we favored this simpler regression formula because it had a  
 393 significantly lower ( $\Delta > 70$ ) AIC score than those with interaction terms between  $Z$  and  $A$ .

394       $U \sim L + P + Z + A$       Eq. 3

395      In this global model, we found significant effects on swimming speed (848 measurements,  
 396 100 videos, 18 species,  $U = 0.29L - 0.60P - 0.2Z - 50.34A$ , pseudo- $R^2 = 0.37$ ,  $p < 0.001$ ) for  $L$ ,  
 397  $Z$ , and  $A$ . We found that our global regression explains 36.8% of the variance in our swimming  
 398 speed data: 5.8% is explained by zooid size, 3.5% by pulsation rate, 0.8% from zooid number,  
 399 and 26.6% by the frontal scaling mode.

400  
 401 *Respiration rates and cost of transport (COT)*  
 402      The respiration rates of swimming and anesthetized salps revealed broad differences  
 403 between species (Fig. 6, S2A). After estimating COT, we found a few significant differences

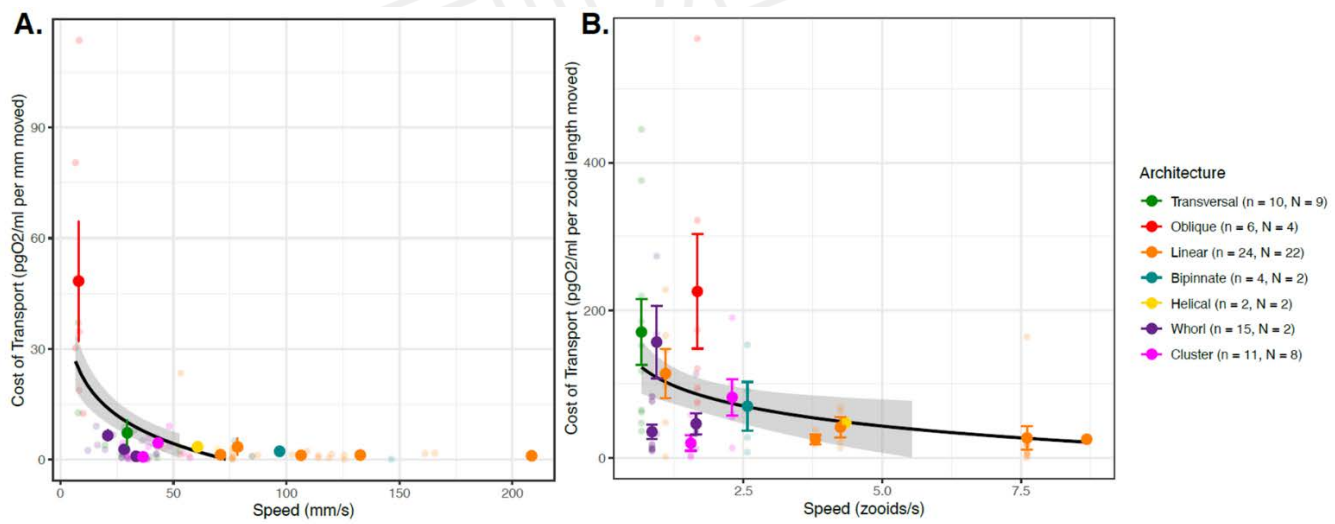
404 between architectures (Fig. 6, ANOVA  $F > 5.9$ ,  $p < 0.001$ , Table S2B). In terms of absolute COT  
 405 per mm traveled, all architectures except oblique chains had similar high transport efficiencies  
 406 under 13 pgO<sub>2</sub>/ml. Every one of these architectures was significantly more efficient per mm  
 407 traveled than oblique architectures (Tukey's  $p < 0.001$ ). In terms of relative COT per zooid length  
 408 traveled, linear chains, clusters, and whorls had similar transport efficiencies that are significantly  
 409 faster than transversal and oblique chains (Tukey's  $p < 0.05$ ). Some of the differences between  
 410 COT per mm and COT per zooid length are likely due to scaling with body size, as can be  
 411 observed with the relative shift in the minuscule *Thalia* sp. (5.2 mm zooids) and the massive *Salpa*  
 412 *maxima* (93.4 mm zooids).



413  
 414 Figure 6. Mean cost-of-transport per mm (A) and per zooid length (B) moved for each salp  
 415 species, and for each colonial architecture (C, D) with standard errors. Bar colors indicate colonial  
 416 architecture. Sample sizes and Tukey's post-hoc pairwise comparisons across architecture types  
 417 are listed in Dataset 1B and Table S2B, respectively.

418  
 419 When comparing the proportion of investment of metabolic costs into swimming  
 420 (compared to the species mean baseline) across salp species (Fig. S2B), eight species had  
 421 locomotion budgets under 50%, and the other seven have budgets above 50%. We then

422 compared the proportion of energetic investment in swimming to the COT values across species  
 423 (Fig. S3A,B). We found no relationship with absolute COT ( $N = 74$ , 14 species,  $p = 0.24$ ). We  
 424 found a positive relationship with zooid-length scaled COT ( $N = 74$ , 14 species, Swimming % =  
 425  $0.11 \times \text{COT per zooid length} + 34.4$ , adjusted  $R^2 = 0.22$ ,  $p < 0.001$ ), indicating that species with  
 426 more costly locomotion per zooid length invest a larger proportion of their energy budget in  
 427 swimming. Finally, we compared the proportion of energetic investment in swimming with speed  
 428 (Fig. S3C,D). We found no relationship (neither in mm/s nor in zooids/s), indicating that faster  
 429 swimmers do not invest more of their energy budget into their locomotion efforts. We found that  
 430 regardless of whether we consider transport in terms of absolute distances (Fig. 7A,  $N = 64$ , 14  
 431 species, linear regression: COT per mm =  $-0.12 \times \text{Speed mm/s} + 13.46$ , adjusted  $R^2 = 0.09$ ,  $p <$   
 432  $0.005$ ; exponential regression:  $\log\text{COT per mm} = -0.015 \times \text{Speed mm/s} + 1.39$ , adjusted  $R^2 = 0.14$ ,  
 433  $p < 0.001$ ) or relative to body lengths (Fig. 7B, 64 specimens, 14 species, linear regression COT  
 434 per zooid length =  $-12.9 \times \text{Speed zooid lengths/s} + 116.1$ , adjusted  $R^2 = 0.07$ ,  $p < 0.01$ , exponential  
 435 regression  $\log\text{COT per zooid length} = -0.24 \times \text{Speed zooid lengths/s} + 4.28$ , adjusted  $R^2 = 0.14$   $p$   
 436  $< 0.001$ ), the COT decreases in species with faster swimming speeds.  
 437  
 438



439  
 440 Figure 7. COT (specimen mean with standard error,  $n=75$ ) per mm (A) and zooid length (B) moved  
 441 across the specimen mean absolute (A) or relative (B) swimming speeds. The dot color indicates  
 442 colonial architecture. Gray areas represent the 95% confidence intervals of the exponential  
 443 regressions (black lines).

444

## 445 Discussion

446 We compared the swimming speeds and costs of transport of salp colonies across the  
447 most comprehensive representation of salp species diversity. Our results show a wide range of  
448 colonial swimming speeds across salp species and architectures with linear species swimming  
449 fastest (Fig. 3). Moreover, this study shows for the first time how salp colonial swimming speed  
450 scales with the number of zooids in the colony (Fig. 5), suggesting that incremental propulsive  
451 power from additional zooids does can produce higher swimming speeds for species with a  
452 constant frontal area. Across species, salps have a low COT (Fig. 6) and as speed increases,  
453 COT decreases (Fig. 7), which may be a unique advantage of multi-jet swimmers.

454 *Architectural determinants of salp swimming speed*

455 Colonial architecture was the strongest predictor of swimming speed, though there is a  
456 large amount of unexplained variation which may relate to species-specific differences,  
457 behavioral, or environmental factors (see global GLM results). We expected that swimming speed  
458 in colonial salps would be predicted by pulsation rate as a measure of swimming effort. Our results  
459 indicate that this relationship only exists when accounting for zooid size (Fig. S1B), suggesting  
460 an underlying relationship between pulsation rate and zooid length that may be masking its  
461 predictive power over absolute speeds. This is consistent with the distribution of our data and our  
462 observations in the field where larger salps pulsate at a slower rate than smaller ones. We find a  
463 significant increase in speed with larger zooid sizes (Fig. S1C,D), consistent with previous findings  
464 of jet propelled invertebrates (Gemmell et al 2021; Bone and Trueman 1983) and more broadly  
465 across aquatic swimmers (Andersen et al. 2016).

466 The relationship between the number of zooids and speed in linear chains is complicated  
467 by shifts in zooid orientation during development. Salp colonies start their free-living phase when  
468 the developing buds detach from the solitary oozooid. The newly released colony has the  
469 maximum number of zooids since the zooid number only gets reduced as the colony splits or  
470 loses zooids to turbulence, disease, or predation. Therefore, colonies with higher numbers of  
471 zooids are typically composed of smaller, younger zooids. In linear architectures, these younger  
472 colonies could still be developing their dorsoventral rotation (Damian-Serrano & Sutherland 2023),  
473 thus effectively being more like oblique architecture. A less acute dorsoventral rotation angle  
474 would explain why these more numerous linear chains are not as fast as we would expect, given  
475 that our results support a significant relationship between this angle and swimming speed (Fig.  
476 4). Finding a strong relationship between zooid number and speed in whorls was surprising given  
477 their less streamlined configuration (Fig. 5). This could be due to the smaller range of slow speeds  
478 and few zooids in the data we obtained for these species. Our regression results on pooled  
479 architectures, as well as finding a significant relationship between number of zooids and speed

480 for linear and bipinnate chains but not for clusters nor transversal chains, support our primary  
481 hypothesis that the different frontal area scaling relationships across architectures has an impact  
482 on swimming speed.

483 Linear chains swam faster than all other architectures, including those that share a  
484 constant frontal area feature like bipinnate chains ([Fig. 3, Table S2](#)). One potential explanation  
485 for this difference could come from the relative thrust provided by the jets. Linear chains eject  
486 their jet plumes at very small angles (near parallel) to the axis of locomotion (Sutherland et al.  
487 2024), just wide enough to avoid interaction between jet plumes (Sutherland & Weihs 2017).  
488 Bipinnate and helical chains (both with constant frontal area) have the atrial siphons (point of jet  
489 ejection) of their constituent blastozooids oriented at a wider angle (Madin 1990), which may lead  
490 to wider angles of their jets relative to the axis of locomotion. This in turn would result in a larger  
491 proportion of the force exerted by the jet to be applied as torque rather than thrust onto the colony.  
492 This hypothesis could be tested by measuring the 3D angles of the actual jets instead of the  
493 angles of the zooids since salps can use their atrial muscles and siphon morphology to direct the  
494 angle of their jets.

495 Finding that clusters can swim at speeds comparable to those of bipinnate and helical  
496 chains, even faster than whorls, defies our intuitive understanding of the mechanical properties  
497 of these colonies and thus warrants further investigation into how these species coordinate their  
498 jets to produce forward thrust. While oblique chains are architectural intermediates between  
499 transversal and linear chains ([Damian-Serrano & Sutherland 2023](#)), our data indicate that oblique  
500 chains may be the slowest swimmers among salps. This incongruence may be explained by the  
501 fact that we only had speed data from one oblique specimen (of *Thalia* sp.) with very small zooid  
502 sizes. Small salps might operate at notably lower Reynolds numbers than large ones, which may  
503 require a non-linear size correction for meaningful speed comparisons. Swimming speed data  
504 from the much larger oblique chains of *Thetys vagina* may provide a more comparable example  
505 of the locomotory performance of this oblique colonial configuration.

506 The questions addressed in this study focus on the effect of frontal area of colonial  
507 architectures on swimming speed. This effect may be associated with form and pressure drag  
508 differences between more and less streamlined colony shapes. To test whether these are the  
509 forces responsible for differences in swimming speed, drag would have to be measured or  
510 calculated, which is beyond the scope of this study. Other unaccounted forces may be significant  
511 energetic contributors to the system that explain the remainder of the observed variation. Chain  
512 length for the streamlined forms (helical, linear, and bipinnate chains) could have negative effects  
513 on swimming speeds that may partially counteract the positive effect of increased propeller thrust.

514 For example, skin drag increases proportionally to the surface area of the system, and the  
515 smoothness of the chain may increase pressure drag through vortex shredding (Vogel 1981).  
516 While added (virtual) mass could also be an issue, asynchronously swimming colonies do not  
517 suffer as much from these acceleration-related costs, since their speed is maintained near  
518 constant while cruising (Bone & Trueman 1983). Chain length could also lead to reduced stability  
519 and efficiency, though some linear species capitalize on this by swimming in corkscrew orbital  
520 spirals (Sutherland et al. 2024). However, if friction drag, chain stability, or vortex shredding were  
521 indeed more important contributors than frontal form drag, we would predict that linear chains  
522 would appear slower than other more stable and compact architectures. Future studies may  
523 unravel these potential confounding effects on the biomechanics of colonial salp swimming.

524 *Salp swimming speed and diel vertical migration*

525 Salps are important players in the oceanic carbon cycle, grazing upon both phytoplankton  
526 and bacteria (Henschke et al. 2016). Their carcasses and fecal pellets export large quantities of  
527 fixed carbon into the deep sea, accelerating carbon sequestration in the biological carbon pump  
528 (Wiebe et al. 1979, Décima et al. 2023). Part of this process is enhanced by the diel vertical  
529 migrations by some salp species though the distribution of this behavior across species diversity  
530 is poorly known. Off Bermuda, Madin et al. (1996) reported *Pegea* spp., *B. rostrata*, and *C. polae*  
531 as non-migratory, all of which we found to have slow swimming speeds. Other slow-swimmer  
532 species like *C. affinis* were found to only migrate a few meters through the diel cycle. The species  
533 *S. aspera*, *S. fusiformis*, *S. zonaria*, *I. punctata*, and *R. retracta* have been observed vertically  
534 migrating off Bermuda (Madin et al 1996, Stone & Steinberg 2014), which is congruent with our  
535 observations during fieldwork. These species all have constant frontal area and fast swimming  
536 speeds.

537 Vertical migrators need to be fast enough to follow the dark isolumes as they shift during  
538 dawn and dusk in time to maximize their exploitation of the food resources near the surface. Thus,  
539 absolute speed is important to the autoecology of these animals. Other *Salpa* species have also  
540 been reported as strong vertical migrators throughout the literature (Henschke et al. 2021, Madin  
541 et al. 2006, Pascual et al. 2017). A species that does not fit this pattern is *I. cylindrica*, a fast-  
542 swimming non-migratory species that spends night and day near the surface (Madin et al 1996;  
543 and pers. obs.). However, other studies do report moderate diel vertical migration for this species  
544 (Stone & Steinberg 2014), so it may be adapted for facultative vertical migration under specific  
545 oceanographic conditions. Some migratory species, such as *S. aspera*, are known to travel  
546 distances of over 800m at dawn and dusk, at rates predicted to require 5-10 m/min (83-166 mm/s)

547 based on MOCNESS trawl intervals (Wiebe et al. 1979). These predictions are consistent with  
548 the speeds we recorded for this species (88-145 mm/s) and similar congeners.

549 *Ecophysiological implications*

550 While the importance of a few well-studied linear chain salp species in the biological  
551 carbon pump has been delineated, the question of whether this ecological role is generalizable to  
552 other salp species remains unanswered. In addition to vertical migration behavior, another likely  
553 important factor in their carbon flow is their respiration rate. The higher their respiration rate, the  
554 larger the proportion of assimilated carbon that will be released back into the water as dissolved  
555 carbon dioxide. This study provides the broadest taxonomic perspective on respiration rates (18  
556 species, Fig. S2A) and swimming cost of transport (14 species), finding 17-fold differences in their  
557 respiration rates and over 77-fold differences in their mean COT. Except for a few species with  
558 extremely high and low values, most respiration rates are centered between 0.2 and 1  
559  $\mu\text{mol/g/hour}$ , assuming a salp tissue density of 1.025 g/ml. In general, the respiration rates we  
560 estimated for salps are within the range of those reported in the literature (Trueblood 2019, Iguchi  
561 and Ikeda 2004). Compared to the metabolic rates estimated for the broader diversity of marine  
562 pelagic animals (Seibel & Drazen 2007), the rates that we measured for salps are in a similar  
563 range to those measured for *Salpa thompsoni* (Iguchi and Ikeda 2004). Our values are also similar  
564 to those measured by Seibel & Drazen (2007) in nemerteans, chaetognaths, and most fishes (0.1-  
565 1  $\mu\text{molO}_2/\text{g/h}$ ), which are generally higher than other gelatinous animals like ctenophores or  
566 scyphomedusae (0.01-0.1  $\mu\text{molO}_2/\text{g/h}$ ), but generally lower than those of cephalopods,  
567 crustaceans, or large fish (1-10  $\mu\text{molO}_2/\text{g/h}$ ). Salp species known to have strong vertical migration  
568 behaviors (*Salpa* spp., *S. zonaria*, *I. punctata*, and *R. retracta*) have low basal metabolic rates  
569 (Fig. S2A) and low costs of transport. These results indicate that many non-migratory species,  
570 while likely still being important players in the biological carbon pump via their fecal pellet  
571 production, are releasing more of the consumed carbon as carbon dioxide near the surface than  
572 their more metabolically efficient relatives. The ultimate ecological outcome of each species  
573 needs to be assessed holistically, considering their microbial filtration and pellet deposition rate  
574 as well as their relative abundance in the water column.

575 Our metabolically calculated costs of transport range between 5-50 J/kg/m when  
576 converting the mg of oxygen to J via aerobic respiration free energy equations at 23°C. **These**  
577 values are higher than the highly efficient 1-2 J/kg/m reported for salps in the literature (Bone &  
578 Trueman 1983, Gemmell et al. 2021), **and approach** the less-efficient values found in single jet-  
579 propelled invertebrates like scallops or squids. We suspect that COT calculated from mechanical  
580 parameters such as the displacement of water mass is not directly comparable to the COT

581 calculated from respiration rates. Furthermore, the standard aerobic respiration free-energy  
582 equation based on glucose may not fully represent the metabolic energy-conversion processes  
583 in salps, which could rely on a combination of sugars and fatty acids derived from their  
584 microscopic prey.

585 While COT increases with swimming speed fishes (Rubio-Gracia et al. 2020) and jet-  
586 propelled squid (Bi & Zhu 2019), multi-jet swimmers may circumvent this tradeoff by having  
587 multiple swimming units. In colonial siphonophores, as zooid number increases swimming speed  
588 increases together with a decrease in COT (Du Clos et al. 2022). Our results show that faster  
589 swimming species have lower COT (Fig. 6), which suggests that faster speeds and higher  
590 locomotory efficiency have a common cause, where both speed and efficiency depend on frontal  
591 area which may partly drive form and pressure drag forces. However, this hypothesis is not  
592 supported by the distribution of COT across architectures (Fig 6C, D), where except for oblique  
593 and transversal chains, all architectures present similarly efficient COT values. Perhaps there are  
594 other underlying explanatory factors linking swimming speed and swimming efficiency, such as  
595 shared ancestry, muscle content, jet coordination, or jetting angles (thrust-to-torque ratios).

#### 596 *Evolutionary implications*

597 Across the evolutionary history of salps, linear chains have evolved multiple times  
598 independently from oblique ancestors (Damian-Serrano et al. 2023), suggesting the adaptive role  
599 of this architecture as a functional trait. Linear chain architectures evolved independently in *M.*  
600 *hexagona*, *S. zonaria*, *I. punctata*, and before the common ancestor of *Iasis* and *Salpa*. Our results  
601 show that going from an oblique form to a linear one may confer significant advantages in  
602 locomotory speed and energetic efficiency. However, multiple colonial architectures, which we  
603 find to be slower swimmers (such as transversal chains, helical chains, whorls, and clusters in  
604 the genus *Pegea* and the Cyclosalpidae family) had also evolved from oblique and linear  
605 ancestors. This is incongruent with a scenario where natural selection strongly favors locomotion  
606 efficiency across all ecological niches of salps. Therefore, the evolution of colonial architecture  
607 may be driven by ecological trade-offs with other non-locomotory functions. Alternatively, in some  
608 of these lineages, locomotion at the colonial stage may not be important enough for selection to  
609 maintain these highly streamlined forms, allowing for neutral evolutionary processes to produce  
610 a diversity of non-adaptive forms. In the current study, we did not use phylogenetic comparative  
611 methods in our analysis because like other investigators comparing biomechanical properties  
612 across species (e.g. Dabiri et al. 2010, DiSanto et al. 2021) we were interested in inherent  
613 mechanical relationships dictated by the colony architectures. For instance, a linear arrangement  
614 of zooids inherently reduces drag due to a cluster arrangement, leading to faster swimming

615 speeds and potentially higher efficiency regardless of phylogenetic history. In other words, any  
616 phylogenetic inertia is irrelevant in instantaneous relationships between traits (Felsenstein 1985).  
617 Moreover, independence of data is often incorrectly assumed to be an assumption of standard  
618 (nonphylogenetic) regressions (Uyeda et al. 2018), when in reality the assumptions relate to the  
619 independence and distribution of the error terms. Thus, when all the phylogenetic signal is present  
620 in the predictor, as it is in the case with colonial architecture (Damian-Serrano et al. 2022) and its  
621 associated characteristics, there is no need for any “phylogenetic correction” (Uyeda et al. 2018).  
622 However, there may be unaccounted factors explaining the residual variation in our analyses that  
623 may bear phylogenetic signal. For example, tunic stiffness, tunic smoothness, muscle band  
624 number, muscle fiber density, swimming behavior, as well as metabolic and physiological  
625 baselines may be more similar between more closely related species, potentially erasing some of  
626 the architecture-specific signal. Future studies could address the role of phylogeny and heritable  
627 factors in salp swimming speed and cost of transport using phylogenetic comparative methods.  
628 These analyses could reveal whether these factors have co-evolved with each other and/or with  
629 respiration rate or colonial architecture.

### 630 *Insights for bioinspired underwater vehicle design*

631 Pulsatile jet propulsion is a promising avenue for bioinspired aquatic vehicles and robots  
632 (Mohensi 2006, Gohardini 2014, Yue et al. 2015). Multijet propulsion systems with multiple  
633 propellers akin to salp colonies have been explored in an engineering context (Chao et al. 2017,  
634 Costello et al. 2015) with direct inspiration from gelatinous animals (Marut 2014, Krummel 2019,  
635 Bi et al 2022, Du Clos et al. 2022). Salp diversity provides a natural laboratory to explore the  
636 hydrodynamic implications of different multijet arrangement designs. Our findings underscore the  
637 importance of considering the scaling hydrodynamic properties of propeller arrangements to  
638 optimize speed and energy efficiency in bioinspired underwater vehicle design. While linear chain  
639 arrangements were the fastest and among the most energy efficient, robot (or vehicle)  
640 configurations such as a cluster form may confer unique object manipulation or maneuverability  
641 advantages. Our results show that these seemingly inefficient propeller configurations do not  
642 impose large disadvantages in terms of speed and fuel efficiency.

### 643 **Acknowledgments:**

644 We are grateful to the crew of Aquatic Life Divers, Kona Honu Divers for their assistance  
645 and support in hosting our offshore diving operations. We also wish to thank Marc Hughes, Jeff  
646 Milisen, Rebecca Gordon, Matt Connelly, Clint Collins, Paul Richardson, and Anne Thompson for  
647 their assistance during diving, collections, and filming operations in the field. We would like to

648 thank Tiffany Bachtel for her valuable advice on the respirometry experiment design. We thank  
649 the associate editor and two anonymous reviewers for their helpful comments.

650 **Funding**

651 This research was supported by the Gordon and Betty Moore Foundation [grant number  
652 8835] and the Office of Naval Research [grant number N00014-23-1-2171].

653 **Data availability**

654 Data used to generate the results presented in this paper are available in the supplementary  
655 information. Any other datasets used directly or indirectly for this study are available from the  
656 authors upon reasonable request.

657 **Competing interests**

658 No competing interests declared.

659 **Literature cited**

660 Alexander, A. J. (1968). Forward Speed Effects on Annular Jet Cushions. *The Aeronautical  
661 Journal*, 72(689), 438-441.

662 Andersen, K. H., Berge, T., Gonçalves, R. J., Hartvig, M., Heuschele, J., Hylander, S., ... &  
663 Kiørboe, T. (2016). Characteristic sizes of life in the oceans, from bacteria to whales.  
664 *Annual review of marine science*, 8(1), 217-241.

665 Bi, X., & Zhu, Q. (2019). Dynamics of a squid-inspired swimmer in free swimming. *Bioinspiration  
666 & Biomimetics*, 15(1), 016005.

667 Bi, X., Tang, H., & Zhu, Q., 2022. Feasibility of hydrodynamically activated valves for 416 salp-  
668 like propulsion. *Physics of Fluids*, 34(10), 101903.

669 Biggs, D. C. (1977). Respiration and ammonium excretion by open ocean gelatinous zooplankton  
670 1. *Limnology and Oceanography*, 22(1), 108-117.

671 Bone, Q., Anderson, P. A. V., & Pulsford, A. (1980). Morphology of salp chain communication.  
672 *Proceedings of the Royal Society of London. Series B. Biological Sciences*, 210(1181),  
673 549-558.

674 Bone, Q., & Trueman, E. R. (1983). Jet propulsion in salps (Tunicata: Thaliacea). *Journal of  
675 Zoology*, 201(4), 481-506.

676 Cetta, C. M., Madin, L. P., & Kremer, P. (1986). Respiration and excretion by oceanic salps.  
677 *Marine Biology*, 91, 529-537.

678 Chao, S., Guan, G., & Hong, G. S., 2017, September. Design of a finless torpedo-shaped micro  
679 AUV with high maneuverability. In OCEANS 2017-Anchorage (pp. 425 1-6). IEEE.

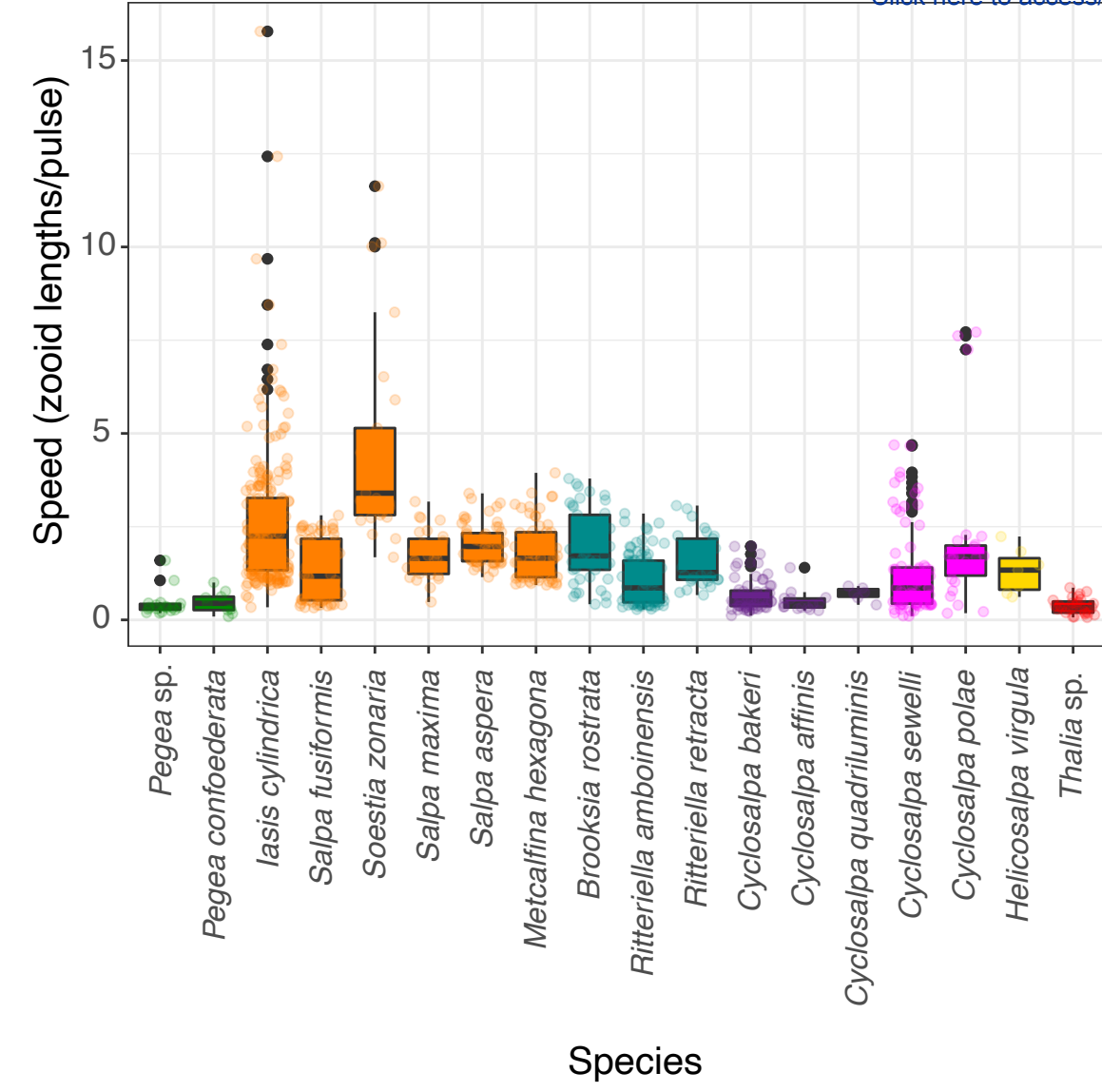
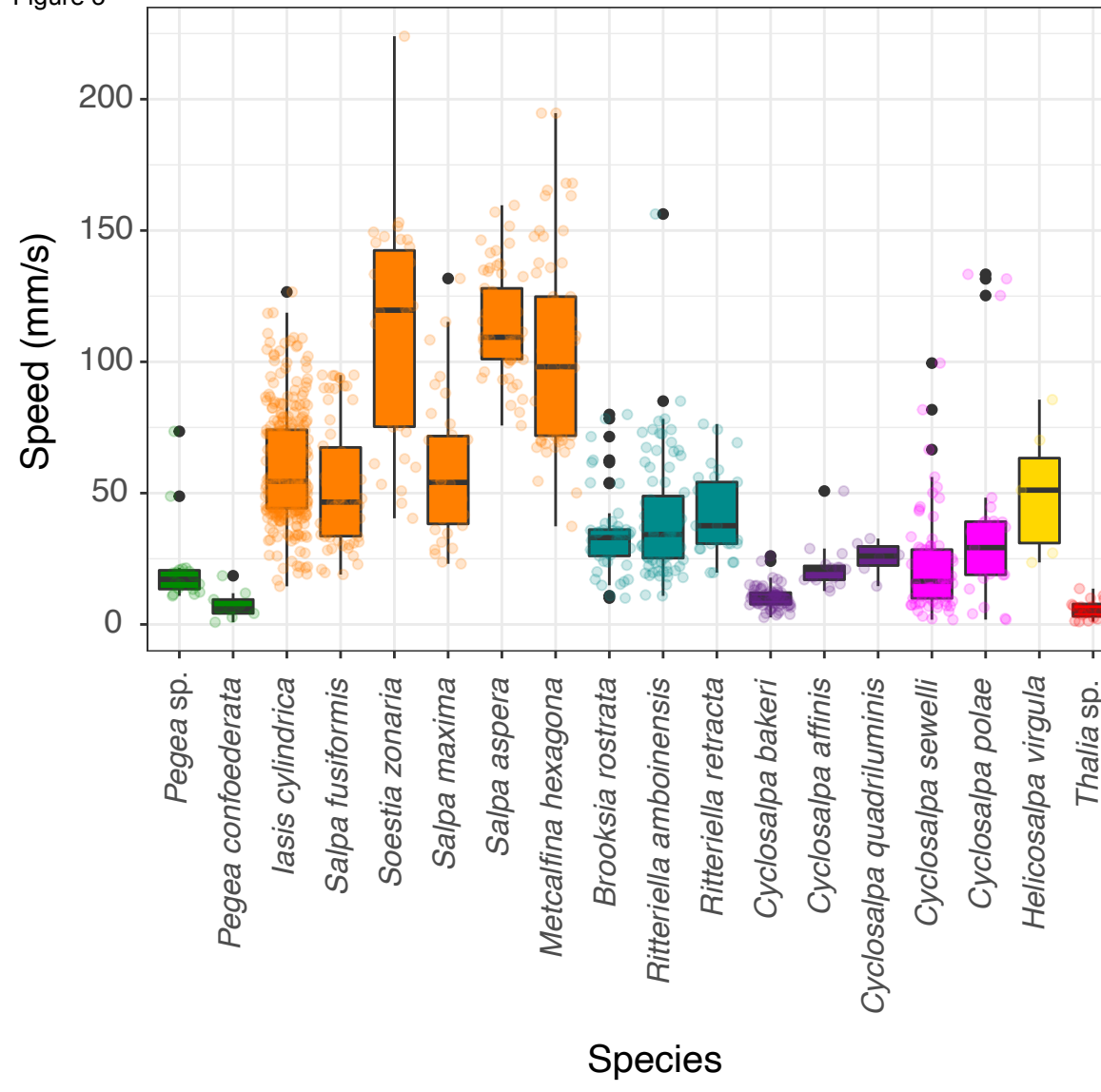
680 Colin, S. P., Gemmell, B. J., Costello, J. H., & Sutherland, K. R. (2022). In situ high-speed  
681 brightfield imaging for studies of aquatic organisms. *Protocols.io*.

- 682 Costello, J. H., Colin, S. P., Gemmell, B. J., Dabiri, J. O., & Sutherland, K. R., 2015. 429 Multi-jet  
683 propulsion organized by clonal development in a colonial siphonophore. 430 *Nature*  
684 communications, 6(1), 8158.
- 685 Dabiri, J. O., Colin, S. P., Katija, K., & Costello, J. H. (2010). A wake-based correlate of  
686 swimming performance and foraging behavior in seven co-occurring jellyfish species.  
687 *Journal of experimental biology*, 213(8), 1217-1225.
- 688 Damian-Serrano, A., & Sutherland, K. R. (2023). A developmental ontology for the colonial  
689 architecture of salps. *The Biological Bulletin*, 245(1), 9-18..
- 690 Damian-Serrano, A., Hughes, M., & Sutherland, K. R. (2023). A new molecular phylogeny of salps  
691 (Tunicata: thalicea: salpida) and the evolutionary history of their colonial architecture.  
692 *Integrative Organismal Biology*, 5(1), obad037.
- 693 Décima, M., Stukel, M. R., Nodder, S. D., Gutiérrez-Rodríguez, A., Selph, K. E., Dos Santos, A.  
694 L., ... & Pinkerton, M. (2023). Salp blooms drive strong increases in passive carbon export  
695 in the Southern Ocean. *Nature communications*, 14(1), 425.
- 696 Di Santo, V., Goerig, E., Wainwright, D. K., Akanyeti, O., Liao, J. C., Castro-Santos, T., & Lauder,  
697 G. V. (2021). Convergence of undulatory swimming kinematics across a diversity of fishes.  
698 *Proceedings of the National Academy of Sciences*, 118(49), e2113206118.
- 699 Du Clos, K. T., Gemmell, B. J., Colin, S. P., Costello, J. H., Dabiri, J. O., and Sutherland, K. R.  
700 2022. Distributed propulsion enables fast and efficient swimming modes in physonect  
701 siphonophores. *Proceedings of the National Academy of Sciences*. 119:e2202494119.
- 702 Felsenstein, J. (1985). Phylogenies and the comparative method. *The American  
703 Naturalist*, 125(1), 1-15.
- 704 Gemmell, B. J., Dabiri, J. O., Colin, S. P., Costello, J. H., Townsend, J. P., & Sutherland, K. R.  
705 (2021). Cool your jets: biological jet propulsion in marine invertebrates. *Journal of  
706 Experimental Biology*, 224(12), jeb222083.
- 707 Gohardani, A. S. Distributed Propulsion Technology Nova Science Publishers (2014).
- 708 Haddock, S. H. (2004). A golden age of gelata: past and future research on planktonic  
709 ctenophores and cnidarians. *Hydrobiologia*, 530, 549-556.
- 710 Haddock, S. H., & Heine, J. N. (2005). Scientific blue-water diving.
- 711 Hamner, W. M., Madin, L. P., Alldredge, A. L., Gilmer, R. W., & Hamner, P. P. (1975). Underwater  
712 observations of gelatinous zooplankton: Sampling problems, feeding biology, and  
713 behavior 1. *Limnology and Oceanography*, 20(6), 907-917.

- 714 Henschke, N., Cherel, Y., Cotté, C., Espinasse, B., Hunt, B.P. and Pakhomov, E.A., 2021. Size  
715 and stage specific patterns in *Salpa thompsoni* vertical migration. *Journal of Marine*  
716 *Systems*, 222, p.103587.
- 717 Krummel, G. M. (2019). Locomotion and Control of Cnidarian-Inspired Robots (Doctoral  
718 dissertation, Virginia Tech).
- 719 Mackie, G. O. (1986). From aggregates to integrates: physiological aspects of modularity in  
720 colonial animals. *Philosophical Transactions of the Royal Society of London. B, Biological*  
721 *Sciences*, 313(1159), 175-196.
- 722 Madin, L. P. (1990). Aspects of jet propulsion in salps. *Canadian Journal of Zoology*, 68(4), 765-  
723 777.
- 724 Madin, L. P., & Deibel, D. (1998). Feeding and energetics of Thaliacea. *The biology of pelagic*  
725 *tunicates*, 81-104.
- 726 Madin, L. P., Kremer, P., & Hacker, S. (1996). Distribution and vertical migration of salps  
727 (Tunicata, Thaliacea) near Bermuda. *Journal of Plankton Research*, 18(5), 747-755.
- 728 Madin, L.P., Kremer, P., Wiebe, P.H., Purcell, J.E., Horgan, E.H. and Nemazie, D.A., 2006.  
729 Periodic swarms of the salp *Salpa aspera* in the Slope Water off the NE United States:  
730 Biovolume, vertical migration, grazing, and vertical flux. *Deep Sea Research Part I:*  
731 *Oceanographic Research Papers*, 53(5), pp.804-819.
- 732 Marut, K. J. (2014). Underwater Robotic Propulsors Inspired by Jetting Jellyfish (Doctoral  
733 dissertation, Virginia Tech).
- 734 Mayzaud, P., Boutoute, M., Gasparini, S., Mousseau, L., & Lefevre, D. (2005). Respiration in  
735 marine zooplankton—the other side of the coin: CO<sub>2</sub> production. *Limnology and*  
736 *Oceanography*, 50(1), 291-298.
- 737 Mohensi, K., 2006. Pulsatile vortex generators for low-speed maneuvering of small 482  
738 underwater vehicles. *Ocean Eng.* 33, 2209–2223.
- 739 Pascual, M., Acuña, J.L., Sabatés, A., Raya, V. and Fuentes, V., 2017. Contrasting diel vertical  
740 migration patterns in *Salpa fusiformis* populations. *Journal of Plankton Research*, 39(5),  
741 pp.836-842.
- 742 R Core Team, R. (2021). R: A language and environment for statistical computing.
- 743 Rubio-Gracia, F., García-Berthou, E., Guasch, H., Zamora, L., & Vila-Gispert, A. (2020). Size-  
744 related effects and the influence of metabolic traits and morphology on swimming  
745 performance in fish. *Current Zoology*, 66(5), 493-503.

- 746 Schneider, G. (1992). A comparison of carbon-specific respiration rates in gelatinous and non-  
747 gelatinous zooplankton: a search for general rules in zooplankton metabolism.  
748 *Helgoländer Meeresuntersuchungen*, 46, 377-388.
- 749 Seibel, B. A., & Drazen, J. C. (2007). The rate of metabolism in marine animals: environmental  
750 constraints, ecological demands and energetic opportunities. *Philosophical Transactions  
751 of the Royal Society B: Biological Sciences*, 362(1487), 2061-2078.
- 752 Stone, J. P., & Steinberg, D. K. (2014). Long-term time-series study of salp population dynamics  
753 in the Sargasso Sea. *Marine Ecology Progress Series*, 510, 111-127.
- 754 Sutherland, K. R., & Weihs, D. (2017). Hydrodynamic advantages of swimming by salp chains.  
755 *Journal of The Royal Society Interface*, 14(133), 20170298.
- 756 Sutherland, K. R., Damian-Serrano, A., Du Clos, K. T., Gemmell, B. J., Colin, S. P., Costello, J.  
757 H. (2024). Spinning and corkscrewing of oceanic macroplankton revealed through in situ  
758 imaging. *Science Advances* 10(20).
- 759 Sutherland, K. R., & Madin, L. P. (2010). Comparative jet wake structure and swimming  
760 performance of salps. *Journal of Experimental Biology*, 213(17), 2967-2975.
- 761 Trueblood, L. A. (2019). Salp metabolism: temperature and oxygen partial pressure effect on the  
762 physiology of *Salpa fusiformis* from the California Current. *Journal of Plankton Research*,  
763 41(3), 281-291.
- 764 Trueman, E. R., Bone, Q., & Braconnor, J. C. (1984). Oxygen consumption in swimming salps  
765 (Tunicata: Thaliacea). *Journal of Experimental Biology*, 110(1), 323-327.
- 766 Uyeda, J. C., Zenil-Ferguson, R., & Pennell, M. W. (2018). Rethinking phylogenetic comparative  
767 methods. *Systematic Biology*, 67(6), 1091-1109.
- 768 Vogel, S. (1981). Life in moving fluids. *Princeton University Press*, Princeton, NJ.
- 769 Vogel, S. (2008). Modes and scaling in aquatic locomotion. *Integrative and Comparative Biology*,  
770 48(6), 702-712.
- 771 Wiebe, P. H., Madin, L. P., Haury, L. R., Harbison, G. R., & Philbin, L. M. (1979). Diel vertical  
772 migration by *Salpa aspera* and its potential for large-scale particulate organic matter  
773 transport to the deep-sea. *Marine Biology*, 53, 249-255.
- 774 World Register of Marine Species (WoRMS). (2024). WoRMS Editorial Board. Accessed January  
775 30, 2024. Available online at <http://www.marinespecies.org>
- 776 Yue, C. et al., 2015. Mechantronic system and experiments of a spherical underwater 510 robot:  
777 SUR-II. *J. Intell. Robot Syst.* Doi:10.1007/s10846-015-0177-3.

Figure 3

[Click here to access/download;Figure;F2\\_jitterplus.pdf](#)


**Architecture**

- Transversal (n = 27, N = 4)
- Oblique (n = 28, N = 1)
- Linear (n = 443, N = 52)
- Bipinnate (n = 157, N = 18)
- Helical (n = 7, N = 1)
- Whorl (n = 84, N = 10)
- Cluster (n = 102, N = 14)

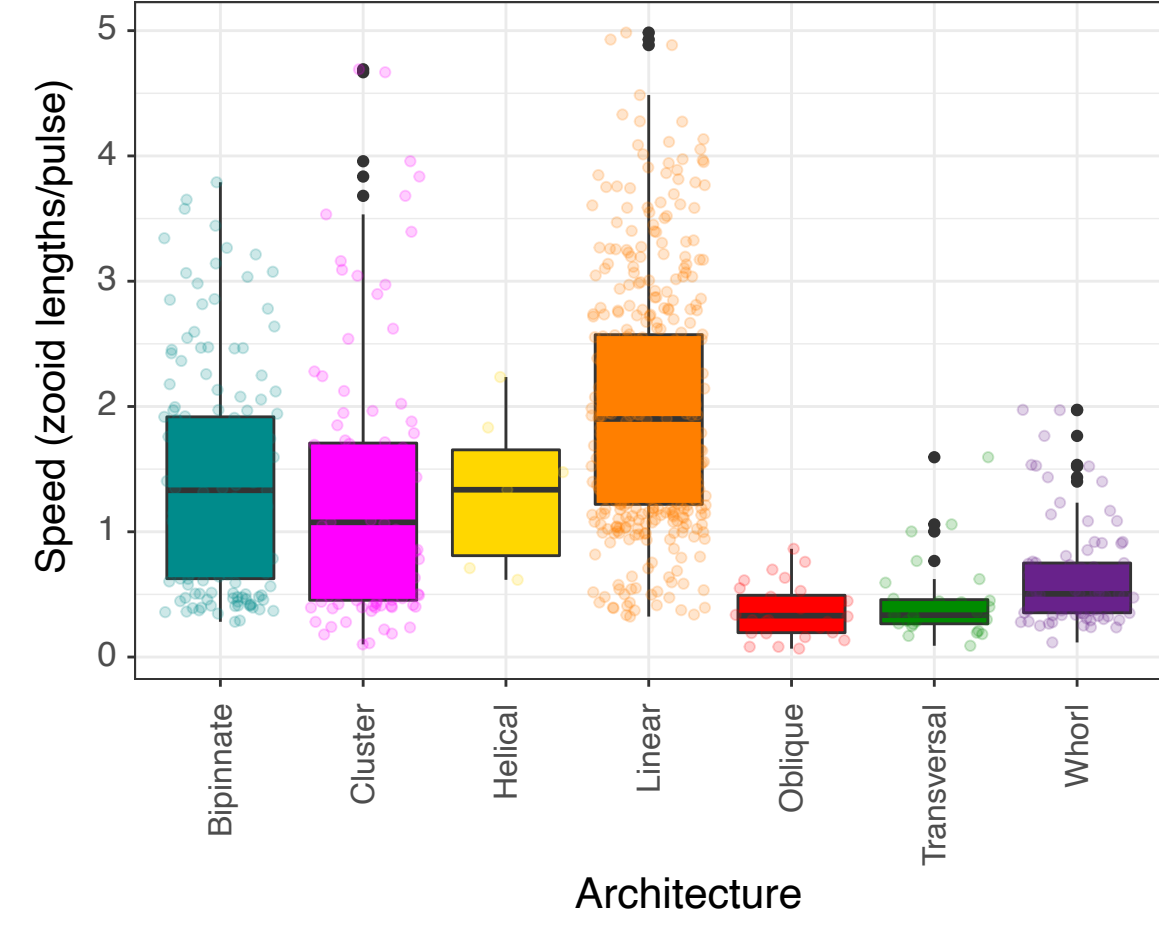
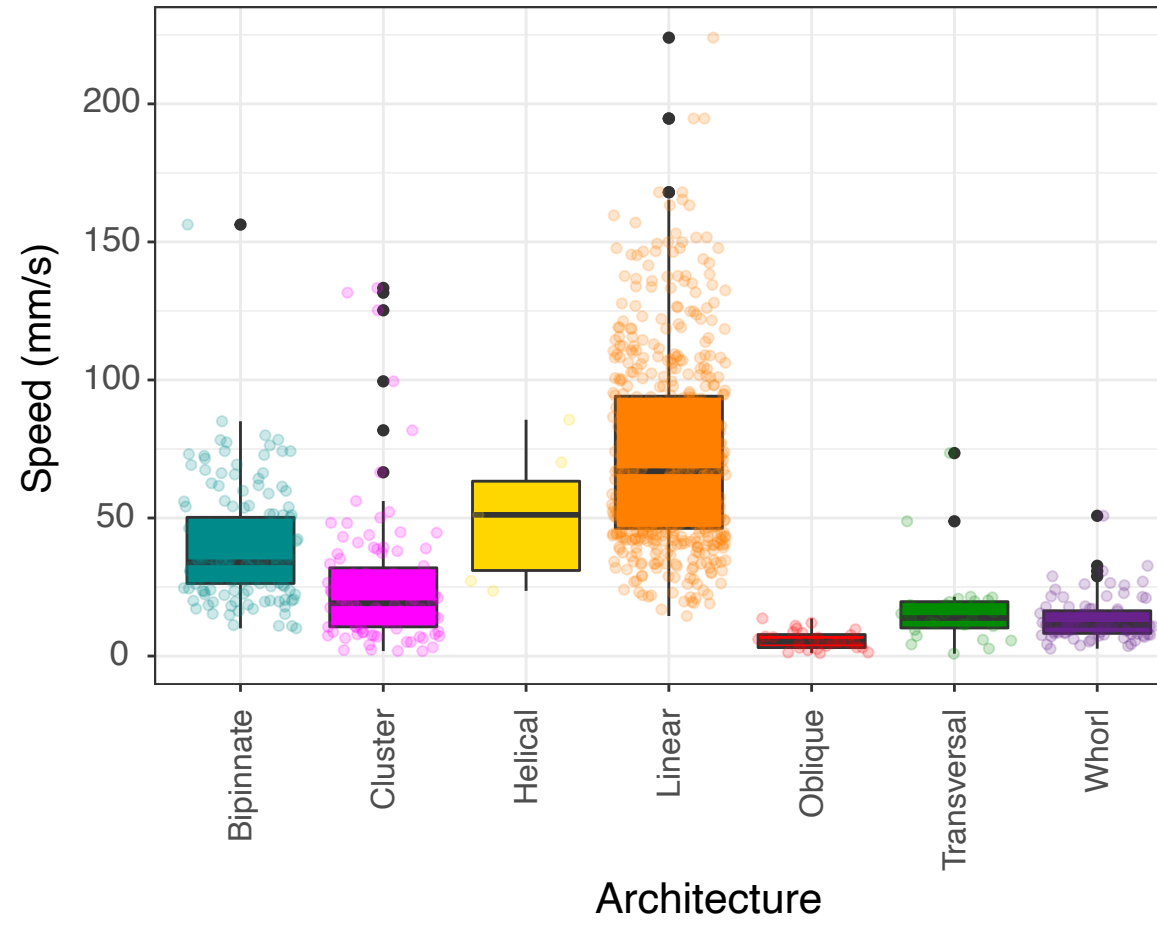
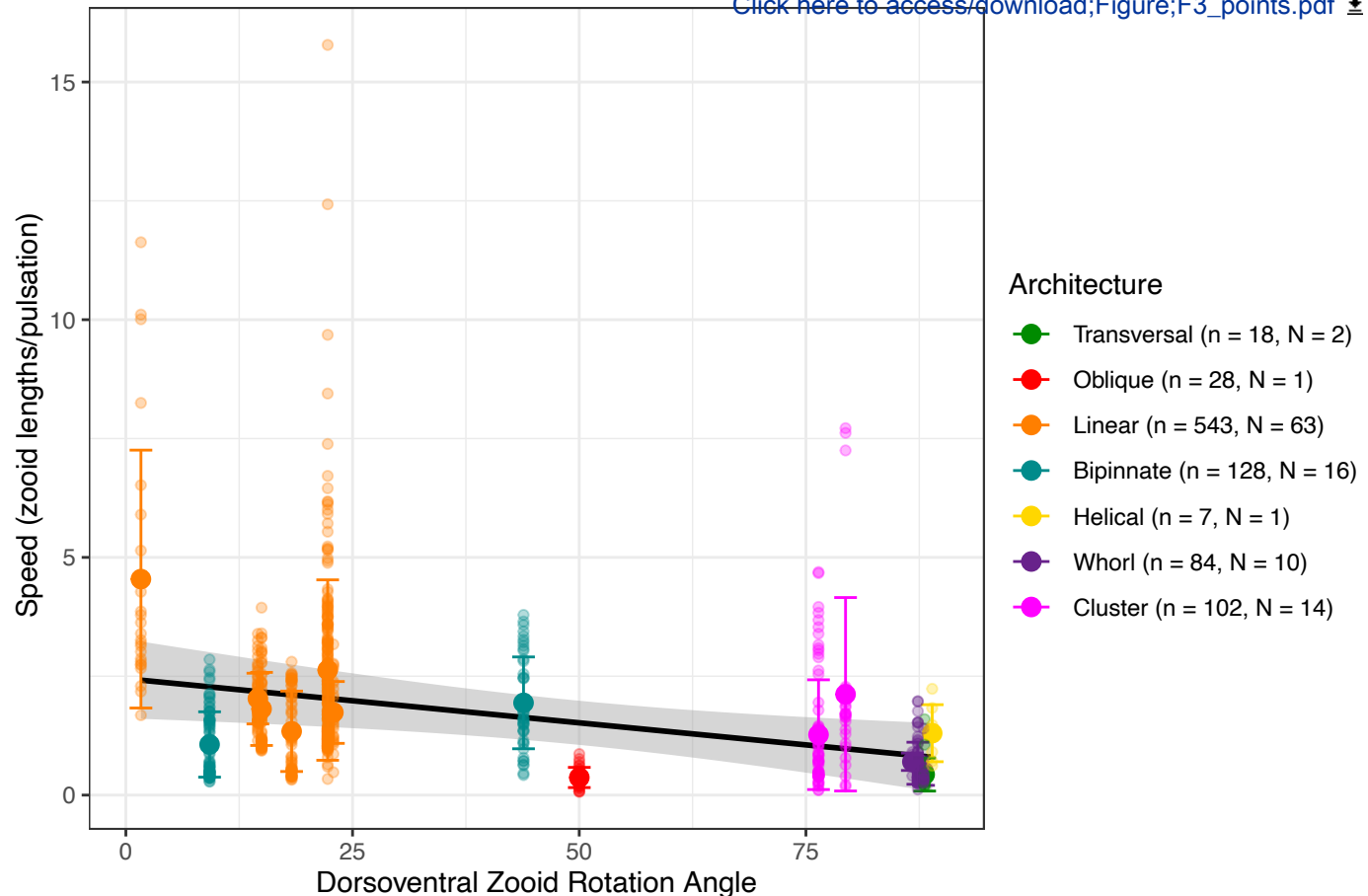
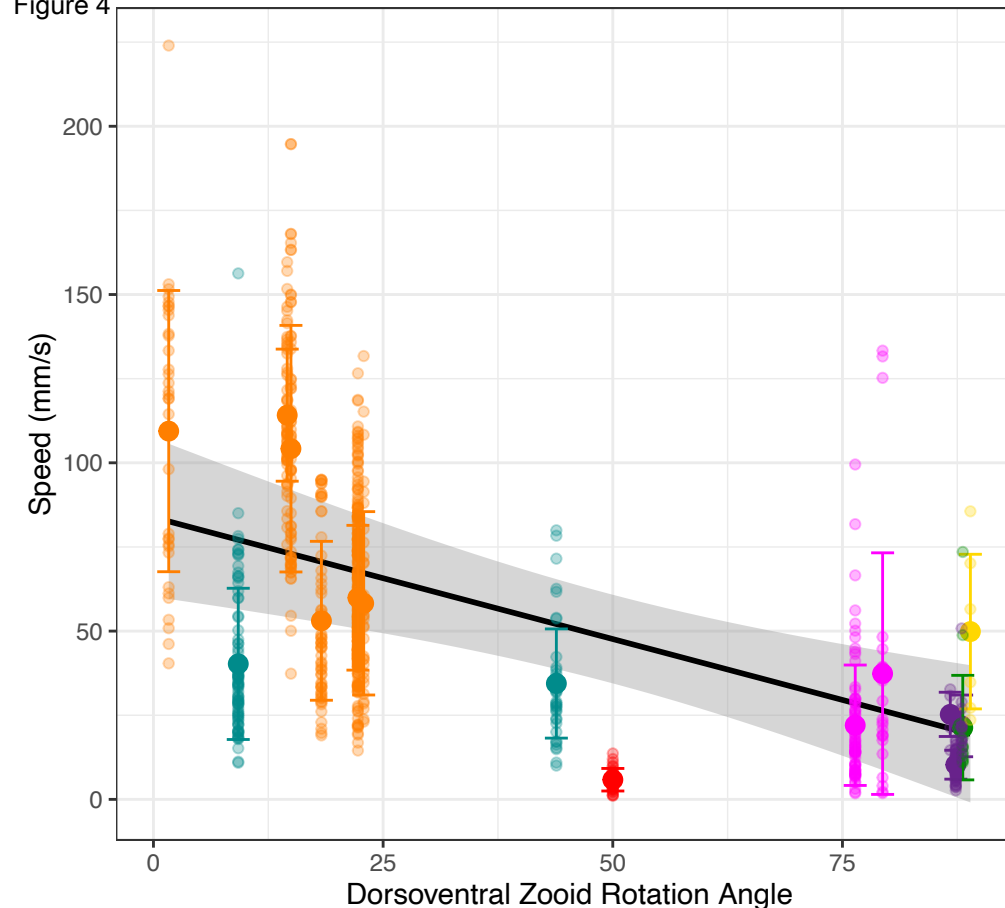


Figure 4

[Click here to access/download;Figure;F3\\_points.pdf](#)


#### Architecture

- Transversal ( $n = 18, N = 2$ )
- Oblique ( $n = 28, N = 1$ )
- Linear ( $n = 543, N = 63$ )
- Bipinnate ( $n = 128, N = 16$ )
- Helical ( $n = 7, N = 1$ )
- Whorl ( $n = 84, N = 10$ )
- Cluster ( $n = 102, N = 14$ )

Figure 5

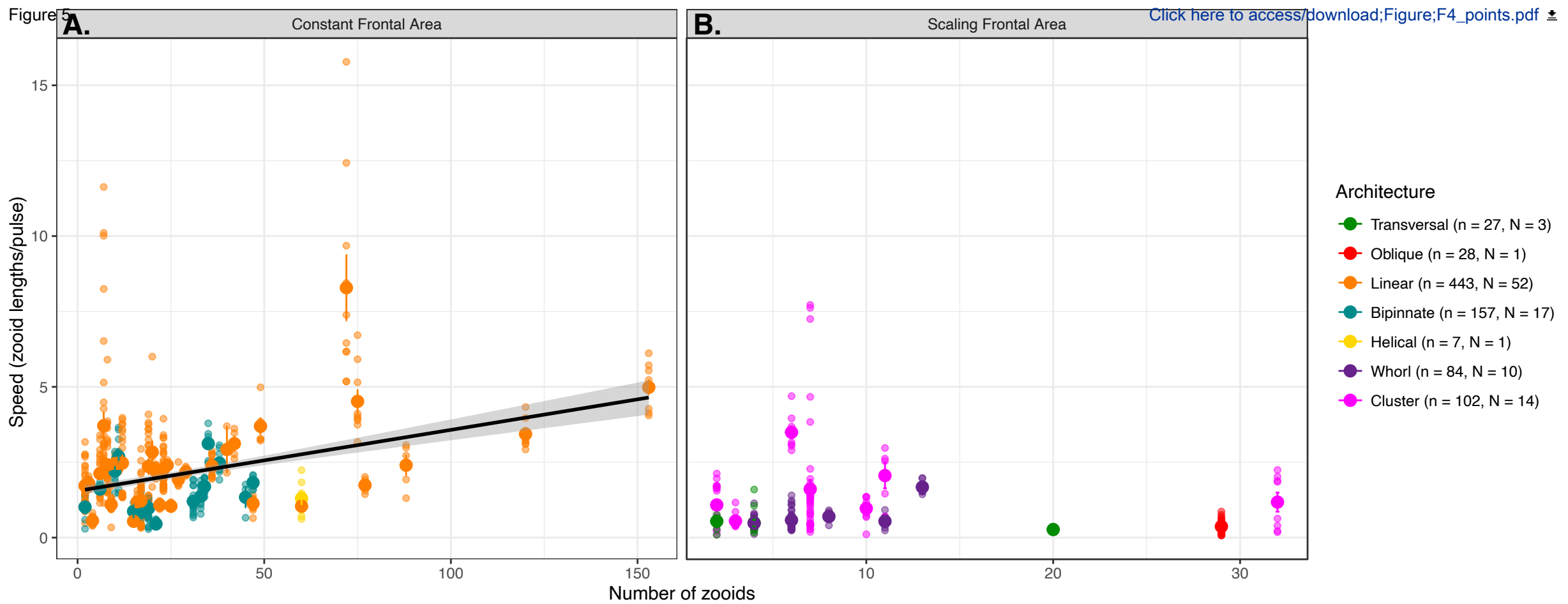
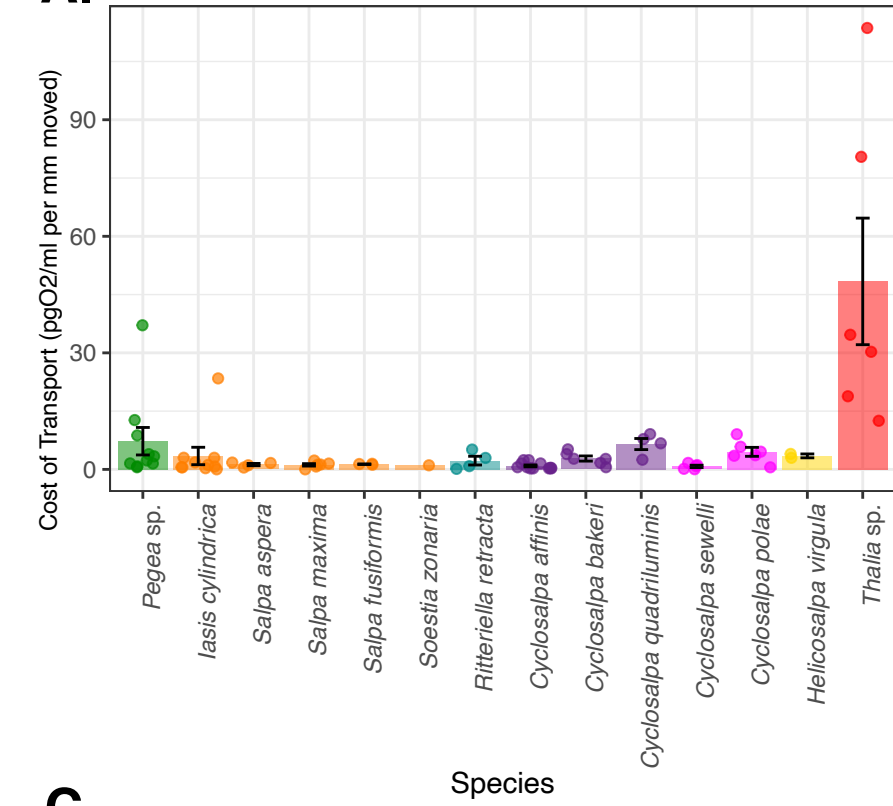
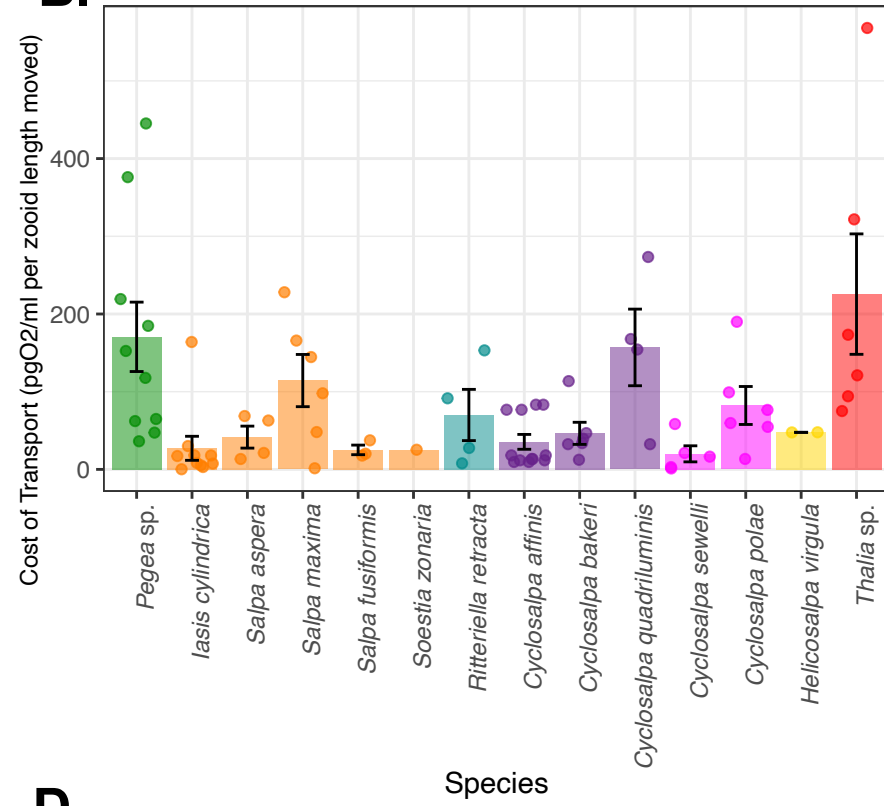


Figure 6

[Click here to access/download;Figure;F5\\_jitter.pdf](#)
**A.****B.****Architecture**

- Transversal (n = 10, N = 9)
- Oblique (n = 6, N = 4)
- Linear (n = 24, N = 22)
- Bipinnate (n = 4, N = 2)
- Helical (n = 2, N = 2)
- Whorl (n = 15, N = 2)
- Cluster (n = 11, N = 8)

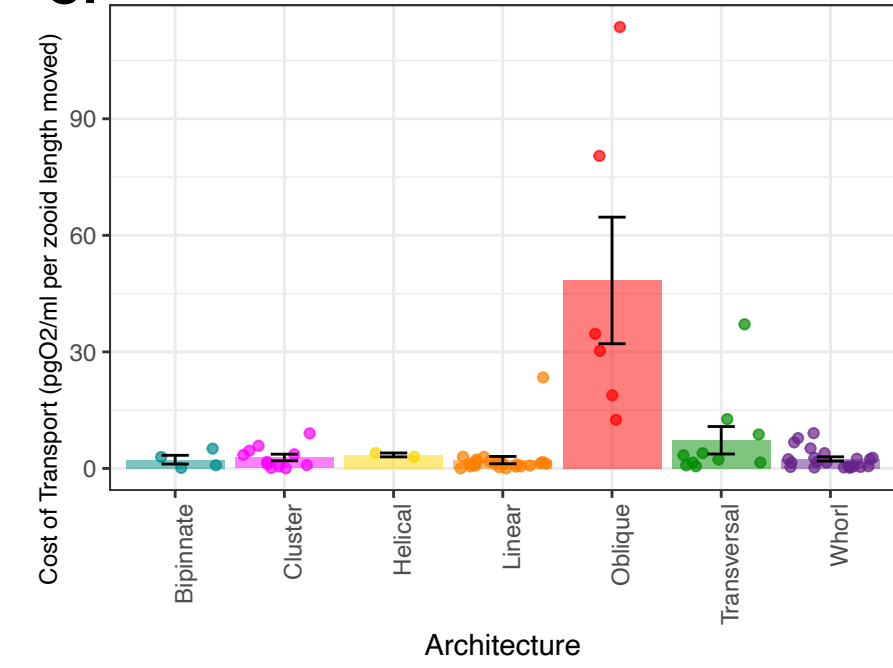
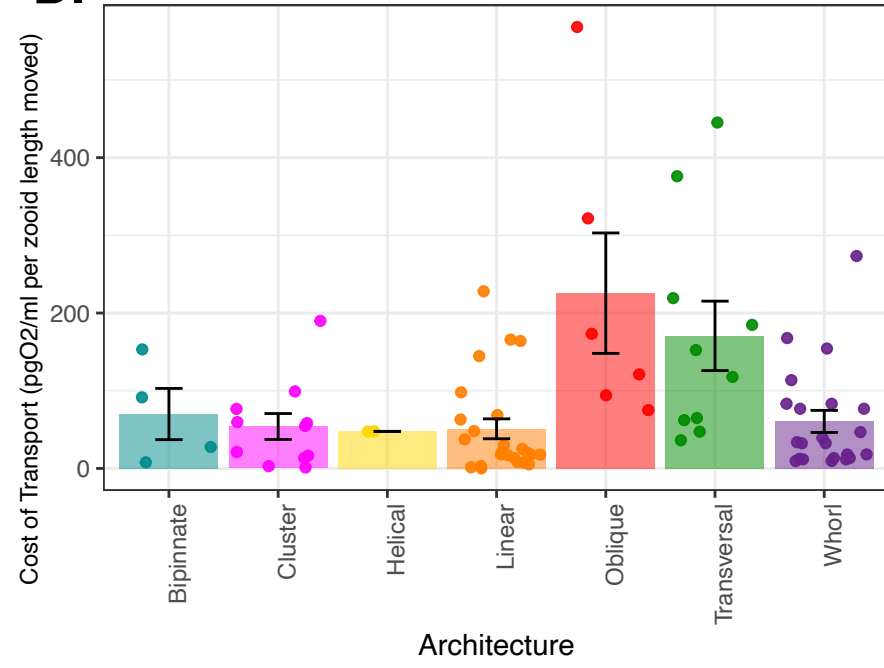
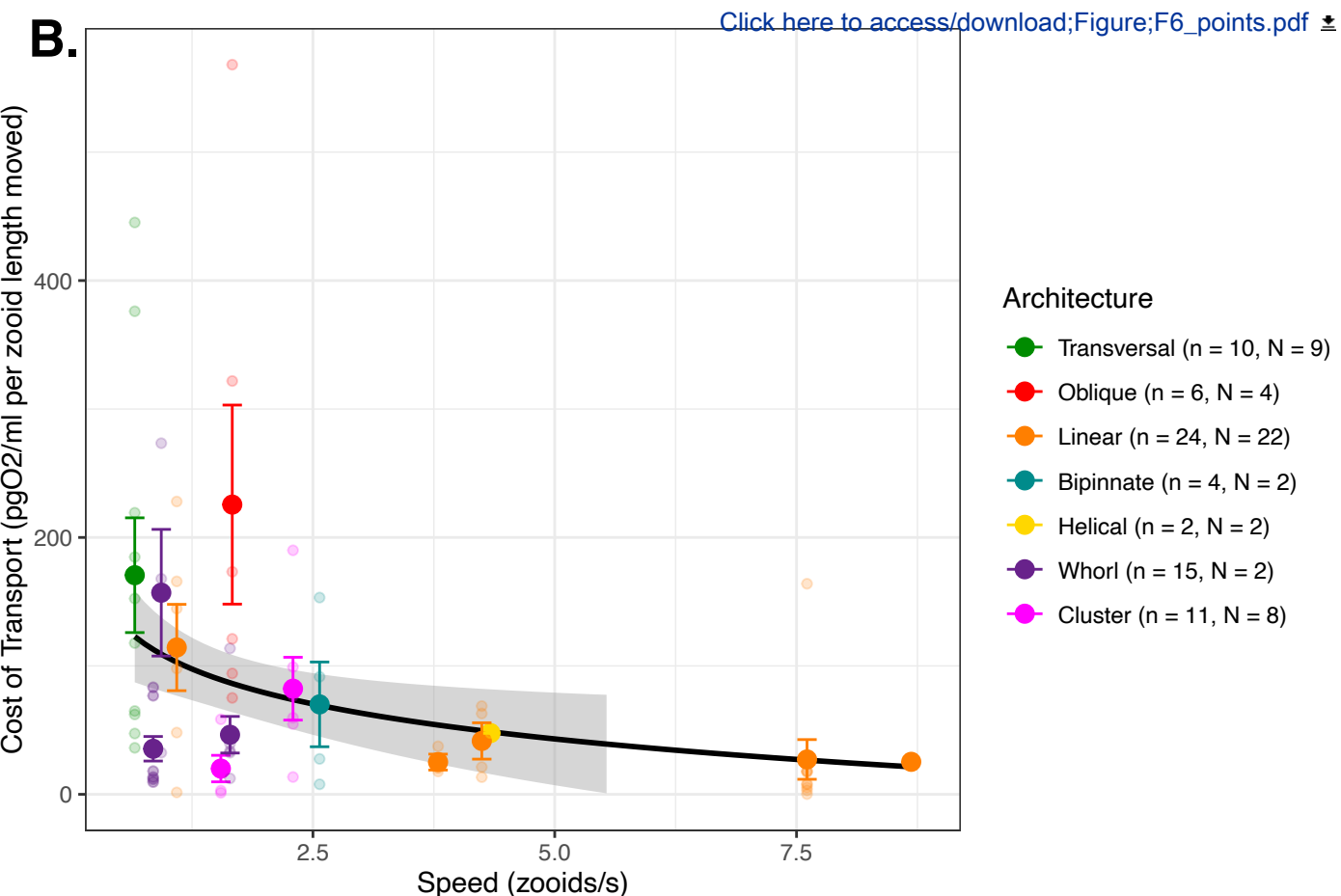
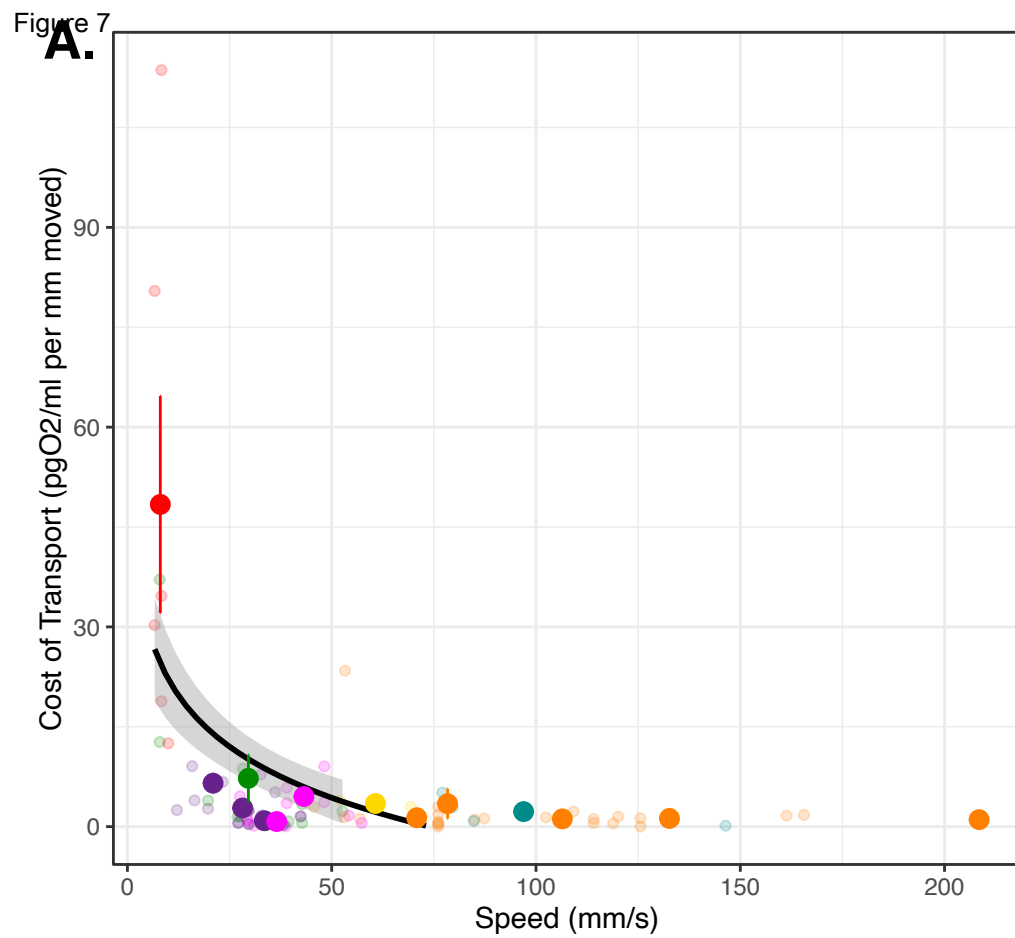
**C.****D.**

Figure 7

[Click here to access/download;Figure;F6\\_points.pdf](#)

1  
2  
3  
4   1 **Title: Colonial Architecture Modulates the Speed and**  
5   2 **Efficiency of Multi-Jet Swimming in Salp Colonies**

6   3  
7   4 **Authors:** Alejandro Damian-Serrano<sup>1</sup>, Kai A. Walton<sup>1</sup>, Anneliese Bishop-Perdue<sup>1</sup>, Sophie  
8   5 Bagoye<sup>1</sup>, Kevin T. Du Clos<sup>2</sup>, Bradford J. Gemmell<sup>3</sup>, Sean P. Colin<sup>4,5</sup>, John H. Costello<sup>6</sup>, Kelly R.  
9   6 Sutherland<sup>1</sup>

10   7  
11   8 **Author Affiliations:**

12   9  
13   10 (1) Institute of Ecology and Evolution, Department of Biology, University of Oregon. 473 Onyx  
14   11 Bridge, 5289 University of Oregon, Eugene, OR 97403-5289, USA.

15   12 (2) Louisiana Universities Marine Consortium, 8124 Highway 56, Chauvin, LA 70344, USA.

16   13 (3) Department of Integrative Biology, University of South Florida, 4202 East Fowler Avenue,  
17   14 Tampa, FL 33620, USA.

18   15 (4) Marine Biology and Environmental Science, Roger Williams University, Bristol, RI 02809, USA.

19   16 (5) Whitman Center, Marine Biological Laboratory, Woods Hole, MA 02543, USA.

20   17 (6) Biology Department, Providence College, Providence, RI 02918, USA.

21   19 **Running title:** Architecture Modulates Salp Swimming

22   20  
23   21 **Summary Statement (30 words)**

24   22 Linear arrangements in multi-jet propelled marine colonial invertebrates are faster than less  
25   23 streamlined architectures without incurring in higher costs of transport, offering insights for  
26   24 bioinspired underwater vehicle design.

1  
2  
3  
4   34 **Abstract**  
5   35

6   36 Salps are marine pelagic tunicates with a complex life cycle including a solitary and colonial stage.  
7   37 Salp colonies are composed of asexually budded individuals that coordinate their swimming by  
8   38 multi-jet propulsion. Colonies develop into species-specific architectures with distinct zooid  
9   39 orientations. These distinct colonial architectures vary in how frontal area scales with the number  
10   40 of zooids in the colony. Here, we address how differences in frontal area drive differences in  
11   41 swimming speed and the relationship between swimming speed and cost of transport in salps.  
12   42 We (1) compare swimming speed across salp species and architectures, (2) evaluate how  
13   43 swimming speed scales with the number of zooids across colony in architectures, and (3)  
14   44 compare the metabolic cost of transport across species and how it scales with swimming speed.  
15   45 To measure swimming speeds, we recorded swimming salp colonies using in situ videography  
16   46 while SCUBA diving in the open ocean. To estimate the cost of transport, we measured the  
17   47 respiration rates of swimming and anesthetized salps collected in situ using jars equipped with  
18   48 non-invasive oxygen sensors. We found that linear colonies swim faster, which supports idea that  
19   49 their differential advantage in frontal area scales with an increasing number of zooids. We also  
20   50 found that higher swimming speeds predict lower costs of transport in salps. These findings  
21   51 underscore the importance of considering propeller arrangement to optimize speed and energy  
22   52 efficiency in bioinspired underwater vehicle design, leveraging lessons learned from the diverse  
23   53 natural laboratory provided by salp diversity.

24   54  
25  
26   55 **Keywords:** salps, colonial architecture, multi-jet propulsion, swimming, cost of transport  
27  
28

29   56  
30   57 **Introduction**  
31

32   58 Salps (Tunicata: Thaliacea: Salpida) are planktonic invertebrates that have a two-phase  
33   59 life cycle comprised of a solitary oozooid that asexually buds colonies of sexually reproducing  
34   60 blastozooids. Salp colonies are composed of up to hundreds of genetically identical, physically  
35   61 and neurophysiologically integrated pulsatile zooids (Bone et al. 1980, Mackie 1986). Zooids in  
36   62 the colony feed and propel themselves by drawing water in through the oral siphon, using muscle  
37   63 contraction to compress their pharyngeal chamber, and ejecting a jet of water from their atrial  
38   64 siphon (Bone & Trueman 1983). While solitary oozooids move using single-jet propulsion, salp  
39   65 blastozooid colonies integrate multiple propelling jets, which increases their thrust and reduces  
40   66 the drag that results from periodical acceleration and deceleration via asynchronous swimming  
41   67 (Sutherland & Weihs 2017).

1  
2  
3  
4 68 Currently, there are 48 described species of salps (WoRMS, 2024) and while salps are  
5 69 widely distributed, most species are restricted to open ocean environments, far from the coast,  
6 70 which poses unique challenges to accessing them for direct study in their environment (Hamner  
7 et al 1975, Haddock 2004). Moreover, salps cannot be maintained alive in containers beyond a  
8 72 few hours since they are extremely fragile and sensitive to the presence of solid walls. Therefore,  
9 73 many morphological, ecological, and functional aspects of salp diversity, such as swimming  
10 74 speeds and metabolic demands, have remained unexplored. One such aspect is colonial  
11 75 architecture or the way that the zooids are arranged relative to each other in the colony. Salp  
12 76 colonies develop into species-specific architectures with distinct zooid orientations, including  
13 77 transversal, oblique, linear, helical, and bipinnate chains; as well as whorls, and clusters (Damian-  
14 78 Serrano & Sutherland, 2023). These architectures likely drive aspects of swimming performance  
15 79 (Madin 1990, Damian-Serrano et al. 2023).

24 80 Linear salp chains have been described as more efficient swimmers due to the reduction  
25 81 of drag associated with a more streamlined form (Bone & Trueman 1983). In a multi-jet system,  
26 82 having a larger number of propellers can improve the hydrodynamic and inertial benefits granted  
27 83 by asynchronous multijet propulsion, in addition to providing additional thrust to the colony (Madin  
28 84 1990, Sutherland & Weihs 2017). The effect of varying numbers of propeller zooids on swimming  
29 85 speed has never been investigated in salps, nor how this relationship may vary across their  
30 86 diverse colonial architectures. Salp colonial architectures differ in how the number of zooids in  
31 87 the colony scales with their frontal area relative to motion (Madin 1990). Some architectures  
32 88 (linear, bipinnate, and helical) have a constant frontal area, regardless of zooid number. These  
33 89 architectures may benefit from increased thrust delivered by larger numbers of zooids while  
34 90 maintaining a constant frontal area. However, the rest of the architectures (oblique, transversal,  
35 91 whorl, and cluster) have an increasing (directly proportional) frontal area as the number of zooids  
36 92 increases (Fig. 1). Therefore, we expect the latter architectures to not only obtain more thrust, but  
37 93 to also experience more frontal water resistance as zooid number increases. As a result, we  
38 94 anticipate that swimming speed will be greater in colonies that bear a larger number of zooids,  
39 95 but only (or more so) for species with architectures that have a constant frontal area.

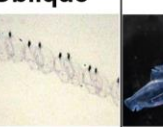
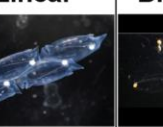
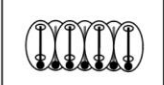
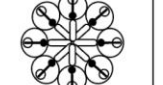
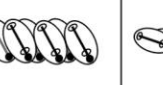
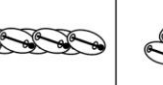
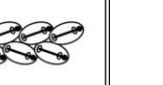
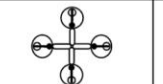
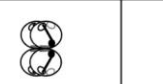
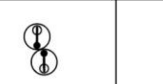
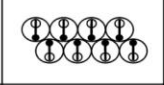
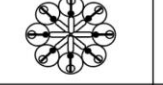
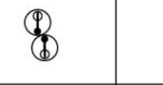
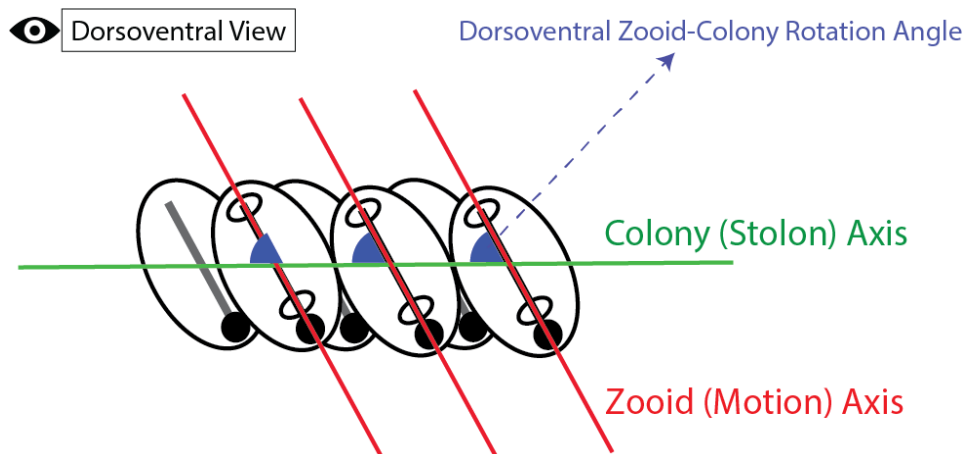
	Transversal	Whorl	Cluster	Helical	Oblique	Linear	Bipinnate
Architecture							
							
Frontal area 4 zooids							
Frontal area 8 zooids							
Scaling	2	2	2	1	$1 \times 2$	1	1

Figure 1. Salp colonial architectures with representative species photos (*Pegea* sp. for transversal, *Cyclosalpa affinis* for whorl, *Cyclosalpa sewelli* for cluster, *Helicosalpa virgula* for helical, *Thalia cicatricosa* for oblique, *Soestia zonaria* for linear, and *Ritteriella retracta* for bipinnate) and diagrams showing the distinct zooid orientations. The subsequent rows show the frontal view of colonies with four and eight zooids, with the final row indicating the expected frontal area increase factor between the four and the eight zooid colonies. Full black circles in the diagrams represent viscerae (guts) while the open circle represent siphons. Black straight lines inside the zooids indicate gill bars while gray straight lines represent endostyles.

Linearity of colonies, as well as zooid size and pulsation rates, are additional factors that could influence swimming performance. The degree of linearity in a colony can be expressed as the degree of parallelism between the zooids and the elongation axis of the colony (Fig. 2). This angle is determined by the degree of developmental dorsoventral zooid rotation, which can span from 90°, in transversal chains with no rotation, to 0° (perfect linearity), in some linear chains such as those from the species *Soestia zonaria* (Damian-Serrano & Sutherland, 2023). Strong reductions in the dorsoventral zooid rotation angle toward linear forms have evolved multiple times independently (Damian-Serrano et al. 2023), possibly due to adaptive advantages related to their swimming efficiency. Body size predicts swimming velocity in many animals (Andersen et al. 2016), however colonies with multiple swimming units may circumvent this size-speed relationship by having multiple propellers. Pulsation rates may also influence swimming speed as has been shown in solitary salps (Madin 1990). Pulsation by salps serves the dual role of locomotion and filter feeding. The relationship between pulsation and speed might therefore be particularly relevant for species that undergo diel vertical migration (Madin et al. 1996) and in other species pulsation may serve to maximize filtration rates. Considering the tradeoffs between

1  
2  
3  
4 121 swimming and filtering, the eco-evolutionary relevance of swimming speed, and the hydrodynamic  
5 efficiency likely varies between species (Damian-Serrano et al. 2023).  
6  
7 123  
8  
9 124



10  
11  
12  
13  
14  
15  
16  
17  
18  
19  
20  
21  
22  
23  
24  
25 125 Figure 2. Schematic of an oblique chain from the dorsoventral perspective showing the zooid and  
26  
27 stolon axes and the zooid rotation angle (degree of linearity) relative to those axes. Black lines  
28  
29 indicate gill bars (mostly occluded by zooid axis) while gray lines represent endostyles.  
30  
31  
32

33 129 The energetic costs of salp locomotion from mechanically estimated propulsive efficiency  
34 suggest that like other jet-propelled swimmers, salps are hydrodynamically efficient (Sutherland  
35 & Madin 2010, Gemmell et al. 2021, Trueman et al. 1984). The few metabolic measurements of  
36 swimming salps show that more active species-- in terms of swimming speed and pulsation rates--  
37 have the highest respiration rates (Cetta et al. 1986) and that salps have higher respiration rates  
38 than other gelatinous taxa (Biggs 1977, Schneider 1992, Mayzaud et al. 2005, Trueblood 2019).  
39  
40 133 However, the specific costs incurred by their swimming activity and their relationship to swimming  
41 speed have never been examined across the diversity of salp species.  
42  
43 136

44 In this study, we compare swimming speeds across 17 salp species and energetic costs  
45 of swimming across 15 species, encompassing all seven known salp colony architectures (Fig. 1,  
46 Table S1). In addition, we investigate how swimming speed varies with the number of propeller  
47 zooids and differences in frontal area scaling between colonial architectures. Finally, we compare  
48 cost of transport (COT) across salp species and assess how COT scales with swimming speed  
49 and pulsation effort.  
50  
51 143

52  
53  
54  
55 144 **Materials and Methods**  
56  
57  
58  
59  
60  
61  
62  
63  
64  
65

1  
2  
3  
4 145         *Fieldwork* – We observed salps via 48 bluewater SCUBA dives (Haddock & Heine, 2005)  
5 from a small vessel off the coast of Kailua-Kona (Hawai'i Big Island, 19°42'38.7" N 156°06'15.8"  
6 W), over 2000 m of offshore water during September 2021, April 2022, September 2022 and May  
7 147 2023. We spent a total of 42.2 hours (84.4 person hours: ADS & KRS) collecting and imaging  
8 148 salp colonies. Some dives were diurnal, where we collected most of the specimens of *Iasis*  
9 149 *cylindrica*, *Cyclosalpa affinis*, *Cyclosalpa sewelli*, and *Brooksia rostrata*. We observed and  
10 150 collected most specimens of other species during night dives (blackwater diving). We recorded in  
11 151 situ underwater videos of salp colonies swimming using a variety of cameras including primarily  
12 152 a dark field stereovideography system (Sutherland et al. 2024), as well as a lightweight dual  
13 153 GoPro stereo system, a brightfield single-camera system (Colin et al. 2022), and a darkfield  
14 154 single-camera system. The primary stereovideography system was comprised of two  
15 155 synchronized high-resolution cameras (Z Cam E2, Nan Shan, Shenzhen, China and Sync Cable;  
16 156 4K at 60 or 120 fps) with 17mm f/1.8 lenses (Olympus M.Zuiko Digital) housed in custom  
17 157 aluminum housings (Sexton Company, Salem, OR, USA). Each field of view was 23 x 42 mm and  
18 158 in-focus depth was 20-25 mm. The image from the right-hand camera was viewed using an  
19 159 external monitor (Aquatica Digital, Montreal, Quebec, Canada), and illumination was provided  
20 160 with two 10,000-lumen lights (Keldan, Bruegg, Switzerland). An L-shaped plastic framer helped  
21 161 the videographer position colonies in the field of view of both cameras. Before diving, the stereo  
22 162 system was calibrated in a swimming pool using a cube with reflective landmarks. Calibration  
23 163 images were processed using the CAL software package (SeaGIS measurement science,  
24 164 Bacchus Marsh, Victoria, Australia). Over the course of the study, we observed 241 salp colonies  
25 165 (N) from 18 species and recorded 1,946 measurements (n) (Dataset1A, Table S1). Throughout  
26 166 the manuscript, we refer to the number of specimens as N and the number of measurements as  
27 167 n.  
28 168

44 169         *Measuring salp colony swimming speed* – For most species, we collected and analyzed  
45 170 footage from multiple specimens (Dataset1A, Table S1). We analyzed the swimming behavior of  
46 171 salp colonies arranged in linear (six species, 64 specimens), bipinnate (three species, 17  
47 172 specimens), whorl (three species, 10 specimens), cluster (two species, eight specimens), and  
48 173 transversal (one species, two specimens) architectures, with oblique and helical architectures  
49 174 represented by a single specimen. We used a combination of spatially calibrated stereo video  
50 175 and 2D videos with a reference scale in the frame. From the stereo videos, we manually selected  
51 176 and measured the relative XYZ positions of salp colony zooids in EventMeasure (SeaGIS). We  
52 177 implemented a cutoff in the RMS (root mean squared) point error estimate of < 2 mm.  
53  
54  
55  
56  
57  
58  
59  
60  
61  
62  
63  
64  
65

1  
2  
3  
4 178 We complemented gaps in taxon sampling with archived 2D videos in the lab from  
5 previous expeditions to West Palm Beach (FL, USA) and the Pacific coast of Panama. These two-  
6 dimensional single-camera videos were collected using a Sony FDR-AX700 4K Camcorder  
7 (3840x2160 pixels, 60-120 fps) with a Gates Underwater Housing (Poway, CA, USA) using  
8 brightfield illumination (Colin et al 2022) or darkfield illumination. For these 2D videos, we used  
9 the FFmpeg plugin in ImageJ to manually select and measure the relative XY positions of salp  
10 zooids in sequences where the colony was swimming horizontally within the focal plane. The  
11 colonies were assumed to be in the same plane as the scale bar so at same distance from the  
12 camera. However, in videos with a broad focal depth, this may not always had been the case,  
13 thus potentially introducing some measurement error.  
14

15 188 We tracked and manually selected the position of the first zooid's viscera (using a contrast-  
16 based centering macro to mark the center point) as well as the position of a reference particle in  
17 the water (methods described in Sutherland et al. 2024) in 10-30 frames across 50-500 frame  
18 windows spanning 2-4s of swimming on the synchronized left and right videos in EventMeasure.  
19 The reference particle was a non-swimming organism (such as a foraminiferan or radiolarian) or  
20 a non-living particle. In addition, we recorded the pulsation rates of the specimens measured by  
21 counting the number of times the atrial siphon contracted in a known period. For each analyzed  
22 frame, we calculated the horizontal x, vertical y, and depth z (in the case of the stereo video  
23 measurement files) components of the relative positions of the frontal zooid to the reference  
24 particle as shown in Eq. 1.  
25

26 198  
27 199  $x_n = x_{n\ animal} - x_{n\ particle}$   
28 200  $y_n = y_{n\ animal} - y_{n\ particle}$  Eq. 1  
29 201  $z_n = z_{n\ animal} - z_{n\ particle}$   
30

31 203 Then we calculated the instantaneous relative speeds of the frontal zooid using Eq. 2  
32 (without the z component in the case of the 2D videos) given the known frame rate of each video.  
33

34 205  
35 206  $U = \frac{\sqrt{(x_2-x_1)^2 + (y_2-y_1)^2 + (z_2-z_1)^2}}{t_2-t_1}$  Eq. 2  
36

37 208 *Salp colonial architecture* – To examine the relationships between locomotory variables  
38 209 and colonial architecture, we adopted the species-specific architecture characterizations and  
39 210 dorsoventral zooid rotation angle measurements for each species from Damian-Serrano et al.  
40

1  
2  
3  
4 211 (2023). Using stills from the underwater videos, we measured zooid length, zooid width, and  
5 number of zooids in ImageJ manually selecting the point coordinates. These measurements were  
6 repeated in at least three locations from each colony. When a distinct zooid size gradient was  
7 observed, we measured zooids in locations from the proximal, middle, and distal regions to  
8 capture the full range of variation in the specimen.  
9  
10

11 215  
12 216        *Respiration measurements* – We collected healthy, adult blastozooid (aggregate stage)  
13 colonies across 18 salp species (Dataset S1B) during blue- and black-water SCUBA dives off the  
14 coast of Kona (Hawaii, USA) between September 2021 and May 2023. We analyzed the  
15 respiration rates of salp colonies arranged in linear (seven species, N = 46), bipinnate (three  
16 species, N = 29), whorl (three species, N = 23), cluster (two species, N = 18), and transversal  
17 (one species, N = 13) architectures, oblique chains (*Thalia* sp., N = 7), and helical architectures  
18 represented by *Helicosalpa virgula* (N = 2). Specimens were sealed *in situ* with their surrounding  
19 water in plastic jars equipped with a PreSens oxygen sensor spot (Regensburg, Germany) and a  
20 self-healing rubber port to allow for the injection of solutions without the introduction of air bubbles.  
21  
22 We removed as many symbiotic animals from the salps as possible before closing the lid without  
23 damaging the colony. The same method was applied to one or more seawater controls to account  
24 for the oxygen demand of the local seawater's microbiome. Several collection events occurred  
25 during each 20-60 min long SCUBA dive. Jars with larger animals were opened during the safety  
26 stop to allow them to re-oxygenate. Upon the divers' return to the boat, we measured the initial  
27 oxygen concentration (mg/l) and temperature, and then repeated the measurements at intervals  
28 between 15min and 3h, for total periods ranging between 2h and 5h, depending on logistic  
29 constraints in the field and the rate of oxygen depletion. The exact interval time for each  
30 measurement was variable but recorded (Dataset S1B).  
31  
32

33 233  
34 234        To estimate the energetic expenditure of different salp species while actively swimming,  
35 we recorded the oxygen consumption of intact specimens while swimming inside the jar. To obtain  
36 a baseline of basal respiration rate (while not swimming), we anesthetized some specimens  
37 before the start of the first oxygen measurement time. A few specimens were used for paired  
38 experiments, where their swimming respiration was recorded for a few hours, then inoculated with  
39 the anesthetic, and recorded anesthetized for another set of hours. To anesthetize salps, we  
40 injected their jars with small volumes of concentrated (50 g/l) bicarbonate-buffered MS-222  
41 through the rubber ports on the lids. We tailored the injection volume to the jar size aiming for a  
42 final concentration of 0.2g/l, following the methods in Trueman et al. (1984). We also injected  
43 some seawater control jars to evaluate the effect of MS-222 on oxygen concentration in seawater  
44 and found no effect.  
45  
46  
47  
48  
49  
50  
51  
52  
53  
54  
55  
56  
57  
58  
59  
60  
61  
62  
63  
64  
65

1  
2  
3  
4 245 When multiple seawater controls were collected using jars of different sizes, we paired  
5 each jar with the control that had the most similar volume. If among multiple controls only some  
6 were jars injected with anesthetic, we paired the anesthetized specimen jars with the injected  
7 controls and the intact specimen jars with the intact controls. In experiment 26 (see Dataset S1B  
8 for experiment numbers), the control jar was lost due to an encounter with an oceanic white tip  
9 shark, thus we paired those measurements with the nearest relative time points from the control  
10 jar in experiment 25, collected the same day hours earlier. At the end of each experiment, we  
11 identified the salp specimens used in the experiments to the species level, counted the number  
12 of zooids, measured the zooid length (total length including projections), and measured the  
13 biovolume of the colony using a graduated cylinder. For those specimens where colony or zooid  
14 volume was not measured directly, we estimated the colony volume from their zooid length and  
15 the number of zooids using a Generalized Additive Model with the measured specimens.  
16 256

17 257 We estimated the oxygen consumption rate for each specimen by fitting a linear  
18 regression of consumed oxygen mass (concentration by container volume) against the duration  
19 of the measurement series. We subtracted the slope calculated for the relevant control jar to the  
20 estimated slope of the animal jar. Since our seawater controls were not filtered, some experiments  
21 had abnormally high estimated background respiration rates, leading to negative values. We  
22 removed these data points before the analysis. To estimate biovolume-specific rates, we divided  
23 the rates by the colony volumes. We then compared the biovolume-specific respiration rates of  
24 active (swimming) and anesthetized specimens within each species, calculating the difference as  
25 a measure of biovolume-specific swimming cost respiration rate. Biovolume was used instead of  
26 dry mass to normalize measurements due to the inherent difficulties of accurately measuring dry  
27 mass of these fragile gelatinous organisms in the field. Biovolume provides a consistent and  
28 reliable measure of the live size of the colony, which is directly relevant to the volume of water  
29 being displaced during swimming. We also calculated the relative investment in swimming as the  
30 proportion of biovolume-specific respiration rate comprised by the swimming-specific rate. To  
31 capture variability within species, we calculated the mean respiration rate of anesthetized  
32 specimens for each species and subtracted it from each intact specimen's total respiration rate to  
33 get multiple swimming-specific rate values within each species. We noticed that some species  
34 had higher average respiration rates among the anesthetized specimens than among the  
35 swimming specimens, leading to negative swimming-specific respiration estimates. We  
36 interpreted this anomaly as a systematic error due to the extremely low respiration rates of some  
37 species that fall within the effective detection limit of our experimental setup given the random  
38 variation range of respiration rates in seawater both in experimental jars and in control jars. Small  
39 278

40  
41  
42  
43  
44  
45  
46  
47  
48  
49  
50  
51  
52  
53  
54  
55  
56  
57  
58  
59  
60  
61  
62  
63  
64  
65

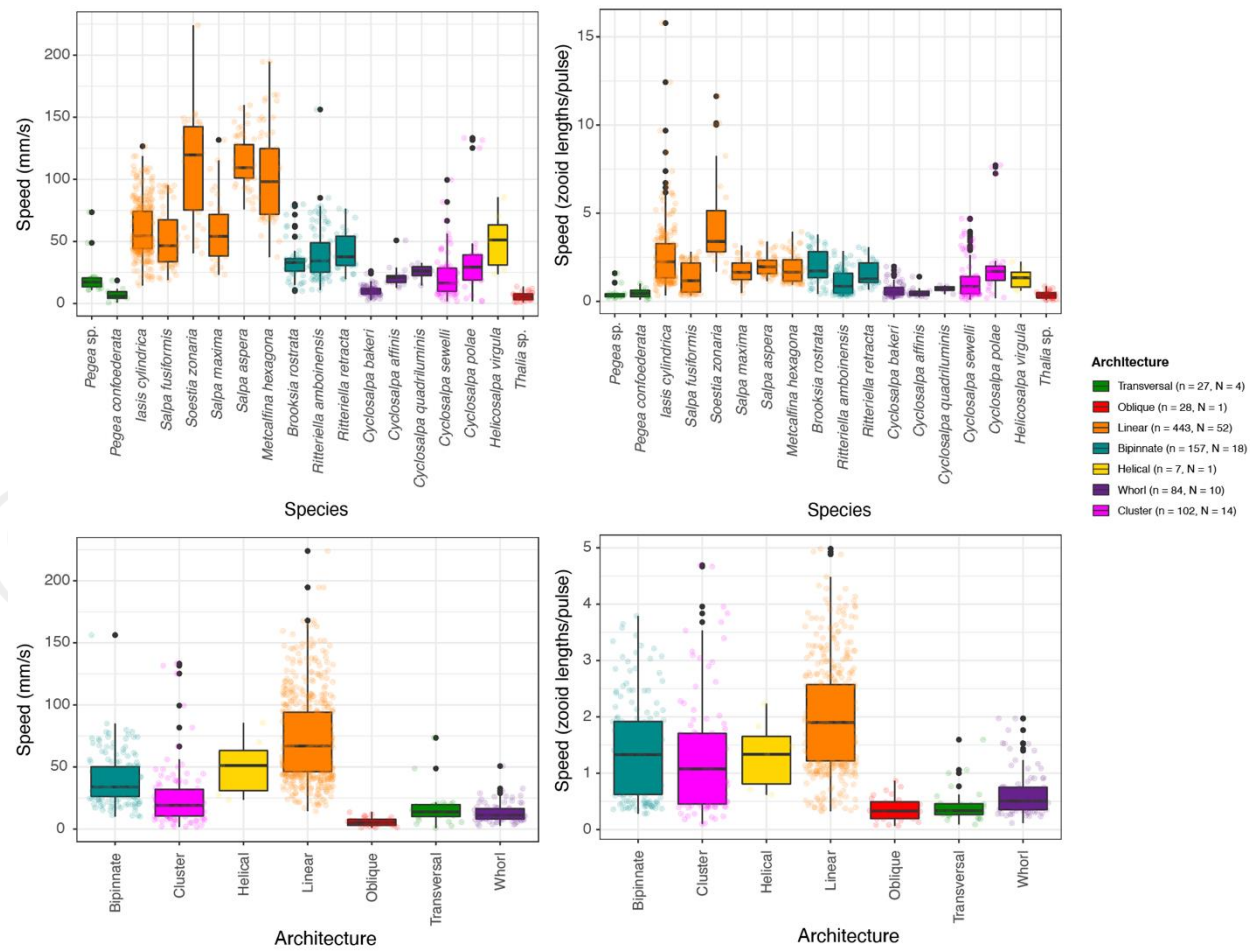
absolute negative values get amplified into large relative values, especially in small animals with a minuscule biovolume denominator. Therefore, we removed the swimming specimens that had lower respiration rates than the mean anesthetized respiration rate for their species. We also removed two respirometry outliers of *Thalia* sp. which had extremely high swimming respiration rates (>7500 pgO<sub>2</sub>/ml/min, whereas all other measurements across species including other *Thalia* sp. were limited to 0-1700 pgO<sub>2</sub>/ml/min), which were likely due to amplification of experimental error (presence of organic matter or symbionts, underestimation of colony volume due to loss of tiny zooids in the sieves) with the small biovolume denominators in this species.

*Estimating costs of transport* – We define the cost of transport (COT) as the amount of oxygen consumed per tissue volume per distance traveled by the colony. To estimate the COT, we divided the swimming-specific respiration rates by the mean swimming speed for each species measured from the stereo and 2D video data. Since the specimens used for speed measurements in the videos and those used in the respirometry experiments had different zooid sizes, we used the mean zooid-lengths per second speeds from the video measurements and then multiplied them by the actual zooid lengths of the respirometry specimens to estimate their absolute (mm/s) speeds. Pulsation rate estimates were taken from species averages from the video specimens. We also calculated the size-specific COT by transforming the swimming distances into zooid lengths measured from the respirometry specimens.

*Statistical Analyses* – All data wrangling and statistics were carried out in R 3.6.3 (R Core Team 2021). To test for differences between architectures, we used ANOVAs with Tukey's post-hoc pairwise contrasts, reporting the difference magnitude and the adjusted p-value in supplementary tables S2A and S2B. To test the relationships between pairs of continuous variables across architectures (e.g. swimming speed vs. number of zooids), we used linear regressions. We evaluated the significance of the slope parameter when compared against a flat slope (one-tailed t-test) to test whether changes in the independent variable (e.g. number of zooids) were associated with changes in the dependent variable (e.g. swimming speed). Owing to the patchiness of some species despite 80+ hours spent underwater (Table S1), we used replicate measurements (n) from each specimen (N) in swimming speed ANOVAs and regressions. We used an exponential regression to test the relationship between speed and COT. Specimen means (N) were used for all COT comparisons and regressions. Individual measurements (n) were used up to determine oxygen consumption rates. To evaluate the relative contribution of zooid size, pulsation rate, zooid number, and architecture type on swimming speed, we fitted a generalized linear model and evaluated the significance and proportion of variance explained by each factor using their partial R<sup>2</sup>.

1  
2  
3  
4 313  
5  
6 **Results**

7  
8  
9  
10  
11  
12  
13  
14  
15  
16  
17  
18  
19  
20 314  
Salp colony swimming speeds, pulsation rates, and respiration rates varied within and across species and colony architectures. When considering speed in terms of mm/s, we found a relationship between pulsation rate (effort) and absolute speed ( $n = 947$ ,  $N = 111$ , 18 species, Speed mm/s =  $0.41 \times$  Pulsation rate + 52.14,  $p < 0.0001$ , Fig. S1A), as well as with zoid-size corrected swimming speed ( $n = 848$ ,  $N = 100$ , 18 species, Speed zoid lengths/s =  $0.96 \times$  Pulsation rate + 1.73, adjusted  $R^2 = 0.18$ ,  $p < 0.0001$ , Fig. S1B). Normalized swimming speeds (zoid lengths per pulse) allow for a more direct comparison of swimming speed across colonial architectures.



51  
52 323  
53  
54 324 Figure 3. Boxplots showing the absolute (A) and corrected for body size and pulsation rate (B)  
55  
56  
57 325 swimming speeds recorded for each salp species and architecture (C, D) respectively. Colors  
correspond to colonial architecture types. Sample sizes are included in the legend and Tukey's  
58  
59  
60  
61  
62  
63  
64  
65

1  
2  
3  
4 327 post-hoc pairwise comparisons across architecture types are listed in Dataset 1A and Table S2A,  
5  
6 328 respectively.  
7  
8 329

9 330 *Swimming speeds across salp architectures*  
10

11 331 Swimming speed varied significantly (5 architectures, 16 species, N = 109, n = 913,  
12  
13 332 ANOVA F > 38, p < 0.001) between colonial architecture types (Fig. 3C, D, Table S2A). Speeds  
14  
15 333 measured with 2D methods were slightly slower than those measured with 3D methods within the  
16  
17 334 species in which they overlapped. This is to be expected since 2D methods cannot account for  
18  
19 335 the z (depth) component of the speed vector. Measurements of helical and oblique chains were  
20  
21 336 limited to a single specimen, so they were excluded from the analysis. In terms of absolute speed  
22  
23 337 (mm/s), linear architectures were significantly faster than every other architecture (Tukey's p <  
24  
25 338 0.001). While bipinnate chains were significantly slower than linear chains, they were significantly  
26  
27 339 faster than transversal chains, clusters, and whorls (Tukey's p < 0.002). Clusters were not  
28  
29 340 significantly faster than transversal chains nor whorls. Transversal chains were on par to whorls,  
30  
31 341 with no significant differences between them.

32  
33 342 In terms of relative speed (zooid lengths/pulse), linear architectures were significantly  
34  
35 343 faster than every other architecture (Tukey's p < 0.001). Bipinnate chains were significantly faster  
36  
37 344 than whorls and transversal chains (Tukey's p < 0.01), but not significantly different from clusters.  
38  
39 345 Clusters were significantly faster than whorls (Tukey's p < 0.001) in relative speed. Whorls and  
40  
41 346 transversal chains presented similar relative swimming speeds with no significant differences.  
42

43  
44 347 Since linear architectures had the fastest mean swimming speeds (Fig. 3C, D), we  
45  
46 348 investigated the relationship between swimming speeds with the dorsoventral zooid rotation  
47  
48 349 angle, which represents the degree of linearity of the colony (Fig. 4). Species with more parallel  
49  
50  
51  
52  
53  
54  
55  
56  
57  
58  
59  
60  
61  
62  
63  
64  
65 (lower angles) dorsoventral zooid rotation presented faster absolute speeds (n = 910, N = 107,  
16 species, Speed mm/s = -0.78\*DV Zooid angle + 81.25, adjusted R<sup>2</sup> = 0.33, p < 0.0001) and  
faster size-and-effort corrected swimming speeds (n = 810, N = 96, 16 species, Speed  
zooids/pulse = -0.016\*DV Zooid angle + 2.37, adjusted R<sup>2</sup> = 0.09, p < 0.0001).

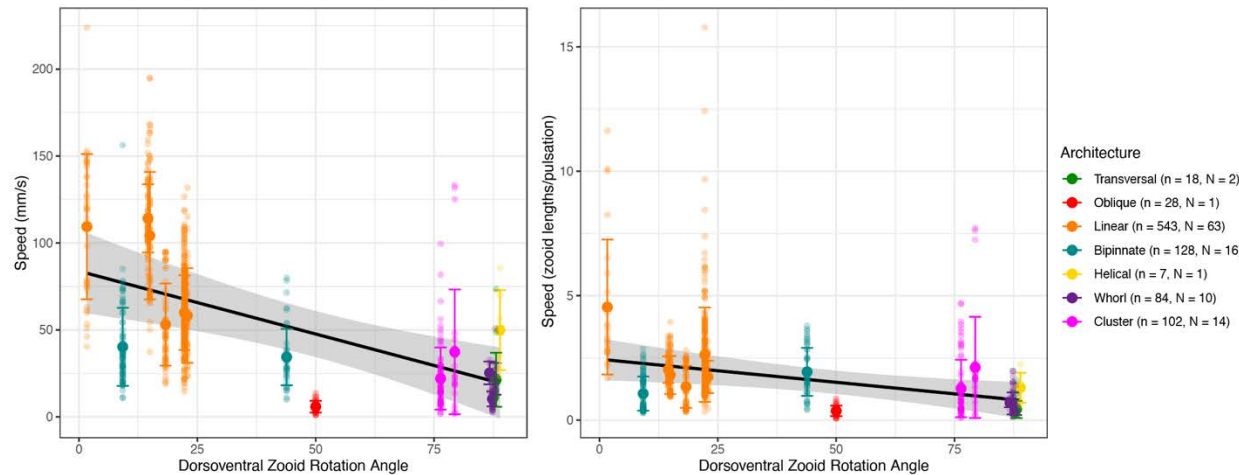
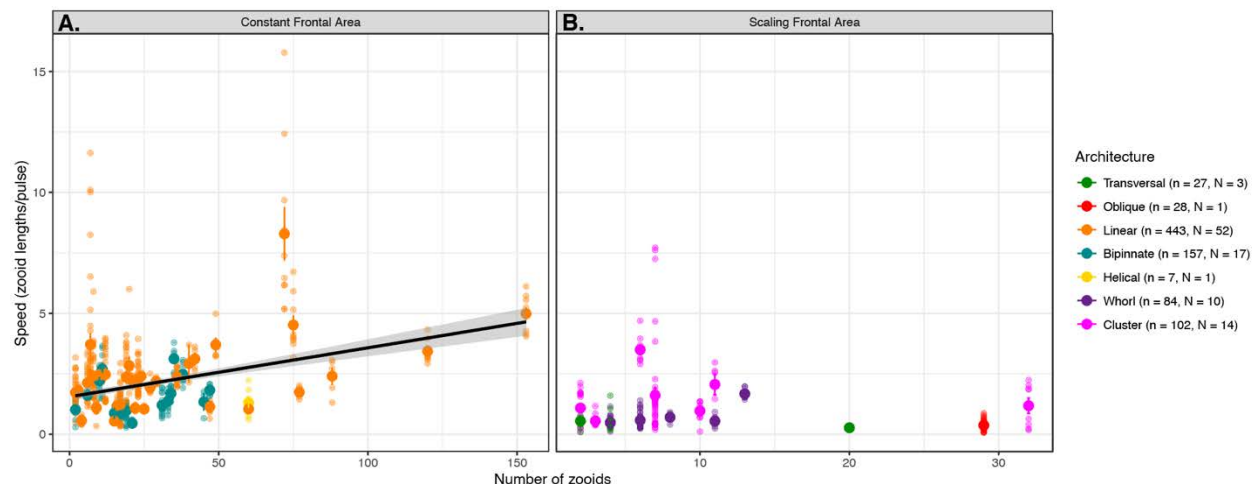


Figure 4. Absolute (A) and relative (B) colony swimming speed (specimen mean with standard errors, total n=103) for each salp species across their degree of dorsoventral zooid rotation. Error bars indicate standard error. The color indicates colonial architecture. Gray areas indicate the 95% confidence interval of the linear regression (black line).

We compared how swimming speeds scale with the number of zooids in the colony and found differences between colonial architectures. Swimming speed in whorls increased with number of zooids ( $n = 84$ ,  $N = 10$ , 3 species, Speed mm/s =  $0.08 \times \text{Number of zooids} + 0.12$ , adjusted  $R^2 = 0.3$ ,  $p < 0.0001$ ), though the data for this architecture was limited to small numbers of zooids (4 to 13) and relatively slow speeds (under 51 mm/s). Linear chain architectures did increase in relative speed with the number of zooids ( $n = 443$ ,  $N = 52$ , 6 species, Speed mm/s =  $0.02 \times \text{Number of zooids} + 1.77$ , adjusted  $R^2 = 0.14$ ,  $p < 0.001$ ), as did bipinnate chains ( $n = 157$ ,  $N = 18$ , 3 species, Speed mm/s =  $0.015 \times \text{Number of zooids} + 1.05$ , adjusted  $R^2 = 0.04$ ,  $p < 0.02$ ). This relationship was not significant for any of the other architectures.

We pooled the data from multiple architectures into scaling modes to evaluate the overall relationship in colonies with a constant frontal area (linear, bipinnate, and helical species) and in colonies with scaling frontal area (transversal, whorl, cluster, and oblique species) with linear regressions (Fig. 1). This aggregation allowed the inclusion of data from architectures for which we only have one specimen (helical and oblique). When pooled by scaling mode (Fig. 5), the regression on colonies with a constant frontal area had a higher intercept on the swimming speed axis than in those with a scaling frontal area (1.54 and 1.09 zoid lengths/pulse, respectively), reflecting the generally higher swimming speed of the former. Moreover, the regression on colonies with constant frontal area had a significant positive slope ( $n = 607$ ,  $N = 71$ , 10 species, Speed mm/s =  $0.02 \times \text{Number of zooids} + 1.55$ , adjusted  $R^2 = 0.12$ ,  $p < 0.001$ ), while the regression



382  
 383 Figure 5. Linear relationships between relative swimming speed (zoid lengths per pulsation,  
 384 specimen mean with standard errors) and number of zooids in the colony for constant (A) and  
 385 scaling ( $N=71$ ) (B) frontal motion-orthogonal frontal area ( $N=29$ ) scaling modes. Gray areas  
 386 represent the 95% confidence intervals of the regressions.  
 387

388 Putting together all the different organismal factors that we analyzed in this study, we  
 389 calculated a generalized linear regression model to predict absolute salp swimming speed ( $U$ )  
 390 from zooid length ( $L$ ), pulsation rate ( $P$ ), number of zooids ( $Z$ ), and colonial architecture  
 391 represented as frontal area scaling mode ( $A$ ) as expressed in Eq. 3. While our results suggest  
 392 that the effect of  $Z$  depends on  $A$ , we favored this simpler regression formula because it had a  
 393 significantly lower ( $\Delta > 70$ ) AIC score than those with interaction terms between  $Z$  and  $A$ .

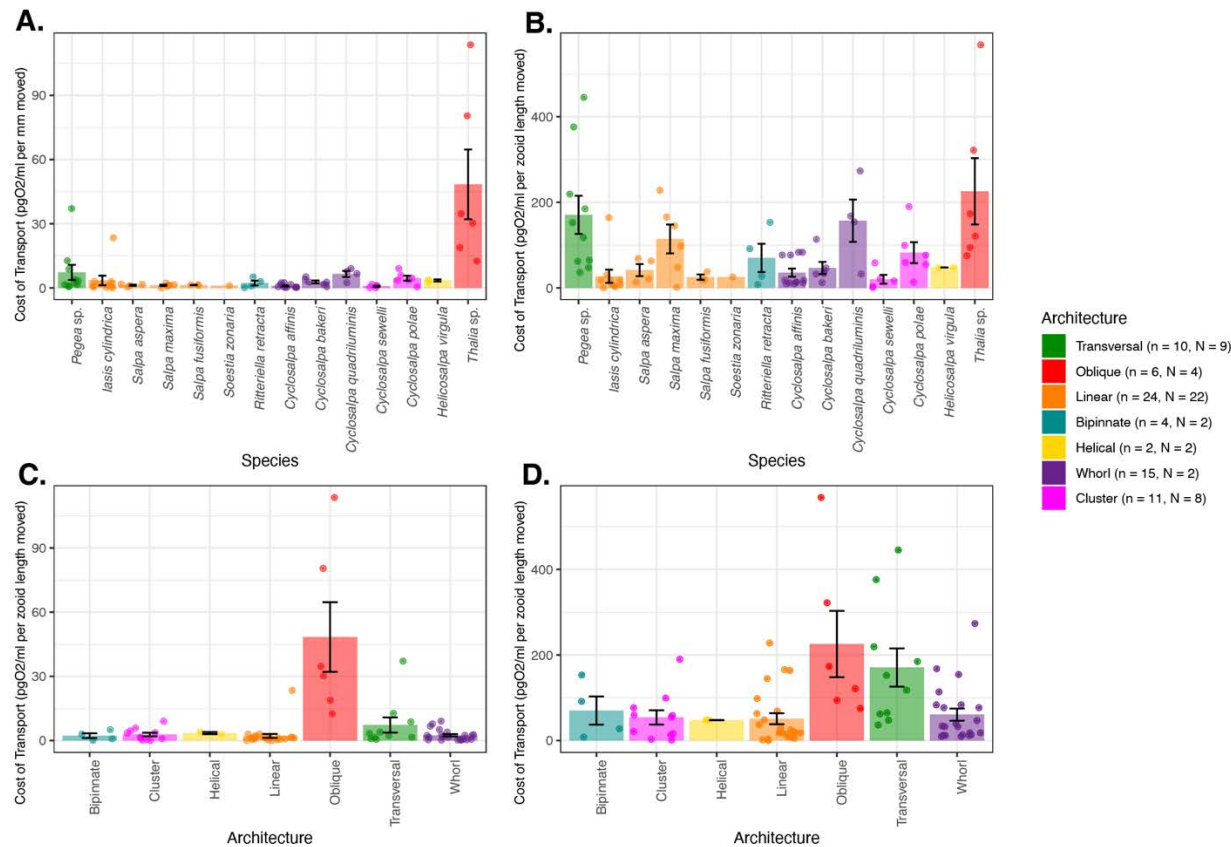
44 394       $U \sim L + P + Z + A$       Eq. 3  
 45

46 395      In this global model, we found significant effects on swimming speed (848 measurements,  
 47 396 100 videos, 18 species,  $U = 0.29L - 0.60P - 0.2Z - 50.34A$ ,  $\text{pseudo-}R^2 = 0.37$ ,  $p < 0.001$ ) for  $L$ ,  
 48 397  $Z$ , and  $A$ . We found that our global regression explains 36.8% of the variance in our swimming  
 49 398 speed data: 5.8% is explained by zooid size, 3.5% by pulsation rate, 0.8% from zooid number,  
 50 399 and 26.6% by the frontal scaling mode.  
 51  
 52  
 53

54 400  
 55  
 56 401 *Respiration rates and cost of transport (COT)*  
 57

58 402      The respiration rates of swimming and anesthetized salps revealed broad differences  
 59 403 between species (Fig. 6, S2A). After estimating COT, we found a few significant differences  
 60  
 61  
 62

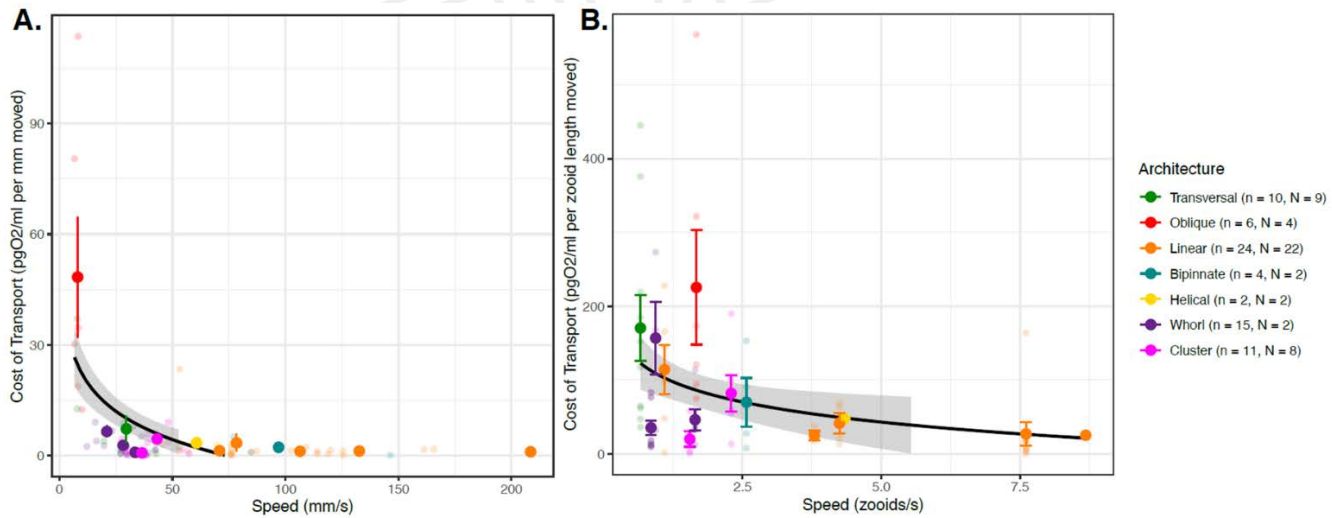
1  
 2  
 3  
 4 404 between architectures (Fig. 6, ANOVA  $F > 5.9$ ,  $p < 0.001$ , Table S2B). In terms of absolute COT  
 5 per mm traveled, all architectures except oblique chains had similar high transport efficiencies  
 6 under 13 pgO<sub>2</sub>/ml. Every one of these architectures was significantly more efficient per mm  
 7 traveled than oblique architectures (Tukey's  $p < 0.001$ ). In terms of relative COT per zooid length  
 8 traveled, linear chains, clusters, and whorls had similar transport efficiencies that are significantly  
 9 faster than transversal and oblique chains (Tukey's  $p < 0.05$ ). Some of the differences between  
 10 COT per mm and COT per zooid length are likely due to scaling with body size, as can be  
 11 observed with the relative shift in the minuscule *Thalia* sp. (5.2 mm zooids) and the massive *Salpa*  
 12 *maxima* (93.4 mm zooids).



413  
 414 Figure 6. Mean cost-of-transport per mm (A) and per zooid length (B) moved for each salp  
 415 species, and for each colonial architecture (C, D) with standard errors. Bar colors indicate colonial  
 416 architecture. Sample sizes and Tukey's post-hoc pairwise comparisons across architecture types  
 417 are listed in Dataset 1B and Table S2B, respectively.

418  
 419 When comparing the proportion of investment of metabolic costs into swimming  
 420 (compared to the species mean baseline) across salp species (Fig. S2B), eight species had  
 421 locomotion budgets under 50%, and the other seven have budgets above 50%. We then

1  
 2  
 3  
 4 422 compared the proportion of energetic investment in swimming to the COT values across species  
 5 423 (Fig. S3A,B). We found no relationship with absolute COT ( $N = 74$ , 14 species,  $p = 0.24$ ). We  
 6 424 found a positive relationship with zooid-length scaled COT ( $N = 74$ , 14 species, Swimming % =  
 7 425  $0.11 \times \text{COT per zooid length} + 34.4$ , adjusted  $R^2 = 0.22$ ,  $p < 0.001$ ), indicating that species with  
 8 426 more costly locomotion per zooid length invest a larger proportion of their energy budget in  
 9 427 swimming. Finally, we compared the proportion of energetic investment in swimming with speed  
 10 428 (Fig. S3C,D). We found no relationship (neither in mm/s nor in zooids/s), indicating that faster  
 11 429 swimmers do not invest more of their energy budget into their locomotion efforts. We found that  
 12 430 regardless of whether we consider transport in terms of absolute distances (Fig. 7A,  $N = 64$ , 14  
 13 431 species, linear regression: COT per mm =  $-0.12 \times \text{Speed mm/s} + 13.46$ , adjusted  $R^2 = 0.09$ ,  $p <$   
 14 432 0.005; exponential regression: logCOT per mm =  $-0.015 \times \text{Speed mm/s} + 1.39$ , adjusted  $R^2 = 0.14$ ,  
 15 433  $p < 0.001$ ) or relative to body lengths (Fig. 7B, 64 specimens, 14 species, linear regression COT  
 16 434 per zooid length =  $-12.9 \times \text{Speed zooid lengths/s} + 116.1$ , adjusted  $R^2 = 0.07$ ,  $p < 0.01$ , exponential  
 17 435 regression logCOT per zooid length =  $-0.24 \times \text{Speed zooid lengths/s} + 4.28$ , adjusted  $R^2 = 0.14$   $p$   
 18 436 < 0.001), the COT decreases in species with faster swimming speeds.  
 19 437  
 20 438  
 21 439  
 22 440  
 23 441  
 24 442  
 25 443  
 26 444  
 27 445



440 Figure 7. COT (specimen mean with standard error,  $n=75$ ) per mm (A) and zooid length (B) moved  
 441 across the specimen mean absolute (A) or relative (B) swimming speeds. The dot color indicates  
 442 colonial architecture. Gray areas represent the 95% confidence intervals of the exponential  
 443 regressions (black lines).

## Discussion

1  
2  
3  
4 446 We compared the swimming speeds and costs of transport of salp colonies across the  
5 most comprehensive representation of salp species diversity. Our results show a wide range of  
6 colonial swimming speeds across salp species and architectures with linear species swimming  
7 fastest (Fig. 3). Moreover, this study shows for the first time how salp colonial swimming speed  
8 scales with the number of zooids in the colony (Fig. 5), suggesting that incremental propulsive  
9 power from additional zooids does can produce higher swimming speeds for species with a  
10 constant frontal area. Across species, salps have a low COT (Fig. 6) and as speed increases,  
11 COT decreases (Fig. 7), which may be a unique advantage of multi-jet swimmers.  
12  
13 451  
14 452  
15 453  
16 454  
17 455  
18 456  
19 457  
20 458  
21 459  
22 460  
23 461  
24 462  
25 463  
26 464  
27 465  
28 466  
29 467  
30 468  
31 469  
32 470  
33 471  
34 472  
35 473  
36 474  
37 475  
38 476  
39 477  
40 478  
41 479  
42  
43  
44  
45  
46  
47  
48  
49  
50  
51  
52  
53  
54  
55  
56  
57  
58  
59  
60  
61  
62  
63  
64  
65

We compared the swimming speeds and costs of transport of salp colonies across the most comprehensive representation of salp species diversity. Our results show a wide range of colonial swimming speeds across salp species and architectures with linear species swimming fastest (Fig. 3). Moreover, this study shows for the first time how salp colonial swimming speed scales with the number of zooids in the colony (Fig. 5), suggesting that incremental propulsive power from additional zooids does can produce higher swimming speeds for species with a constant frontal area. Across species, salps have a low COT (Fig. 6) and as speed increases, COT decreases (Fig. 7), which may be a unique advantage of multi-jet swimmers.

#### *Architectural determinants of salp swimming speed*

Colonial architecture was the strongest predictor of swimming speed, though there is a large amount of unexplained variation which may relate to species-specific differences, behavioral, or environmental factors (see global GLM results). We expected that swimming speed in colonial salps would be predicted by pulsation rate as a measure of swimming effort. Our results indicate that this relationship only exists when accounting for zooid size (Fig. S1B), suggesting an underlying relationship between pulsation rate and zooid length that may be masking its predictive power over absolute speeds. This is consistent with the distribution of our data and our observations in the field where larger salps pulsate at a slower rate than smaller ones. We find a significant increase in speed with larger zooid sizes (Fig. S1C,D), consistent with previous findings of jet propelled invertebrates (Gemmell et al 2021; Bone and Trueman 1983) and more broadly across aquatic swimmers (Andersen et al. 2016).

The relationship between the number of zooids and speed in linear chains is complicated by shifts in zooid orientation during development. Salp colonies start their free-living phase when the developing buds detach from the solitary oozooid. The newly released colony has the maximum number of zooids since the zooid number only gets reduced as the colony splits or loses zooids to turbulence, disease, or predation. Therefore, colonies with higher numbers of zooids are typically composed of smaller, younger zooids. In linear architectures, these younger colonies could still be developing their dorsoventral rotation (Damian-Serrano & Sutherland 2023), thus effectively being more like oblique architecture. A less acute dorsoventral rotation angle would explain why these more numerous linear chains are not as fast as we would expect, given that our results support a significant relationship between this angle and swimming speed (Fig. 4). Finding a strong relationship between zooid number and speed in whorls was surprising given their less streamlined configuration (Fig. 5). This could be due to the smaller range of slow speeds and few zooids in the data we obtained for these species. Our regression results on pooled architectures, as well as finding a significant relationship between number of zooids and speed

1  
2  
3  
4 480 for linear and bipinnate chains but not for clusters nor transversal chains, support our primary  
5 hypothesis that the different frontal area scaling relationships across architectures has an impact  
6 on swimming speed.  
7  
8

9 483 Linear chains swam faster than all other architectures, including those that share a  
10 constant frontal area feature like bipinnate chains (Fig. 3, Table S2). One potential explanation  
11 for this difference could come from the relative thrust provided by the jets. Linear chains eject  
12 their jet plumes at very small angles (near parallel) to the axis of locomotion (Sutherland et al.  
13 16 486 2024), just wide enough to avoid interaction between jet plumes (Sutherland & Weihs 2017).  
17 487 Bipinnate and helical chains (both with constant frontal area) have the atrial siphons (point of jet  
18 488 ejection) of their constituent blastozooids oriented at a wider angle (Madin 1990), which may lead  
19 489 to wider angles of their jets relative to the axis of locomotion. This in turn would result in a larger  
20 490 proportion of the force exerted by the jet to be applied as torque rather than thrust onto the colony.  
21 491 This hypothesis could be tested by measuring the 3D angles of the actual jets instead of the  
22 492 angles of the zooids since salps can use their atrial muscles and siphon morphology to direct the  
23 493 angle of their jets.  
24 494

25 495 Finding that clusters can swim at speeds comparable to those of bipinnate and helical  
26 496 chains, even faster than whorls, defies our intuitive understanding of the mechanical properties  
27 497 of these colonies and thus warrants further investigation into how these species coordinate their  
28 498 jets to produce forward thrust. While oblique chains are architectural intermediates between  
29 499 transversal and linear chains (Damian-Serrano & Sutherland 2023), our data indicate that oblique  
30 500 chains may be the slowest swimmers among salps. This incongruence may be explained by the  
31 501 fact that we only had speed data from one oblique specimen (of *Thalia* sp.) with very small zooid  
32 502 sizes. Small salps might operate at notably lower Reynolds numbers than large ones, which may  
33 503 require a non-linear size correction for meaningful speed comparisons. Swimming speed data  
34 504 from the much larger oblique chains of *Thetys vagina* may provide a more comparable example  
35 505 of the locomotory performance of this oblique colonial configuration.  
36

37 506 The questions addressed in this study focus on the effect of frontal area of colonial  
38 507 architectures on swimming speed. This effect may be associated with form and pressure drag  
39 508 differences between more and less streamlined colony shapes. To test whether these are the  
40 509 forces responsible for differences in swimming speed, drag would have to be measured or  
41 510 calculated, which is beyond the scope of this study. Other unaccounted forces may be significant  
42 511 energetic contributors to the system that explain the remainder of the observed variation. Chain  
43 512 length for the streamlined forms (helical, linear, and bipinnate chains) could have negative effects  
44 513 on swimming speeds that may partially counteract the positive effect of increased propeller thrust.  
45  
46  
47  
48  
49  
50  
51  
52  
53  
54  
55  
56  
57  
58  
59  
60  
61  
62  
63  
64  
65

1  
2  
3  
4 514 For example, skin drag increases proportionally to the surface area of the system, and the  
5 smoothness of the chain may increase pressure drag through vortex shredding (Vogel 1981).  
6 515 While added (virtual) mass could also be an issue, asynchronously swimming colonies do not  
7 suffer as much from these acceleration-related costs, since their speed is maintained near  
8 constant while cruising (Bone & Trueman 1983). Chain length could also lead to reduced stability  
9 and efficiency, though some linear species capitalize on this by swimming in corkscrew orbital  
10 spirals (Sutherland et al. 2024). However, if friction drag, chain stability, or vortex shredding were  
11 indeed more important contributors than frontal form drag, we would predict that linear chains  
12 would appear slower than other more stable and compact architectures. Future studies may  
13 unravel these potential confounding effects on the biomechanics of colonial salp swimming.  
14 521  
15 522  
16 523  
17 524 *Salp swimming speed and diel vertical migration*  
18 525  
19 526  
20 527  
21 528  
22 529  
23 530  
24 531  
25 532  
26 533  
27 534  
28 535  
29 536  
30  
31  
32  
33  
34  
35  
36  
37  
38  
39  
40  
41  
42  
43  
44  
45  
46  
47  
48  
49  
50  
51  
52  
53  
54  
55  
56  
57  
58  
59  
60  
61  
62  
63  
64  
65

Salps are important players in the oceanic carbon cycle, grazing upon both phytoplankton and bacteria (Henschke et al. 2016). Their carcasses and fecal pellets export large quantities of fixed carbon into the deep sea, accelerating carbon sequestration in the biological carbon pump (Wiebe et al. 1979, Décima et al. 2023). Part of this process is enhanced by the diel vertical migrations by some salp species though the distribution of this behavior across species diversity is poorly known. Off Bermuda, Madin et al. (1996) reported *Pegea* spp., *B. rostrata*, and *C. polae* as non-migratory, all of which we found to have slow swimming speeds. Other slow-swimmer species like *C. affinis* were found to only migrate a few meters through the diel cycle. The species *S. aspera*, *S. fusiformis*, *S. zonaria*, *I. punctata*, and *R. retracta* have been observed vertically migrating off Bermuda (Madin et al 1996, Stone & Steinberg 2014), which is congruent with our observations during fieldwork. These species all have constant frontal area and fast swimming speeds.

Vertical migrators need to be fast enough to follow the dark isolumes as they shift during dawn and dusk in time to maximize their exploitation of the food resources near the surface. Thus, absolute speed is important to the autoecology of these animals. Other *Salpa* species have also been reported as strong vertical migrators throughout the literature (Henschke et al. 2021, Madin et al. 2006, Pascual et al. 2017). A species that does not fit this pattern is *I. cylindrica*, a fast-swimming non-migratory species that spends night and day near the surface (Madin et al 1996; and pers. obs.). However, other studies do report moderate diel vertical migration for this species (Stone & Steinberg 2014), so it may be adapted for facultative vertical migration under specific oceanographic conditions. Some migratory species, such as *S. aspera*, are known to travel distances of over 800m at dawn and dusk, at rates predicted to require 5-10 m/min (83-166 mm/s)

1  
2  
3  
4 547 based on MOCNESS trawl intervals (Wiebe et al. 1979). These predictions are consistent with  
5  
6 548 the speeds we recorded for this species (88-145 mm/s) and similar congeners.  
7  
8 549 *Ecophysiological implications*

9 550 While the importance of a few well-studied linear chain salp species in the biological  
10  
11 551 carbon pump has been delineated, the question of whether this ecological role is generalizable to  
12  
13 552 other salp species remains unanswered. In addition to vertical migration behavior, another likely  
14  
15 553 important factor in their carbon flow is their respiration rate. The higher their respiration rate, the  
16  
17 554 larger the proportion of assimilated carbon that will be released back into the water as dissolved  
18  
19 555 carbon dioxide. This study provides the broadest taxonomic perspective on respiration rates (18  
20  
21 556 species, Fig. S2A) and swimming cost of transport (14 species), finding 17-fold differences in their  
22  
23 557 respiration rates and over 77-fold differences in their mean COT. Except for a few species with  
24  
25 558 extremely high and low values, most respiration rates are centered between 0.2 and 1  
26  
27 559  $\mu\text{mol/g/hour}$ , assuming a salp tissue density of 1.025 g/ml. In general, the respiration rates we  
28  
29 560 estimated for salps are within the range of those reported in the literature (Trueblood 2019, Iguchi  
30  
31 561 and Ikeda 2004). Compared to the metabolic rates estimated for the broader diversity of marine  
32  
33 562 pelagic animals (Seibel & Drazen 2007), the rates that we measured for salps are in a similar  
34  
35 563 range to those measured for *Salpa thompsoni* (Iguchi and Ikeda 2004). Our values are also similar  
36  
37 564 to those measured by Seibel & Drazen (2007) in nemerteans, chaetognaths, and most fishes (0.1-  
38  
39 565 1  $\mu\text{molO}_2/\text{g/h}$ ), which are generally higher than other gelatinous animals like ctenophores or  
40  
41 566 scyphomedusae (0.01-0.1  $\mu\text{molO}_2/\text{g/h}$ ), but generally lower than those of cephalopods,  
42  
43 567 crustaceans, or large fish (1-10  $\mu\text{molO}_2/\text{g/h}$ ). Salp species known to have strong vertical migration  
44  
45 568 behaviors (*Salpa* spp., *S. zonaria*, *I. punctata*, and *R. retracta*) have low basal metabolic rates  
46  
47 569 (Fig. S2A) and low costs of transport. These results indicate that many non-migratory species,  
48  
49 570 while likely still being important players in the biological carbon pump via their fecal pellet  
50  
51 571 production, are releasing more of the consumed carbon as carbon dioxide near the surface than  
52  
53 572 their more metabolically efficient relatives. The ultimate ecological outcome of each species  
54  
55 573 needs to be assessed holistically, considering their microbial filtration and pellet deposition rate  
56  
57 574 as well as their relative abundance in the water column.

58  
59 575 Our metabolically calculated costs of transport range between 5-50 J/kg/m when  
60  
61 576 converting the mg of oxygen to J via aerobic respiration free energy equations at 23°C. These  
62  
63 577 values are higher than the highly efficient 1-2 J/kg/m reported for salps in the literature (Bone &  
64  
65 578 Trueman 1983, Gemmell et al. 2021), and approach the less-efficient values found in single jet-  
propelled invertebrates like scallops or squids. We suspect that COT calculated from mechanical  
parameters such as the displacement of water mass is not directly comparable to the COT

1  
2  
3  
4 581 calculated from respiration rates. Furthermore, the standard aerobic respiration free-energy  
5 equation based on glucose may not fully represent the metabolic energy-conversion processes  
6 in salps, which could rely on a combination of sugars and fatty acids derived from their  
7  
8 584 microscopic prey.  
9

10  
11 585 While COT increases with swimming speed fishes (Rubio-Gracia et al. 2020) and jet-  
12 propelled squid (Bi & Zhu 2019), multi-jet swimmers may circumvent this tradeoff by having  
13 multiple swimming units. In colonial siphonophores, as zooid number increases swimming speed  
14 increases together with a decrease in COT (Du Clos et al. 2022). Our results show that faster  
15 swimming species have lower COT (Fig. 6), which suggests that faster speeds and higher  
16 locomotory efficiency have a common cause, where both speed and efficiency depend on frontal  
17 area which may partly drive form and pressure drag forces. However, this hypothesis is not  
18 supported by the distribution of COT across architectures (Fig 6C, D), where except for oblique  
19 and transversal chains, all architectures present similarly efficient COT values. Perhaps there are  
20 other underlying explanatory factors linking swimming speed and swimming efficiency, such as  
21 shared ancestry, muscle content, jet coordination, or jetting angles (thrust-to-torque ratios).  
22  
23 592  
24 593  
25 594  
26 595  
27 596  
28 597  
29 598  
30 599  
31 600  
32 601  
33 602  
34 603  
35 604  
36 605  
37 606  
38 607  
39 608  
40 609  
41 610  
42 611  
43 612  
44 613  
45 614  
46 615  
47 616  
48 617  
49 618  
50 619  
51 620  
52 621  
53 622  
54 623  
55 624  
56 625  
57 626  
58 627  
59 628  
60 629  
61 630  
62 631  
63 632  
64 633  
65 634

### 30 596 *Evolutionary implications*

31 597 Across the evolutionary history of salps, linear chains have evolved multiple times  
32 598 independently from oblique ancestors (Damian-Serrano et al. 2023), suggesting the adaptive role  
33 599 of this architecture as a functional trait. Linear chain architectures evolved independently in *M.*  
34 600 *hexagona*, *S. zonaria*, *I. punctata*, and before the common ancestor of *Iasis* and *Salpa*. Our results  
35 show that going from an oblique form to a linear one may confer significant advantages in  
36 601 locomotory speed and energetic efficiency. However, multiple colonial architectures, which we  
37 602 find to be slower swimmers (such as transversal chains, helical chains, whorls, and clusters in  
38 603 the genus *Pegea* and the Cyclosalpidae family) had also evolved from oblique and linear  
39 604 ancestors. This is incongruent with a scenario where natural selection strongly favors locomotion  
40 605 efficiency across all ecological niches of salps. Therefore, the evolution of colonial architecture  
41 606 may be driven by ecological trade-offs with other non-locomotory functions. Alternatively, in some  
42 607 of these lineages, locomotion at the colonial stage may not be important enough for selection to  
43 608 maintain these highly streamlined forms, allowing for neutral evolutionary processes to produce  
44 609 a diversity of non-adaptive forms. In the current study, we did not use phylogenetic comparative  
45 610 methods in our analysis because like other investigators comparing biomechanical properties  
46 611 across species (e.g. Dabiri et al. 2010, DiSanto et al. 2021) we were interested in inherent  
47 612 mechanical relationships dictated by the colony architectures. For instance, a linear arrangement  
48 613 of zooids inherently reduces drag due to a cluster arrangement, leading to faster swimming  
49 614 of zooids inherently reduces drag due to a cluster arrangement, leading to faster swimming  
50 615  
51 616  
52 617  
53 618  
54 619  
55 620  
56 621  
57 622  
58 623  
59 624  
60 625  
61 626  
62 627  
63 628  
64 629  
65 630

1  
2  
3  
4 615 speeds and potentially higher efficiency regardless of phylogenetic history. In other words, any  
5 phylogenetic inertia is irrelevant in instantaneous relationships between traits (Felsenstein 1985).  
6 616 Moreover, independence of data is often incorrectly assumed to be an assumption of standard  
7 (nonphylogenetic) regressions (Uyeda et al. 2018), when in reality the assumptions relate to the  
8 independence and distribution of the error terms. Thus, when all the phylogenetic signal is present  
9 in the predictor, as it is in the case with colonial architecture (Damian-Serrano et al. 2022) and its  
10 associated characteristics, there is no need for any “phylogenetic correction” (Uyeda et al. 2018).  
11 619  
12 620  
13 621  
14 622  
15 623  
16 624  
17 625  
18 626  
19 627  
20 628  
21 629  
22 630 These analyses could reveal whether these factors have co-evolved with each other and/or with  
23 respiration rate or colonial architecture.

24 631 *Insights for bioinspired underwater vehicle design*  
25  
26 632 Pulsatile jet propulsion is a promising avenue for bioinspired aquatic vehicles and robots  
27 (Mohensi 2006, Gohardini 2014, Yue et al. 2015). Multijet propulsion systems with multiple  
28 633 propellers akin to salp colonies have been explored in an engineering context (Chao et al. 2017,  
29 634 Costello et al. 2015) with direct inspiration from gelatinous animals (Marut 2014, Krummel 2019,  
30 635 Bi et al 2022, Du Clos et al. 2022). Salp diversity provides a natural laboratory to explore the  
31 636 hydrodynamic implications of different multijet arrangement designs. Our findings underscore the  
32 637 importance of considering the scaling hydrodynamic properties of propeller arrangements to  
33 638 optimize speed and energy efficiency in bioinspired underwater vehicle design. While linear chain  
34 639 arrangements were the fastest and among the most energy efficient, robot (or vehicle)  
35 640 configurations such as a cluster form may confer unique object manipulation or maneuverability  
36 641 advantages. Our results show that these seemingly inefficient propeller configurations do not  
37 642 impose large disadvantages in terms of speed and fuel efficiency.

38 643 **Acknowledgments:**

39 644 We are grateful to the crew of Aquatic Life Divers, Kona Honu Divers for their assistance  
40 and support in hosting our offshore diving operations. We also wish to thank Marc Hughes, Jeff  
41 645 Milisen, Rebecca Gordon, Matt Connelly, Clint Collins, Paul Richardson, and Anne Thompson for  
42 646 their assistance during diving, collections, and filming operations in the field. We would like to  
43 647  
44  
45  
46  
47  
48  
49  
50  
51  
52  
53  
54  
55  
56  
57  
58  
59  
60  
61  
62  
63  
64  
65

1  
2  
3  
4 648 thank Tiffany Bachtel for her valuable advice on the respirometry experiment design. We thank  
5  
6 649 the associate editor and two anonymous reviewers for their helpful comments.  
7  
8 650

## 9 651      **Funding**

10 652      This research was supported by the Gordon and Betty Moore Foundation [grant number  
11 653 8835] and the Office of Naval Research [grant number N00014-23-1-2171].  
12  
13 654

## 14 655      **Data availability**

15 656 Data used to generate the results presented in this paper are available in the supplementary  
16 657 information. Any other datasets used directly or indirectly for this study are available from the  
17 658 authors upon reasonable request.  
18

## 19 659      **Competing interests**

20 660 No competing interests declared.  
21

## 22 661      **Literature cited**

23 662 Alexander, A. J. (1968). Forward Speed Effects on Annular Jet Cushions. *The Aeronautical  
24 663 Journal*, 72(689), 438-441.  
25

26 664 Andersen, K. H., Berge, T., Gonçalves, R. J., Hartvig, M., Heuschele, J., Hylander, S., ... &  
27 665 Kiørboe, T. (2016). Characteristic sizes of life in the oceans, from bacteria to whales.  
28 666 *Annual review of marine science*, 8(1), 217-241.  
29

30 667 Bi, X., & Zhu, Q. (2019). Dynamics of a squid-inspired swimmer in free swimming. *Bioinspiration  
31 668 & Biomimetics*, 15(1), 016005.  
32

33 669 Bi, X., Tang, H., & Zhu, Q., 2022. Feasibility of hydrodynamically activated valves for 416 salp-  
34 670 like propulsion. *Physics of Fluids*, 34(10), 101903.  
35

36 671 Biggs, D. C. (1977). Respiration and ammonium excretion by open ocean gelatinous zooplankton  
37 672 1. *Limnology and Oceanography*, 22(1), 108-117.  
38

39 673 Bone, Q., Anderson, P. A. V., & Pulsford, A. (1980). Morphology of salp chain communication.  
40 674 *Proceedings of the Royal Society of London. Series B. Biological Sciences*, 210(1181),  
41 675 549-558.  
42

43 676 Bone, Q., & Trueman, E. R. (1983). Jet propulsion in salps (Tunicata: Thaliacea). *Journal of  
44 677 Zoology*, 201(4), 481-506.  
45

46 678 Cetta, C. M., Madin, L. P., & Kremer, P. (1986). Respiration and excretion by oceanic salps.  
47 679 *Marine Biology*, 91, 529-537.  
48

49 680 Chao, S., Guan, G., & Hong, G. S., 2017, September. Design of a finless torpedo-shaped micro  
50 681 AUV with high maneuverability. In OCEANS 2017-Anchorage (pp. 425 1-6). IEEE.  
51

52 682 Colin, S. P., Gemmell, B. J., Costello, J. H., & Sutherland, K. R. (2022). In situ high-speed  
53 683 brightfield imaging for studies of aquatic organisms. *Protocols.io*.  
54

- 1  
2  
3
- 4 682 Costello, J. H., Colin, S. P., Gemmell, B. J., Dabiri, J. O., & Sutherland, K. R., 2015. 429 Multi-jet  
5  
6 683 propulsion organized by clonal development in a colonial siphonophore. 430 *Nature*  
7  
8 684 communications, 6(1), 8158.
- 9 685 Dabiri, J. O., Colin, S. P., Katija, K., & Costello, J. H. (2010). A wake-based correlate of  
10  
11 686 swimming performance and foraging behavior in seven co-occurring jellyfish species.  
12  
13 687 *Journal of experimental biology*, 213(8), 1217-1225.
- 14 688 Damian-Serrano, A., & Sutherland, K. R. (2023). A developmental ontology for the colonial  
15  
16 689 architecture of salps. *The Biological Bulletin*, 245(1), 9-18..
- 17 690 Damian-Serrano, A., Hughes, M., & Sutherland, K. R. (2023). A new molecular phylogeny of salps  
18  
19 691 (Tunicata: thalicea: salpida) and the evolutionary history of their colonial architecture.  
20  
21 692 *Integrative Organismal Biology*, 5(1), obad037.
- 22 693 Décima, M., Stukel, M. R., Nodder, S. D., Gutiérrez-Rodríguez, A., Selph, K. E., Dos Santos, A.  
23  
24 694 L., ... & Pinkerton, M. (2023). Salp blooms drive strong increases in passive carbon export  
25  
26 695 in the Southern Ocean. *Nature communications*, 14(1), 425.
- 27 696 Di Santo, V., Goerig, E., Wainwright, D. K., Akanyeti, O., Liao, J. C., Castro-Santos, T., & Lauder,  
28  
29 697 G. V. (2021). Convergence of undulatory swimming kinematics across a diversity of fishes.  
30  
31 698 *Proceedings of the National Academy of Sciences*, 118(49), e2113206118.
- 32 699 Du Clos, K. T., Gemmell, B. J., Colin, S. P., Costello, J. H., Dabiri, J. O., and Sutherland, K. R.  
33  
34 700 2022. Distributed propulsion enables fast and efficient swimming modes in physonect  
35  
36 701 siphonophores. *Proceedings of the National Academy of Sciences*. 119:e2202494119.
- 37 702 Felsenstein, J. (1985). Phylogenies and the comparative method. *The American  
38  
39 703 Naturalist*, 125(1), 1-15.
- 40  
41 704 Gemmell, B. J., Dabiri, J. O., Colin, S. P., Costello, J. H., Townsend, J. P., & Sutherland, K. R.  
42  
43 705 (2021). Cool your jets: biological jet propulsion in marine invertebrates. *Journal of  
44  
45 706 Experimental Biology*, 224(12), jeb222083.
- 46 707 Gohardani, A. S. *Distributed Propulsion Technology* Nova Science Publishers (2014).
- 47  
48 708 Haddock, S. H. (2004). A golden age of gelata: past and future research on planktonic  
49  
50 709 ctenophores and cnidarians. *Hydrobiologia*, 530, 549-556.
- 51 710 Haddock, S. H., & Heine, J. N. (2005). Scientific blue-water diving.
- 52  
53 711 Hamner, W. M., Madin, L. P., Alldredge, A. L., Gilmer, R. W., & Hamner, P. P. (1975). Underwater  
54  
55 712 observations of gelatinous zooplankton: Sampling problems, feeding biology, and  
56  
57 behavior 1. *Limnology and Oceanography*, 20(6), 907-917.
- 58  
59  
60  
61  
62  
63  
64  
65

- 1  
2  
3
- 4 714 Henschke, N., Cherel, Y., Cotté, C., Espinasse, B., Hunt, B.P. and Pakhomov, E.A., 2021. Size  
5 and stage specific patterns in *Salpa thompsoni* vertical migration. *Journal of Marine*  
6 Systems, 222, p.103587.
- 7 716  
8 717 Krummel, G. M. (2019). Locomotion and Control of Cnidarian-Inspired Robots (Doctoral  
9 dissertation, Virginia Tech).
- 10 718  
11 719 Mackie, G. O. (1986). From aggregates to integrates: physiological aspects of modularity in  
12 colonial animals. *Philosophical Transactions of the Royal Society of London. B, Biological*  
13 Sciences, 313(1159), 175-196.
- 14 720  
15 721  
16 722 Madin, L. P. (1990). Aspects of jet propulsion in salps. *Canadian Journal of Zoology*, 68(4), 765-  
17 723 777.
- 18 724 Madin, L. P., & Deibel, D. (1998). Feeding and energetics of Thaliacea. *The biology of pelagic*  
19 725 *tunicates*, 81-104.
- 20 726 Madin, L. P., Kremer, P., & Hacker, S. (1996). Distribution and vertical migration of salps  
21 (Tunicata, Thaliacea) near Bermuda. *Journal of Plankton Research*, 18(5), 747-755.
- 22 727  
23 728 Madin, L.P., Kremer, P., Wiebe, P.H., Purcell, J.E., Horgan, E.H. and Nemazie, D.A., 2006.  
24 729 Periodic swarms of the salp *Salpa aspera* in the Slope Water off the NE United States:  
25 Biovolume, vertical migration, grazing, and vertical flux. *Deep Sea Research Part I:*  
26 730 Oceanographic Research Papers, 53(5), pp.804-819.
- 27 731  
28 732 Marut, K. J. (2014). Underwater Robotic Propulsors Inspired by Jetting Jellyfish (Doctoral  
29 dissertation, Virginia Tech).
- 30 733  
31 734 Mayzaud, P., Boutoute, M., Gasparini, S., Mousseau, L., & Lefevre, D. (2005). Respiration in  
32 marine zooplankton—the other side of the coin: CO<sub>2</sub> production. *Limnology and*  
33 *Oceanography*, 50(1), 291-298.
- 34 735  
35 736 Mohensi, K., 2006. Pulsatile vortex generators for low-speed maneuvering of small  
36 482 underwater vehicles. *Ocean Eng.* 33, 2209–2223.
- 37 737  
38 738 Pascual, M., Acuña, J.L., Sabatés, A., Raya, V. and Fuentes, V., 2017. Contrasting diel vertical  
39 739 migration patterns in *Salpa fusiformis* populations. *Journal of Plankton Research*, 39(5),  
40 740 pp.836-842.
- 41 741  
42 742 R Core Team, R. (2021). R: A language and environment for statistical computing.
- 43 743 Rubio-Gracia, F., García-Berthou, E., Guasch, H., Zamora, L., & Vila-Gispert, A. (2020). Size-  
44 744 related effects and the influence of metabolic traits and morphology on swimming  
45 performance in fish. *Current Zoology*, 66(5), 493-503.
- 46 745  
47  
48  
49  
50  
51  
52  
53  
54  
55  
56  
57  
58  
59  
60  
61  
62  
63  
64  
65

- 1  
2  
3  
4 746 Schneider, G. (1992). A comparison of carbon-specific respiration rates in gelatinous and non-  
5  
6 747 gelatinous zooplankton: a search for general rules in zooplankton metabolism.  
7  
8 748 *Helgoländer Meeresuntersuchungen*, 46, 377-388.  
9  
10 749 Seibel, B. A., & Drazen, J. C. (2007). The rate of metabolism in marine animals: environmental  
11  
12 750 constraints, ecological demands and energetic opportunities. *Philosophical Transactions of the Royal Society B: Biological Sciences*, 362(1487), 2061-2078.  
13  
14 752 Stone, J. P., & Steinberg, D. K. (2014). Long-term time-series study of salp population dynamics  
15  
16 753 in the Sargasso Sea. *Marine Ecology Progress Series*, 510, 111-127.  
17  
18 754 Sutherland, K. R., & Weihs, D. (2017). Hydrodynamic advantages of swimming by salp chains.  
19  
20 755 *Journal of The Royal Society Interface*, 14(133), 20170298.  
21  
22 756 Sutherland, K. R., Damian-Serrano, A., Du Clos, K. T., Gemmell, B. J., Colin, S. P., Costello, J.  
23  
24 757 H. (2024). Spinning and corkscrewing of oceanic macroplankton revealed through in situ  
25  
imaging. *Science Advances* 10(20).  
26  
27 759 Sutherland, K. R., & Madin, L. P. (2010). Comparative jet wake structure and swimming  
28  
29 760 performance of salps. *Journal of Experimental Biology*, 213(17), 2967-2975.  
30  
31 761 Trueblood, L. A. (2019). Salp metabolism: temperature and oxygen partial pressure effect on the  
32  
33 762 physiology of *Salpa fusiformis* from the California Current. *Journal of Plankton Research*,  
41(3), 281-291.  
34  
35 764 Trueman, E. R., Bone, Q., & Braconnor, J. C. (1984). Oxygen consumption in swimming salps  
36  
37 765 (Tunicata: Thaliacea). *Journal of Experimental Biology*, 110(1), 323-327.  
38  
39 766 Uyeda, J. C., Zenil-Ferguson, R., & Pennell, M. W. (2018). Rethinking phylogenetic comparative  
40  
methods. *Systematic Biology*, 67(6), 1091-1109.  
41  
42 768 Vogel, S. (1981). Life in moving fluids. *Princeton University Press*, Princeton, NJ.  
43  
44 769 Vogel, S. (2008). Modes and scaling in aquatic locomotion. *Integrative and Comparative Biology*,  
45  
46 770 48(6), 702-712.  
47  
48 771 Wiebe, P. H., Madin, L. P., Haury, L. R., Harbison, G. R., & Philbin, L. M. (1979). Diel vertical  
49  
50 772 migration by *Salpa aspera* and its potential for large-scale particulate organic matter  
51  
52 773 transport to the deep-sea. *Marine Biology*, 53, 249-255.  
53  
54 774 World Register of Marine Species (WoRMS). (2024). WoRMS Editorial Board. Accessed January  
55  
56 776 Yue, C. et al., 2015. Mechantronic system and experiments of a spherical underwater 510 robot:  
57  
58 SUR-II. *J. Intell. Robot Syst.* Doi:10.1007/s10846-015-0177-3.  
59  
60  
61  
62  
63  
64  
65

## Supplementary Material

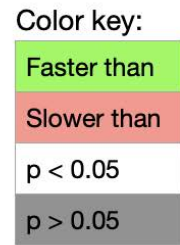
Dataset S1. (A) Salp video specimens analyzed with video specifications, as well as mean morphological and kinematic attributes. (B) Salp specimens used in the respirometry experiments with mean physiological attributes. (Please see attached file.)

Table S1. Summary of numbers of specimens (N), number of measurements (n), and descriptive variable averages per species including both the video speed data and the respiration experiments data.

Species	Architecture	Speed Measurements from Videos						Respiration Measurements from Experiments				
		Mean Number of zooids	Mean zoid length (mm)	Mean Pulsation rate (pulses/s)	Mean swimming speed (mm/s)	N	n	Mean Number of zooids	Mean zoid length (mm)	Mean Colony volume (ml)	N	n
<i>Brookia rostrata</i>	Bipinnate	26	7.4	2.6	34.4	5	45	20.3	6.5	3.7	16	130
<i>Ritterellia amboinensis</i>	Bipinnate	18	25.6	1.9	42.5	9	77	12.7	22.1	8.0	7	44
<i>Ritterellia sp.</i>	Bipinnate	33	21.3	1.3	43.1	3	49	18.7	34.5	22.5	6	42
<i>Cyclosalpa polae</i>	Cluster	5	17.2	1.2	47.6	2	19	7.0	20.0	4.3	7	55
<i>Cyclosalpa sewelli</i>	Cluster	7	15.0	1.4	26.8	6	52	6.2	19.4	7.2	11	88
<i>Helicosalpa virgula</i>	Helical	60	11.5	3.3	49.9	1	7	66.0	14.0	14.8	2	13
<i>Iasis cylindrica</i>	Linear	43	8.9	3.6	61.1	32	308	26.8	10.5	6.5	15	103
<i>Ihlea punctata</i>	Linear	NA	NA	NA	NA	0	0	68	12	3.7	1	7
<i>Metcalflina hexagona</i>	Linear	18	26.8	2.4	109.6	9	105	16.0	28.0	22.0	1	7
<i>Salpa aspera</i>	Linear	9	28.3	2.1	114.3	7	57	16.2	32.0	9.1	6	42
<i>Salpa fusiformis</i>	Linear	16	17.2	3.0	57.2	8	74	13.0	17.7	2.1	7	47
<i>Salpa maxima</i>	Linear	2	61.6	0.7	55.9	4	34	3.6	87.8	27.8	8	52
<i>Soestia zonaria</i>	Linear	11	13.7	1.9	109.2	4	34	9.1	19.6	4.6	8	23
<i>Thalia sp.</i>	Oblique	29	3.5	4.5	5.8	1	28	18.6	5.9	0.3	7	53
<i>Pegasa sp.</i>	Transversal	12	31.0	1.7	20.3	2	18	13.1	43.2	29.2	13	91
<i>Cyclosalpa affinis</i>	Whorl	5	33.0	1.4	24.5	2	15	6.7	37.9	23.4	10	65
<i>Cyclosalpa bakeri</i>	Whorl	7	7.0	2.6	10.4	7	63	6.9	14.6	3.0	7	57
<i>Cyclosalpa quadriluminis</i>	Whorl	8	27.1	1.3	25.3	1	6	8.3	24.5	12.7	6	36

Table S2. Tukey's post-hoc pairwise comparisons from an ANOVA on (A) swimming speed and (B) COT across different colonial architectures reporting magnitude of difference and adjusted p-values.

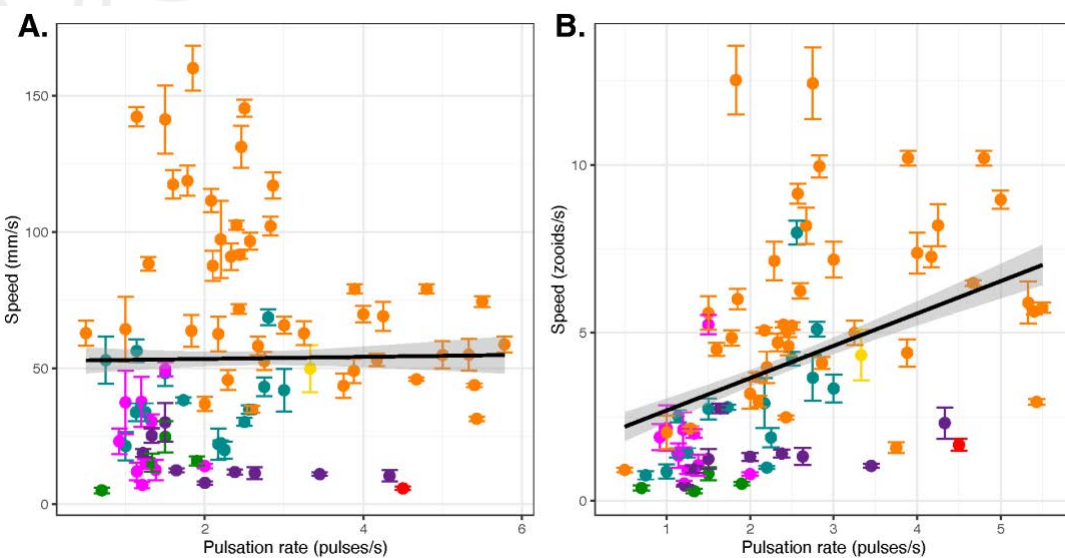
A.		Speed (mm/s)		Speed (zooids/pulse)	
Architecture		Difference	p-value adj.	Difference	p-value adj.
Cluster	Bipinnate	-12.900	0.005	0.082	0.991
Linear	Bipinnate	33.971	0.000	0.896	0.000
Transversal	Bipinnate	-22.314	0.002	-0.969	0.009
Whorl	Bipinnate	-25.559	0.000	-0.774	0.001
Linear	Cluster	46.871	0.000	0.814	0.000
Transversal	Cluster	-9.415	0.570	-1.050	0.006
Whorl	Cluster	-12.659	0.028	-0.856	0.000
Transversal	Linear	-56.286	0.000	-1.864	0.000
Whorl	Linear	-59.530	0.000	-1.670	0.000
Whorl	Transversal	-3.245	0.987	0.195	0.972



B.		COT per mm		COT per zooid length	
Architecture		Difference	p-value adj.	Difference	p-value adj.
Cluster	Bipinnate	0.558	1.000	-16.055	1.000
Linear	Bipinnate	-0.109	1.000	-19.013	0.999
Oblique	Bipinnate	46.132	0.000	155.555	0.099
Transversal	Bipinnate	4.999	0.979	100.580	0.429
Whorl	Bipinnate	0.180	1.000	-9.487	1.000
Linear	Cluster	-0.667	1.000	-2.958	1.000
Oblique	Cluster	45.574	0.000	171.610	0.005
Transversal	Cluster	4.441	0.954	116.636	0.049
Whorl	Cluster	-0.378	1.000	6.568	1.000
Oblique	Linear	46.241	0.000	174.567	0.001
Transversal	Linear	5.108	0.857	119.593	0.010
Whorl	Linear	0.289	1.000	9.526	0.999
Transversal	Oblique	-41.134	0.000	-54.974	0.849
Whorl	Oblique	-45.952	0.000	-165.042	0.003
Whorl	Transversal	-4.819	0.890	-110.067	0.026

Color key:

More efficient than
Less efficient than
p < 0.05
p > 0.05



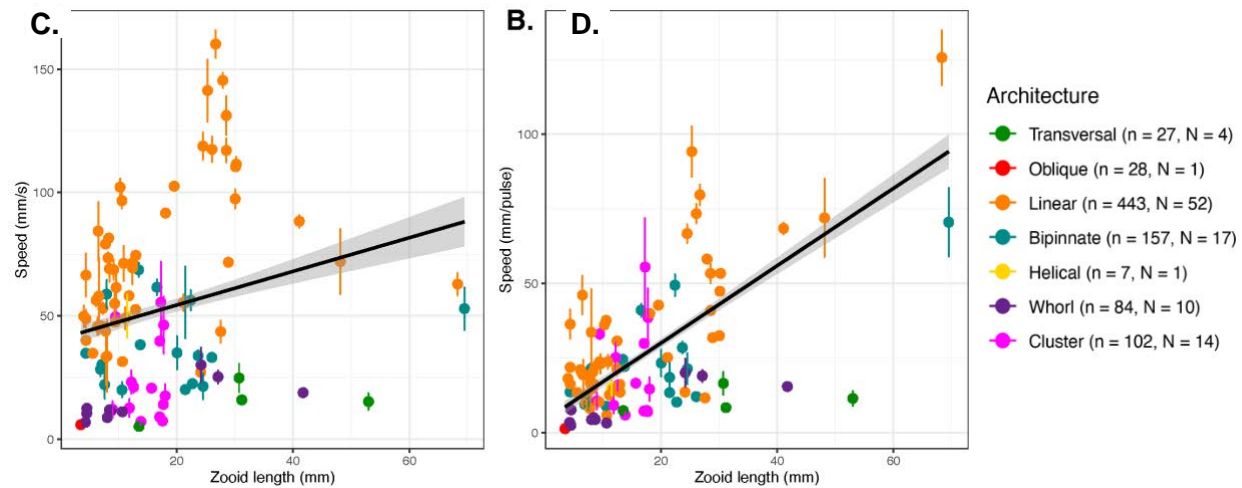
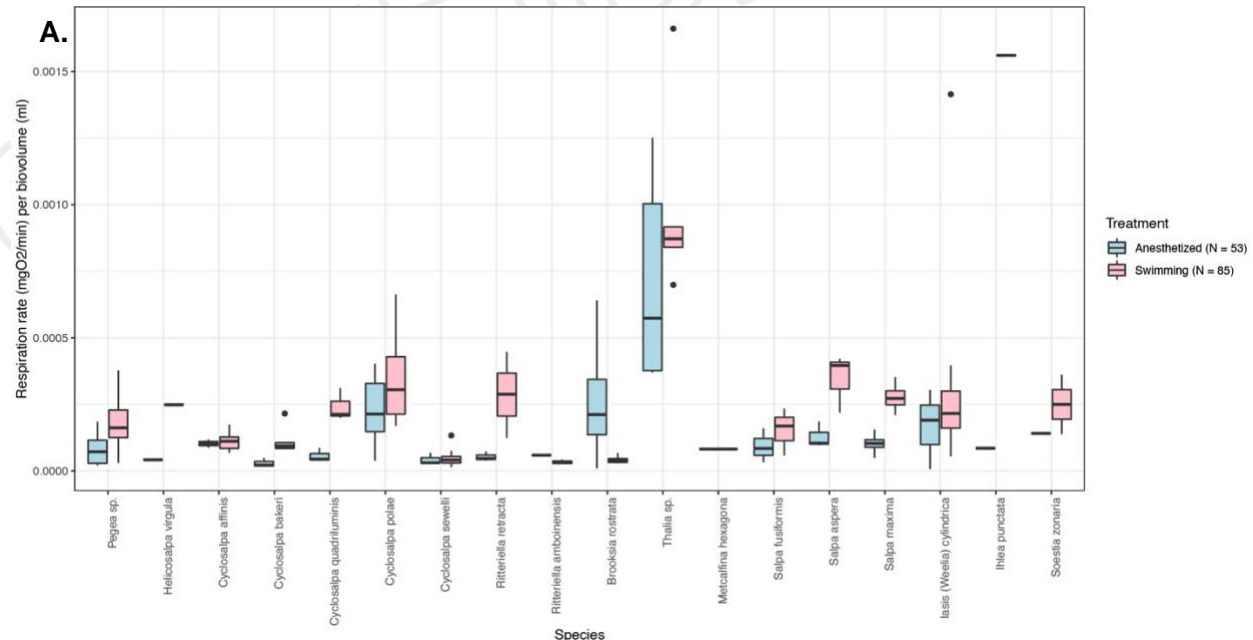


Figure S1. Salp swimming speeds. Distribution of salp colony absolute (A) and zooid size-corrected (B) swimming speed across pulsation rates. Distribution of salp colony absolute (C) and pulsation rate-corrected (D) swimming speed (specimen means with standard errors) across zooid sizes. Lines represent linear regressions with a 95% confidence interval shaded in grey.



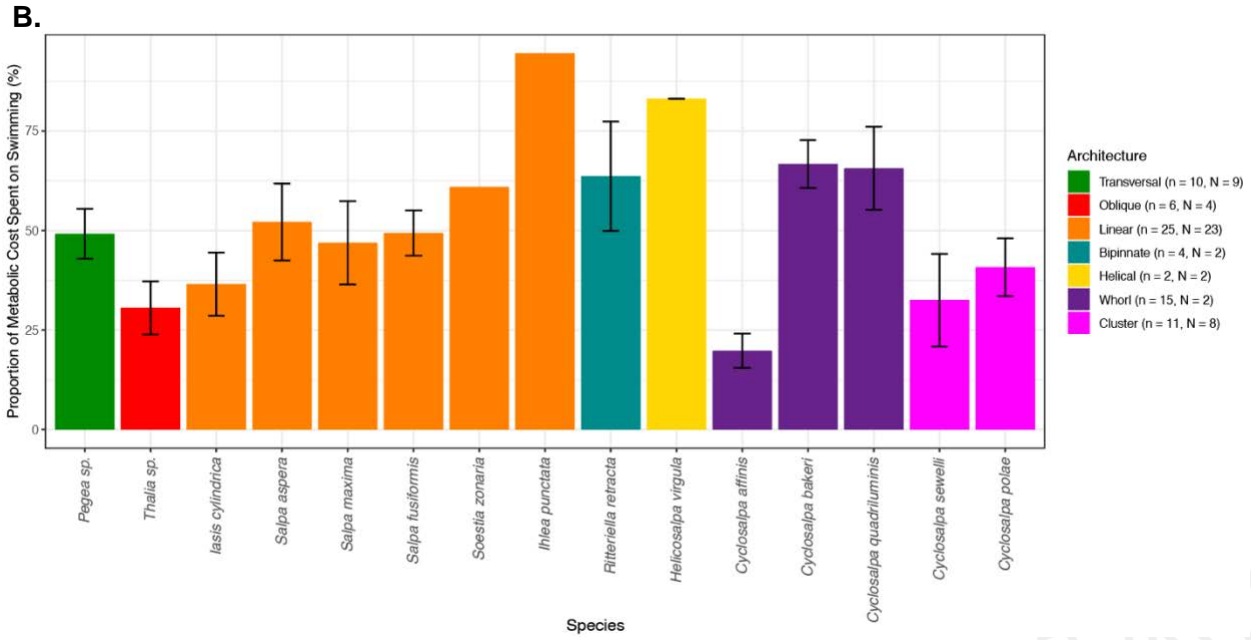
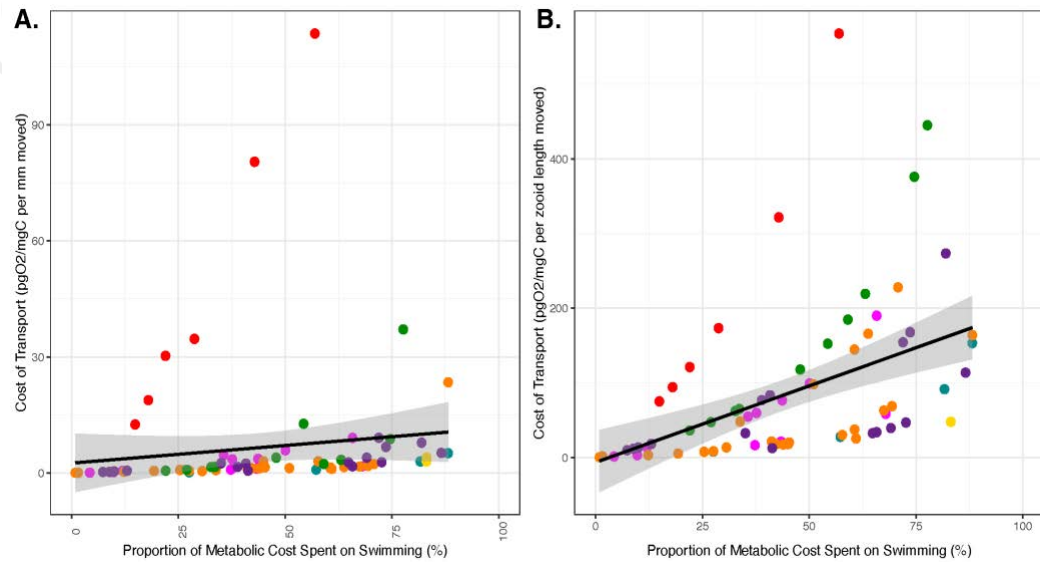


Figure S2. Respiration rates across salp species. (A) Biovolume-normalized respiration rates of swimming (red) and anesthetized (blue) salp colonies across different species. (B) Percentage of the swimming respiration rates matched by the mean anesthetized respiration rate for each salp species. Bars represent species means with black lines representing standard errors. Colors indicate colonial architecture.



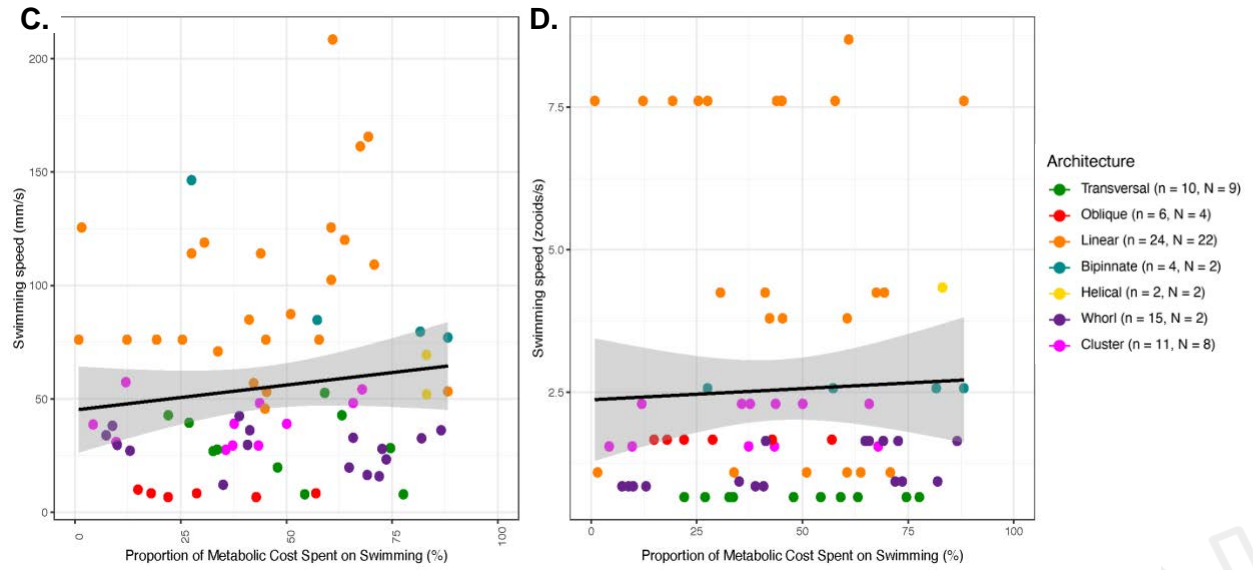


Figure S3. Proportion of metabolic cost spent on swimming. (A and B) Cost of transport (per mm in A, per zooid length in B) for each salp species across their percent swimming respiration rate matched by the species' mean anesthetized respiration rate. (C and D) Swimming speed (in mm/s in A, and zooids/s in B) for each salp species across their percent swimming respiration rate matched by the species mean anesthetized respiration rate. Point color indicates colonial architecture.

[Click here to access/download](#)

**Supplementary Movies, Audio and Datasets**  
Dataset S1A.csv

[Click here to access/download](#)

**Supplementary Movies, Audio and Datasets**  
**Dataset S1B.csv**

1 **Title: Colonial Architecture Modulates the Speed and  
2 Efficiency of Multi-Jet Swimming in Salp Colonies**

3  
4 **Authors:** Alejandro Damian-Serrano<sup>1</sup>, Kai A. Walton<sup>1</sup>, Anneliese Bishop-Perdue<sup>1</sup>, Sophie  
5 Bagoye<sup>1</sup>, Kevin T. Du Clos<sup>2</sup>, Bradford J. Gemmell<sup>3</sup>, Sean P. Colin<sup>4,5</sup>, John H. Costello<sup>6</sup>, Kelly R.  
6 Sutherland<sup>1</sup>

7  
8 **Author Affiliations:**  
9  
10 (1) Institute of Ecology and Evolution, Department of Biology, University of Oregon. 473 Onyx  
11 Bridge, 5289 University of Oregon, Eugene, OR 97403-5289, USA.  
12 (2) Louisiana Universities Marine Consortium, 8124 Highway 56, Chauvin, LA 70344, USA.  
13 (3) Department of Integrative Biology, University of South Florida, 4202 East Fowler Avenue,  
14 Tampa, FL 33620, USA.  
15 (4) Marine Biology and Environmental Science, Roger Williams University, Bristol, RI 02809, USA.  
16 (5) Whitman Center, Marine Biological Laboratory, Woods Hole, MA 02543, USA.  
17 (6) Biology Department, Providence College, Providence, RI 02918, USA.

18  
19 **Running title:** Architecture Modulates Salp Swimming

20  
21 **Summary Statement (30 words)**

22  
23 Linear arrangements in multi-jet propelled marine colonial invertebrates are faster than less  
24 streamlined architectures without incurring in higher costs of transport, offering insights for  
25 bioinspired underwater vehicle design.

26  
27  
28  
29  
30  
31  
32  
33

34     **Abstract**

35

36     Salps are marine pelagic tunicates with a complex life cycle including a solitary and colonial stage.  
37     Salp colonies are composed of asexually budded individuals that coordinate their swimming by  
38     multi-jet propulsion. Colonies develop into species-specific architectures with distinct zooid  
39     orientations. These distinct colonial architectures vary in how frontal area scales with the number  
40     of zooids in the colony. Here, we address how differences in frontal area drive differences in  
41     swimming speed and the relationship between swimming speed and cost of transport in salps.  
42     We (1) compare swimming speed across salp species and architectures, (2) evaluate how  
43     swimming speed scales with the number of zooids across colony in architectures, and (3)  
44     compare the metabolic cost of transport across species and how it scales with swimming speed.  
45     To measure swimming speeds, we recorded swimming salp colonies using in situ videography  
46     while SCUBA diving in the open ocean. To estimate the cost of transport, we measured the  
47     respiration rates of swimming and anesthetized salps collected in situ using jars equipped with  
48     non-invasive oxygen sensors. We found that linear colonies swim faster, which supports idea that  
49     their differential advantage in frontal area scales with an increasing number of zooids. We also  
50     found that higher swimming speeds predict lower costs of transport in salps. These findings  
51     underscore the importance of considering propeller arrangement to optimize speed and energy  
52     efficiency in bioinspired underwater vehicle design, leveraging lessons learned from the diverse  
53     natural laboratory provided by salp diversity.

54

55     **Keywords:** salps, colonial architecture, multi-jet propulsion, swimming, cost of transport

56

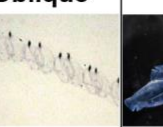
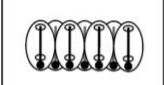
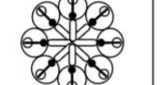
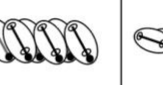
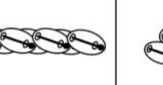
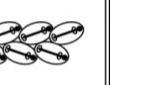
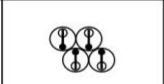
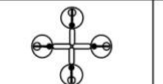
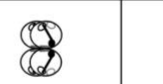
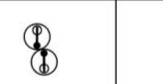
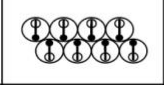
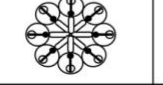
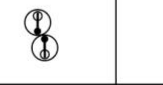
57     **Introduction**

58         Salps (Tunicata: Thaliacea: Salpida) are planktonic invertebrates that have a two-phase  
59     life cycle comprised of a solitary oozooid that asexually buds colonies of sexually reproducing  
60     blastozooids. Salp colonies are composed of up to hundreds of genetically identical, physically  
61     and neurophysiologically integrated pulsatile zooids (Bone et al. 1980, Mackie 1986). Zooids in  
62     the colony feed and propel themselves by drawing water in through the oral siphon, using muscle  
63     contraction to compress their pharyngeal chamber, and ejecting a jet of water from their atrial  
64     siphon (Bone & Trueman 1983). While solitary oozooids move using single-jet propulsion, salp  
65     blastozooid colonies integrate multiple propelling jets, which increases their thrust and reduces  
66     the drag that results from periodical acceleration and deceleration via asynchronous swimming  
67     (Sutherland & Weihs 2017).

68       Currently, there are 48 described species of salps (WoRMS, 2024) and while salps are  
69 widely distributed, most species are restricted to open ocean environments, far from the coast,  
70 which poses unique challenges to accessing them for direct study in their environment (Hamner  
71 et al 1975, Haddock 2004). Moreover, salps cannot be maintained alive in containers beyond a  
72 few hours since they are extremely fragile and sensitive to the presence of solid walls. Therefore,  
73 many morphological, ecological, and functional aspects of salp diversity, such as swimming  
74 speeds and metabolic demands, have remained unexplored. One such aspect is colonial  
75 architecture or the way that the zooids are arranged relative to each other in the colony. Salp  
76 colonies develop into species-specific architectures with distinct zooid orientations, including  
77 transversal, oblique, linear, helical, and bipinnate chains; as well as whorls, and clusters (Damian-  
78 Serrano & Sutherland, 2023). These architectures likely drive aspects of swimming performance  
79 (Madin 1990, Damian-Serrano et al. 2023).

80       Linear salp chains have been described as more efficient swimmers due to the reduction  
81 of drag associated with a more streamlined form (Bone & Trueman 1983). In a multi-jet system,  
82 having a larger number of propellers can improve the hydrodynamic and inertial benefits granted  
83 by asynchronous multijet propulsion, in addition to providing additional thrust to the colony (Madin  
84 1990, Sutherland & Weihs 2017). The effect of varying numbers of propeller zooids on swimming  
85 speed has never been investigated in salps, nor how this relationship may vary across their  
86 diverse colonial architectures. Salp colonial architectures differ in how the number of zooids in  
87 the colony scales with their frontal area relative to motion (Madin 1990). Some architectures  
88 (linear, bipinnate, and helical) have a constant frontal area, regardless of zooid number. These  
89 architectures may benefit from increased thrust delivered by larger numbers of zooids while  
90 maintaining a constant frontal area. However, the rest of the architectures (oblique, transversal,  
91 whorl, and cluster) have an increasing (directly proportional) frontal area as the number of zooids  
92 increases (Fig. 1). Therefore, we expect the latter architectures to not only obtain more thrust, but  
93 to also experience more frontal water resistance as zooid number increases. As a result, we  
94 anticipate that swimming speed will be greater in colonies that bear a larger number of zooids,  
95 but only (or more so) for species with architectures that have a constant frontal area.

96

	Transversal	Whorl	Cluster	Helical	Oblique	Linear	Bipinnate
Architecture							
							
Frontal area 4 zooids							
Frontal area 8 zooids							
Scaling	2	2	2	1	1<<2	1	1

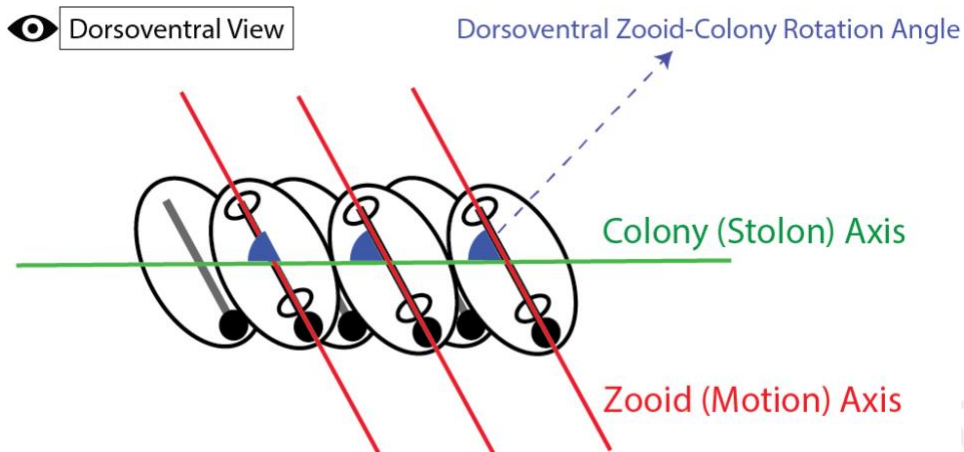
97      Figure 1. Salp colonial architectures with representative species photos (*Pegea* sp. for  
98      transversal, *Cyclosalpa affinis* for whorl, *Cyclosalpa sewelli* for cluster, *Helicosalpa virgula* for  
99      helical, *Thalia cicatricosa* for oblique, *Soestia zonaria* for linear, and *Ritterella retracta* for bipinnate)  
100     and diagrams showing the distinct zooid orientations. The subsequent rows show the frontal view  
101     of colonies with four and eight zooids, with the final row indicating the expected frontal area  
102     increase factor between the four and the eight zooid colonies. Full black circles in the diagrams  
103     represent viscerae (guts) while the open circle represent siphons. Black straight lines inside the  
104     zooids indicate gill bars while gray straight lines represent endostyles.

105     Linearity of colonies, as well as zooid size and pulsation rates, are additional factors that  
106     could influence swimming performance. The degree of linearity in a colony can be expressed as  
107     the degree of parallelism between the zooids and the elongation axis of the colony (Fig. 2). This  
108     angle is determined by the degree of developmental dorsoventral zooid rotation, which can span  
109     from 90°, in transversal chains with no rotation, to 0° (perfect linearity), in some linear chains such  
110     as those from the species *Soestia zonaria* (Damian-Serrano & Sutherland, 2023). Strong  
111     reductions in the dorsoventral zooid rotation angle toward linear forms have evolved multiple  
112     times independently (Damian-Serrano et al. 2023), possibly due to adaptive advantages related  
113     to their swimming efficiency. Body size predicts swimming velocity in many animals (Andersen et  
114     al. 2016), however colonies with multiple swimming units may circumvent this size-speed  
115     relationship by having multiple propellers. Pulsation rates may also influence swimming speed as  
116     has been shown in solitary salps (Madin 1990). Pulsation by salps serves the dual role of  
117     locomotion and filter feeding. The relationship between pulsation and speed might therefore be  
118     particularly relevant for species that undergo diel vertical migration (Madin et al. 1996) and in  
119     other species pulsation may serve to maximize filtration rates. Considering the tradeoffs between  
120

121 swimming and filtering, the eco-evolutionary relevance of swimming speed, and the hydrodynamic  
122 efficiency likely varies between species (Damian-Serrano et al. 2023).

123

124



125  
126 Figure 2. Schematic of an oblique chain from the dorsoventral perspective showing the zooid and  
127 stolon axes and the zooid rotation angle (degree of linearity) relative to those axes. Black lines  
128 indicate gill bars (mostly occluded by zooid axis) while gray lines represent endostyles.

129 The energetic costs of salp locomotion from mechanically estimated propulsive efficiency  
130 suggest that like other jet-propelled swimmers, salps are hydrodynamically efficient (Sutherland  
131 & Madin 2010, Gemmell et al. 2021, Trueman et al. 1984). The few metabolic measurements of  
132 swimming salps show that more active species-- in terms of swimming speed and pulsation rates--  
133 have the highest respiration rates (Cetta et al. 1986) and that salps have higher respiration rates  
134 than other gelatinous taxa (Biggs 1977, Schneider 1992, Mayzaud et al. 2005, Trueblood 2019).  
135 However, the specific costs incurred by their swimming activity and their relationship to swimming  
136 speed have never been examined across the diversity of salp species.

137 In this study, we compare swimming speeds across 17 salp species and energetic costs  
138 of swimming across 15 species, encompassing all seven known salp colony architectures (Fig. 1,  
139 Table S1). In addition, we investigate how swimming speed varies with the number of propeller  
140 zooids and differences in frontal area scaling between colonial architectures. Finally, we compare  
141 cost of transport (COT) across salp species and assess how COT scales with swimming speed  
142 and pulsation effort.

143

#### 144 Materials and Methods

145         *Fieldwork* – We observed salps via 48 bluewater SCUBA dives (Haddock & Heine, 2005)  
146 from a small vessel off the coast of Kailua-Kona (Hawai'i Big Island, 19°42'38.7" N 156°06'15.8"  
147 W), over 2000 m of offshore water during September 2021, April 2022, September 2022 and May  
148 2023. We spent a total of 42.2 hours (84.4 person hours: ADS & KRS) collecting and imaging  
149 salp colonies. Some dives were diurnal, where we collected most of the specimens of *Iasis*  
150 *cylindrica*, *Cyclosalpa affinis*, *Cyclosalpa sewelli*, and *Brooksia rostrata*. We observed and  
151 collected most specimens of other species during night dives (blackwater diving). We recorded in  
152 situ underwater videos of salp colonies swimming using a variety of cameras including primarily  
153 a dark field stereovideography system (Sutherland et al. 2024), as well as a lightweight dual  
154 GoPro stereo system, a brightfield single-camera system (Colin et al. 2022), and a darkfield  
155 single-camera system. The primary stereovideography system was comprised of two  
156 synchronized high-resolution cameras (Z Cam E2, Nan Shan, Shenzhen, China and Sync Cable;  
157 4K at 60 or 120 fps) with 17mm f/1.8 lenses (Olympus M.Zuiko Digital) housed in custom  
158 aluminum housings (Sexton Company, Salem, OR, USA). Each field of view was 23 x 42 mm and  
159 in-focus depth was 20-25 mm. The image from the right-hand camera was viewed using an  
160 external monitor (Aquatica Digital, Montreal, Quebec, Canada), and illumination was provided  
161 with two 10,000-lumen lights (Keldan, Bruegg, Switzerland). An L-shaped plastic framer helped  
162 the videographer position colonies in the field of view of both cameras. Before diving, the stereo  
163 system was calibrated in a swimming pool using a cube with reflective landmarks. Calibration  
164 images were processed using the CAL software package (SeaGIS measurement science,  
165 Bacchus Marsh, Victoria, Australia). Over the course of the study, we observed 241 salp colonies  
166 (N) from 18 species and recorded 1,946 measurements (n) (Dataset1A, Table S1). Throughout  
167 the manuscript, we refer to the number of specimens as N and the number of measurements as  
168 n.

169         *Measuring salp colony swimming speed* – For most species, we collected and analyzed  
170 footage from multiple specimens (Dataset1A, Table S1). We analyzed the swimming behavior of  
171 salp colonies arranged in linear (six species, 64 specimens), bipinnate (three species, 17  
172 specimens), whorl (three species, 10 specimens), cluster (two species, eight specimens), and  
173 transversal (one species, two specimens) architectures, with oblique and helical architectures  
174 represented by a single specimen. We used a combination of spatially calibrated stereo video  
175 and 2D videos with a reference scale in the frame. From the stereo videos, we manually selected  
176 and measured the relative XYZ positions of salp colony zooids in EventMeasure (SeaGIS). We  
177 implemented a cutoff in the RMS (root mean squared) point error estimate of < 2 mm.

178 We complemented gaps in taxon sampling with archived 2D videos in the lab from  
179 previous expeditions to West Palm Beach (FL, USA) and the Pacific coast of Panama. These two-  
180 dimensional single-camera videos were collected using a Sony FDR-AX700 4K Camcorder  
181 (3840x2160 pixels, 60-120 fps) with a Gates Underwater Housing (Poway, CA, USA) using  
182 brightfield illumination (Colin et al 2022) or darkfield illumination. For these 2D videos, we used  
183 the FFmpeg plugin in ImageJ to manually select and measure the relative XY positions of salp  
184 zooids in sequences where the colony was swimming horizontally within the focal plane. The  
185 colonies were assumed to be in the same plane as the scale bar so at same distance from the  
186 camera. However, in videos with a broad focal depth, this may not always had been the case,  
187 thus potentially introducing some measurement error.

188 We tracked and manually selected the position of the first zooid's viscera (using a contrast-  
189 based centering macro to mark the center point) as well as the position of a reference particle in  
190 the water (methods described in Sutherland et al. 2024) in 10-30 frames across 50-500 frame  
191 windows spanning 2-4s of swimming on the synchronized left and right videos in EventMeasure.  
192 The reference particle was a non-swimming organism (such as a foraminiferan or radiolarian) or  
193 a non-living particle. In addition, we recorded the pulsation rates of the specimens measured by  
194 counting the number of times the atrial siphon contracted in a known period. For each analyzed  
195 frame, we calculated the horizontal x, vertical y, and depth z (in the case of the stereo video  
196 measurement files) components of the relative positions of the frontal zooid to the reference  
197 particle as shown in Eq. 1.

$$\begin{aligned} x &= n_{animal} - n_{particle} \\ y &= n_{animal} - n_{particle} \quad \text{Eq. 1} \\ z &= n_{animal} - n_{particle} \end{aligned}$$

203 Then we calculated the instantaneous relative speeds of the frontal zooid using Eq. 2  
204 (without the z component in the case of the 2D videos) given the known frame rate of each video.  
205

$$U = \frac{\sqrt{(x_2 - x_1)^2 + (y_2 - y_1)^2 + (z_2 - z_1)^2}}{t_2 - t_1} \quad \text{Eq. 2}$$

207  
208 *Salp colonial architecture* – To examine the relationships between locomotory variables  
209 and colonial architecture, we adopted the species-specific architecture characterizations and  
210 dorsoventral zooid rotation angle measurements for each species from Damian-Serrano et al.

211 (2023). Using stills from the underwater videos, we measured zooid length, zooid width, and  
212 number of zooids in ImageJ manually selecting the point coordinates. These measurements were  
213 repeated in at least three locations from each colony. When a distinct zooid size gradient was  
214 observed, we measured zooids in locations from the proximal, middle, and distal regions to  
215 capture the full range of variation in the specimen.

216 *Respiration measurements* – We collected healthy, adult blastozooid (aggregate stage)  
217 colonies across 18 salp species (Dataset S1B) during blue- and black-water SCUBA dives off the  
218 coast of Kona (Hawaii, USA) between September 2021 and May 2023. We analyzed the  
219 respiration rates of salp colonies arranged in linear (seven species, N = 46), bipinnate (three  
220 species, N = 29), whorl (three species, N = 23), cluster (two species, N = 18), and transversal  
221 (one species, N = 13) architectures, oblique chains (*Thalia* sp., N = 7), and helical architectures  
222 represented by *Helicosalpa virgula* (N = 2). Specimens were sealed *in situ* with their surrounding  
223 water in plastic jars equipped with a PreSens oxygen sensor spot (Regensburg, Germany) and a  
224 self-healing rubber port to allow for the injection of solutions without the introduction of air bubbles.  
225 We removed as many symbiotic animals from the salps as possible before closing the lid without  
226 damaging the colony. The same method was applied to one or more seawater controls to account  
227 for the oxygen demand of the local seawater's microbiome. Several collection events occurred  
228 during each 20-60 min long SCUBA dive. Jars with larger animals were opened during the safety  
229 stop to allow them to re-oxygenate. Upon the divers' return to the boat, we measured the initial  
230 oxygen concentration (mg/l) and temperature, and then repeated the measurements at intervals  
231 between 15min and 3h, for total periods ranging between 2h and 5h, depending on logistic  
232 constraints in the field and the rate of oxygen depletion. The exact interval time for each  
233 measurement was variable but recorded (Dataset S1B).

234 To estimate the energetic expenditure of different salp species while actively swimming,  
235 we recorded the oxygen consumption of intact specimens while swimming inside the jar. To obtain  
236 a baseline of basal respiration rate (while not swimming), we anesthetized some specimens  
237 before the start of the first oxygen measurement time. A few specimens were used for paired  
238 experiments, where their swimming respiration was recorded for a few hours, then inoculated with  
239 the anesthetic, and recorded anesthetized for another set of hours. To anesthetize salps, we  
240 injected their jars with small volumes of concentrated (50 g/l) bicarbonate-buffered MS-222  
241 through the rubber ports on the lids. We tailored the injection volume to the jar size aiming for a  
242 final concentration of 0.2g/l, following the methods in Trueman et al. (1984). We also injected  
243 some seawater control jars to evaluate the effect of MS-222 on oxygen concentration in seawater  
244 and found no effect.

When multiple seawater controls were collected using jars of different sizes, we paired each jar with the control that had the most similar volume. If among multiple controls only some were jars injected with anesthetic, we paired the anesthetized specimen jars with the injected controls and the intact specimen jars with the intact controls. In experiment 26 (see Dataset S1B for experiment numbers), the control jar was lost due to an encounter with an oceanic white tip shark, thus we paired those measurements with the nearest relative time points from the control jar in experiment 25, collected the same day hours earlier. At the end of each experiment, we identified the salp specimens used in the experiments to the species level, counted the number of zooids, measured the zooid length (total length including projections), and measured the biovolume of the colony using a graduated cylinder. For those specimens where colony or zooid volume was not measured directly, we estimated the colony volume from their zooid length and the number of zooids using a Generalized Additive Model with the measured specimens.

We estimated the oxygen consumption rate for each specimen by fitting a linear regression of consumed oxygen mass (concentration by container volume) against the duration of the measurement series. We subtracted the slope calculated for the relevant control jar to the estimated slope of the animal jar. Since our seawater controls were not filtered, some experiments had abnormally high estimated background respiration rates, leading to negative values. We removed these data points before the analysis. To estimate biovolume-specific rates, we divided the rates by the colony volumes. We then compared the biovolume-specific respiration rates of active (swimming) and anesthetized specimens within each species, calculating the difference as a measure of biovolume-specific swimming cost respiration rate. Biovolume was used instead of dry mass to normalize measurements due to the inherent difficulties of accurately measuring dry mass of these fragile gelatinous organisms in the field. Biovolume provides a consistent and reliable measure of the live size of the colony, which is directly relevant to the volume of water being displaced during swimming. We also calculated the relative investment in swimming as the proportion of biovolume-specific respiration rate comprised by the swimming-specific rate. To capture variability within species, we calculated the mean respiration rate of anesthetized specimens for each species and subtracted it from each intact specimen's total respiration rate to get multiple swimming-specific rate values within each species. We noticed that some species had higher average respiration rates among the anesthetized specimens than among the swimming specimens, leading to negative swimming-specific respiration estimates. We interpreted this anomaly as a systematic error due to the extremely low respiration rates of some species that fall within the effective detection limit of our experimental setup given the random variation range of respiration rates in seawater both in experimental jars and in control jars. Small

279 absolute negative values get amplified into large relative values, especially in small animals with  
280 a minuscule biovolume denominator. Therefore, we removed the swimming specimens that had  
281 lower respiration rates than the mean anesthetized respiration rate for their species. We also  
282 removed two respirometry outliers of *Thalia* sp. which had extremely high swimming respiration  
283 rates (>7500 pgO<sub>2</sub>/ml/min, whereas all other measurements across species including other  
284 *Thalia* sp. were limited to 0-1700 pgO<sub>2</sub>/ml/min), which were likely due to amplification of  
285 experimental error (presence of organic matter or symbionts, underestimation of colony volume  
286 due to loss of tiny zooids in the sieves) with the small biovolume denominators in this species.

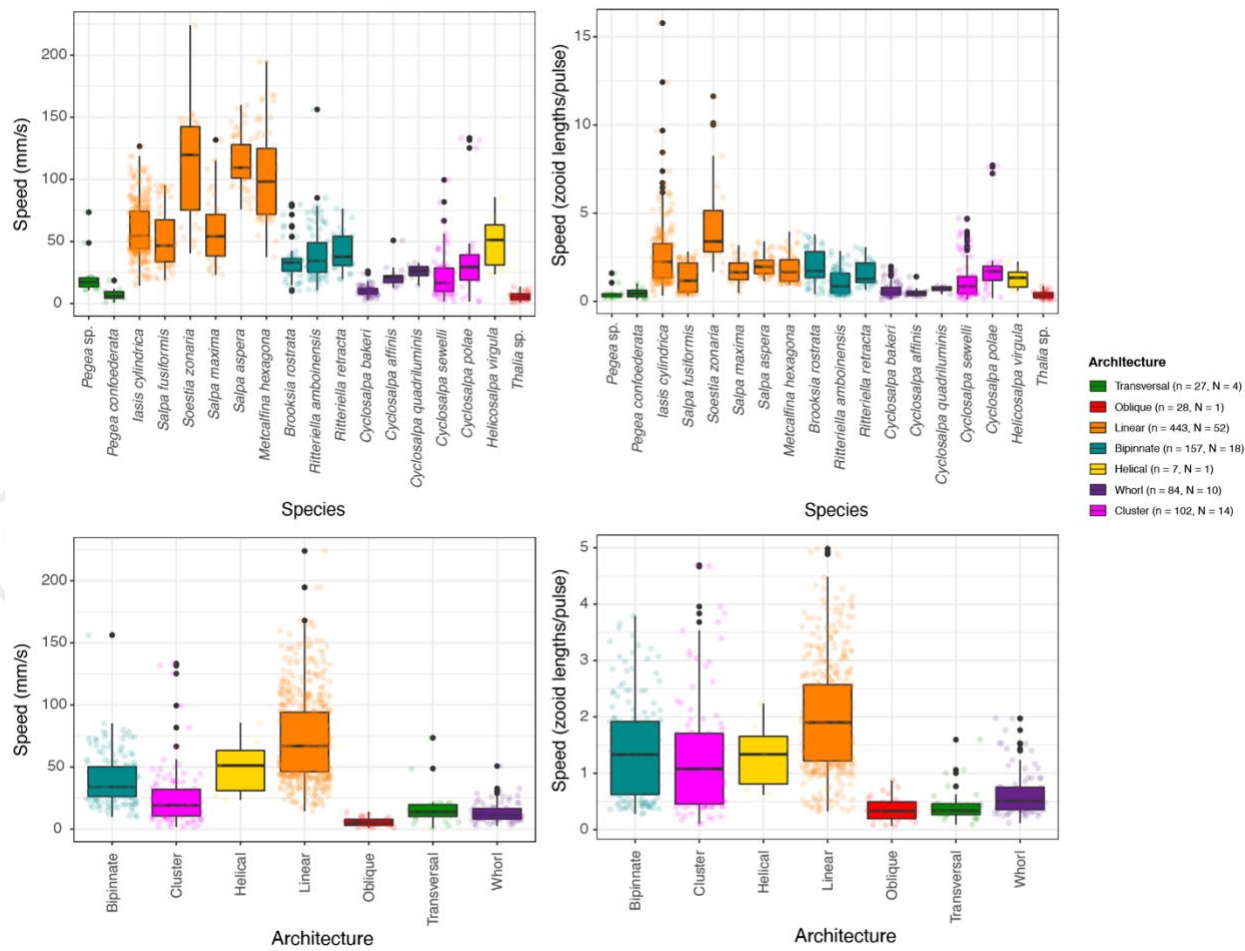
287 *Estimating costs of transport* – We define the cost of transport (COT) as the amount of  
288 oxygen consumed per tissue volume per distance traveled by the colony. To estimate the COT,  
289 we divided the swimming-specific respiration rates by the mean swimming speed for each species  
290 measured from the stereo and 2D video data. Since the specimens used for speed measurements  
291 in the videos and those used in the respirometry experiments had different zooid sizes, we used  
292 the mean zooid-lengths per second speeds from the video measurements and then multiplied  
293 them by the actual zooid lengths of the respirometry specimens to estimate their absolute (mm/s)  
294 speeds. Pulsation rate estimates were taken from species averages from the video specimens.  
295 We also calculated the size-specific COT by transforming the swimming distances into zooid  
296 lengths measured from the respirometry specimens.

297 *Statistical Analyses* – All data wrangling and statistics were carried out in R 3.6.3 (R Core  
298 Team 2021). To test for differences between architectures, we used ANOVAs with Tukey's post-  
299 hoc pairwise contrasts, reporting the difference magnitude and the adjusted p-value in  
300 supplementary tables S2A and S2B. To test the relationships between pairs of continuous  
301 variables across architectures (e.g. swimming speed vs. number of zooids), we used linear  
302 regressions. We evaluated the significance of the slope parameter when compared against a flat  
303 slope (one-tailed t-test) to test whether changes in the independent variable (e.g. number of  
304 zooids) were associated with changes in the dependent variable (e.g. swimming speed). Owing  
305 to the patchiness of some species despite 80+ hours spent underwater (Table S1), we used  
306 replicate measurements (n) from each specimen (N) in swimming speed ANOVAs and  
307 regressions. We used an exponential regression to test the relationship between speed and COT.  
308 Specimen means (N) were used for all COT comparisons and regressions. Individual  
309 measurements (n) were used up to determine oxygen consumption rates. To evaluate the relative  
310 contribution of zooid size, pulsation rate, zooid number, and architecture type on swimming  
311 speed, we fitted a generalized linear model and evaluated the significance and proportion of  
312 variance explained by each factor using their partial R<sup>2</sup>.

313

314 **Results**

315 Salp colony swimming speeds, pulsation rates, and respiration rates varied within and  
 316 across species and colony architectures. When considering speed in terms of mm/s, we found  
 317 a relationship between pulsation rate (effort) and absolute speed ( $n = 947$ ,  $N = 111$ , 18  
 318 species, Speed mm/s =  $0.41 \times$  Pulsation rate + 52.14,  $p < 0.0001$ , Fig. S1A), as well as with  
 319 zoid-size corrected swimming speed ( $n = 848$ ,  $N = 100$ , 18 species, Speed zoid lengths/s  
 320 =  $0.96 \times$  Pulsation rate + 1.73, adjusted  $R^2 = 0.18$ ,  $p < 0.0001$ , Fig. S1B). Normalized swimming  
 321 speeds (zoid lengths per pulse) allow for a more direct comparison of swimming speed across  
 322 colonial architectures.



323

324 Figure 3. Boxplots showing the absolute (A) and corrected for body size and pulsation rate (B)  
 325 swimming speeds recorded for each salp species and architecture (C, D) respectively. Colors  
 326 correspond to colonial architecture types. Sample sizes are included in the legend and Tukey's

327 post-hoc pairwise comparisons across architecture types are listed in Dataset 1A and Table S2A,  
328 respectively.

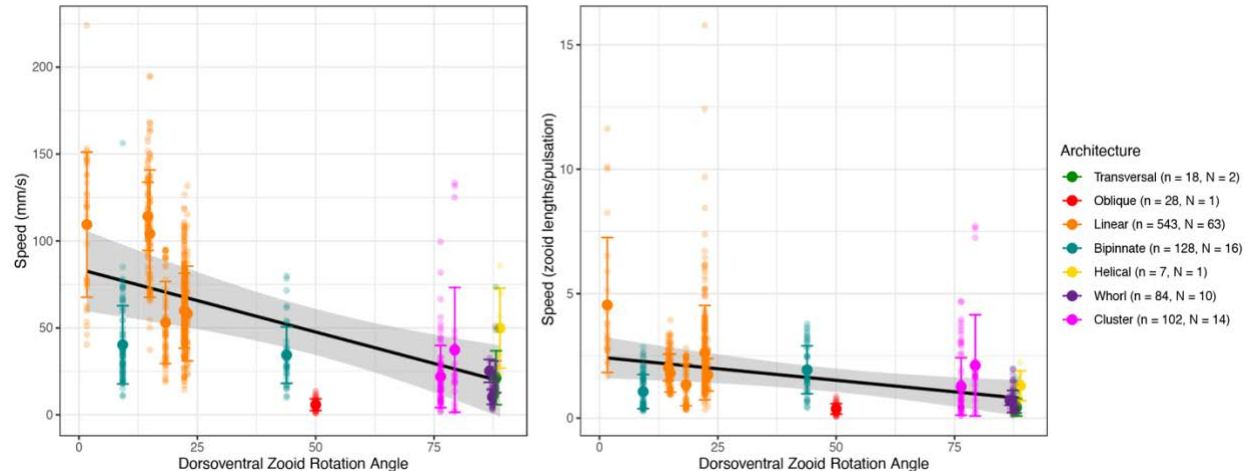
329

330 *Swimming speeds across salp architectures*

331 Swimming speed varied significantly (5 architectures, 16 species, N = 109, n = 913,  
332 ANOVA F > 38, p < 0.001) between colonial architecture types (Fig. 3C, D, Table S2A). Speeds  
333 measured with 2D methods were slightly slower than those measured with 3D methods within the  
334 species in which they overlapped. This is to be expected since 2D methods cannot account for  
335 the z (depth) component of the speed vector. Measurements of helical and oblique chains were  
336 limited to a single specimen, so they were excluded from the analysis. In terms of absolute speed  
337 (mm/s), linear architectures were significantly faster than every other architecture (Tukey's p <  
338 0.001). While bipinnate chains were significantly slower than linear chains, they were significantly  
339 faster than transversal chains, clusters, and whorls (Tukey's p < 0.002). Clusters were not  
340 significantly faster than transversal chains nor whorls. Transversal chains were on par to whorls,  
341 with no significant differences between them.

342 In terms of relative speed (zooid lengths/pulse), linear architectures were significantly  
343 faster than every other architecture (Tukey's p < 0.001). Bipinnate chains were significantly faster  
344 than whorls and transversal chains (Tukey's p < 0.01), but not significantly different from clusters.  
345 Clusters were significantly faster than whorls (Tukey's p < 0.001) in relative speed. Whorls and  
346 transversal chains presented similar relative swimming speeds with no significant differences.

347 Since linear architectures had the fastest mean swimming speeds (Fig. 3C, D), we  
348 investigated the relationship between swimming speeds with the dorsoventral zooid rotation  
349 angle, which represents the degree of linearity of the colony (Fig. 4). Species with more parallel  
350 (lower angles) dorsoventral zooid rotation presented faster absolute speeds (n = 910, N = 107,  
351 16 species, Speed mm/s = -0.78\*DV Zooid angle + 81.25, adjusted R<sup>2</sup> = 0.33, p < 0.0001) and  
352 faster size-and-effort corrected swimming speeds (n = 810, N = 96, 16 species, Speed  
353 zooids/pulse = -0.016\*DV Zooid angle + 2.37, adjusted R<sup>2</sup> = 0.09, p < 0.0001).

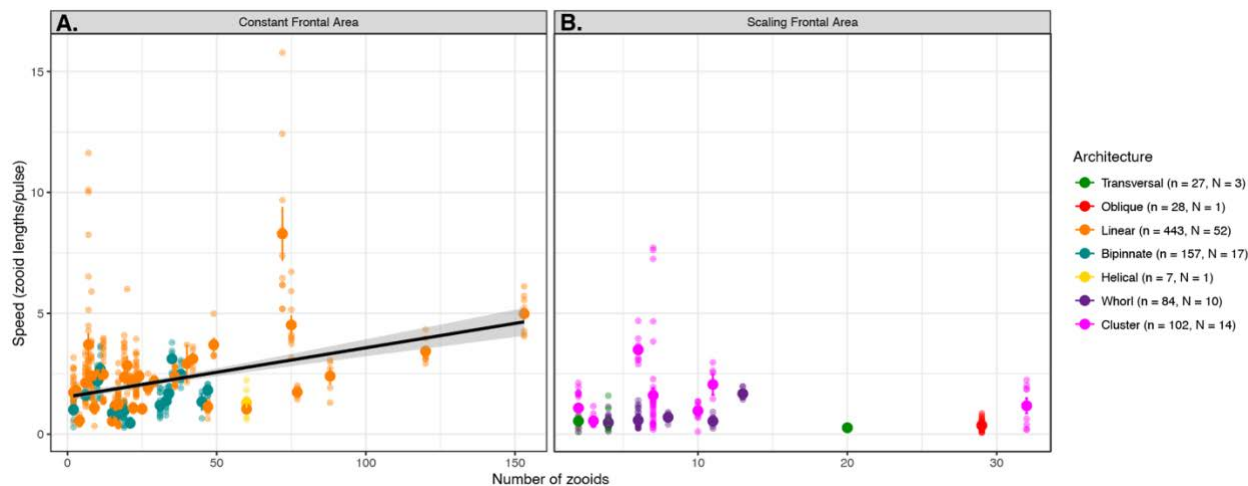


354  
355 Figure 4. Absolute (A) and relative (B) colony swimming speed (specimen mean with standard  
356 errors, total n=103) for each salp species across their degree of dorsoventral zooid rotation. Error  
357 bars indicate standard error. The color indicates colonial architecture. Gray areas indicate the  
358 95% confidence interval of the linear regression (black line).

359  
360 We compared how swimming speeds scale with the number of zooids in the colony and  
361 found differences between colonial architectures. Swimming speed in whorls increased with  
362 number of zooids ( $n = 84$ ,  $N = 10$ , 3 species, Speed mm/s =  $0.08 \times \text{Number of zooids} + 0.12$ ,  
363 adjusted  $R^2 = 0.3$ ,  $p < 0.0001$ ), though the data for this architecture was limited to small numbers  
364 of zooids (4 to 13) and relatively slow speeds (under 51 mm/s). Linear chain architectures did  
365 increase in relative speed with the number of zooids ( $n = 443$ ,  $N = 52$ , 6 species, Speed mm/s =  
366  $0.02 \times \text{Number of zooids} + 1.77$ , adjusted  $R^2 = 0.14$ ,  $p < 0.001$ ), as did bipinnate chains ( $n = 157$ ,  
367  $N = 18$ , 3 species, Speed mm/s =  $0.015 \times \text{Number of zooids} + 1.05$ , adjusted  $R^2 = 0.04$ ,  $p < 0.02$ ).  
368 This relationship was not significant for any of the other architectures.

369 We pooled the data from multiple architectures into scaling modes to evaluate the overall  
370 relationship in colonies with a constant frontal area (linear, bipinnate, and helical species) and in  
371 colonies with scaling frontal area (transversal, whorl, cluster, and oblique species) with linear  
372 regressions (Fig. 1). This aggregation allowed the inclusion of data from architectures for which  
373 we only have one specimen (helical and oblique). When pooled by scaling mode (Fig. 5), the  
374 regression on colonies with a constant frontal area had a higher intercept on the swimming speed  
375 axis than in those with a scaling frontal area (1.54 and 1.09 zoid lengths/pulse, respectively),  
376 reflecting the generally higher swimming speed of the former. Moreover, the regression on  
377 colonies with constant frontal area had a significant positive slope ( $n = 607$ ,  $N = 71$ , 10 species,  
378 Speed mm/s =  $0.02 \times \text{Number of zooids} + 1.55$ , adjusted  $R^2 = 0.12$ ,  $p < 0.001$ ), while the regression

379 on those with scaling frontal area was not significant ( $n = 241$ ,  $N = 29$ , 8 species,  $p = 0.073$ ).  
 380 However, the limited sample sizes for helical and oblique chains prevent us from drawing firm  
 381 conclusions about these architectures.



382  
 383 Figure 5. Linear relationships between relative swimming speed (zoid lengths per pulsation,  
 384 specimen mean with standard errors) and number of zooids in the colony for constant (A) and  
 385 scaling ( $N=71$ ) (B) frontal motion-orthogonal frontal area ( $N=29$ ) scaling modes. Gray areas  
 386 represent the 95% confidence intervals of the regressions.

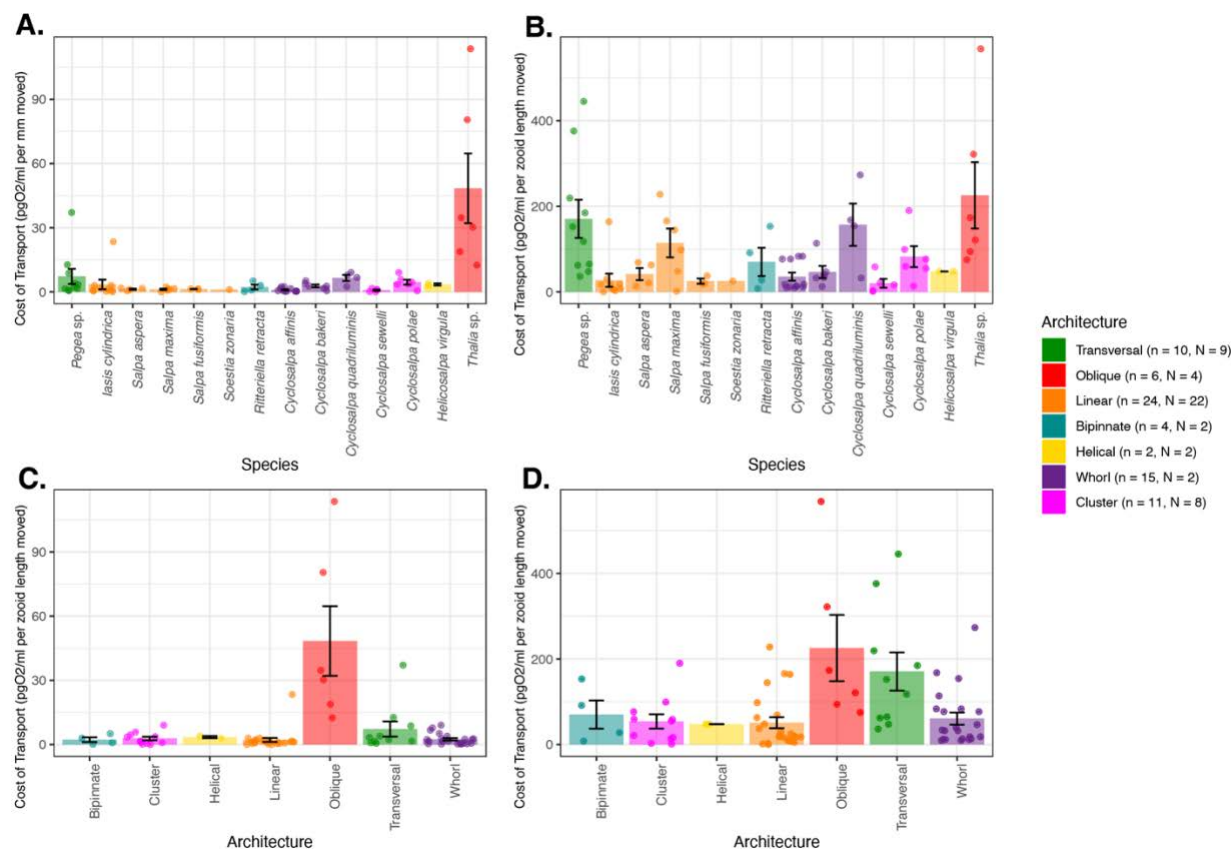
387  
 388 Putting together all the different organismal factors that we analyzed in this study, we  
 389 calculated a generalized linear regression model to predict absolute salp swimming speed ( $U$ )  
 390 from zooid length ( $L$ ), pulsation rate ( $P$ ), number of zooids ( $Z$ ), and colonial architecture  
 391 represented as frontal area scaling mode ( $A$ ) as expressed in Eq. 3. While our results suggest  
 392 that the effect of  $Z$  depends on  $A$ , we favored this simpler regression formula because it had a  
 393 significantly lower ( $\Delta > 70$ ) AIC score than those with interaction terms between  $Z$  and  $A$ .

394 
$$U \sim L + P + Z + A \quad \text{Eq. 3}$$

395 In this global model, we found significant effects on swimming speed (848 measurements,  
 396 100 videos, 18 species,  $U = 0.29L - 0.60P - 0.2Z - 50.34A$ ,  $\text{pseudo-}R^2 = 0.37$ ,  $p < 0.001$ ) for  $L$ ,  
 397  $Z$ , and  $A$ . We found that our global regression explains 36.8% of the variance in our swimming  
 398 speed data: 5.8% is explained by zooid size, 3.5% by pulsation rate, 0.8% from zooid number,  
 399 and 26.6% by the frontal scaling mode.

400  
 401 *Respiration rates and cost of transport (COT)*  
 402 The respiration rates of swimming and anesthetized salps revealed broad differences  
 403 between species (Fig. 6, S2A). After estimating COT, we found a few significant differences

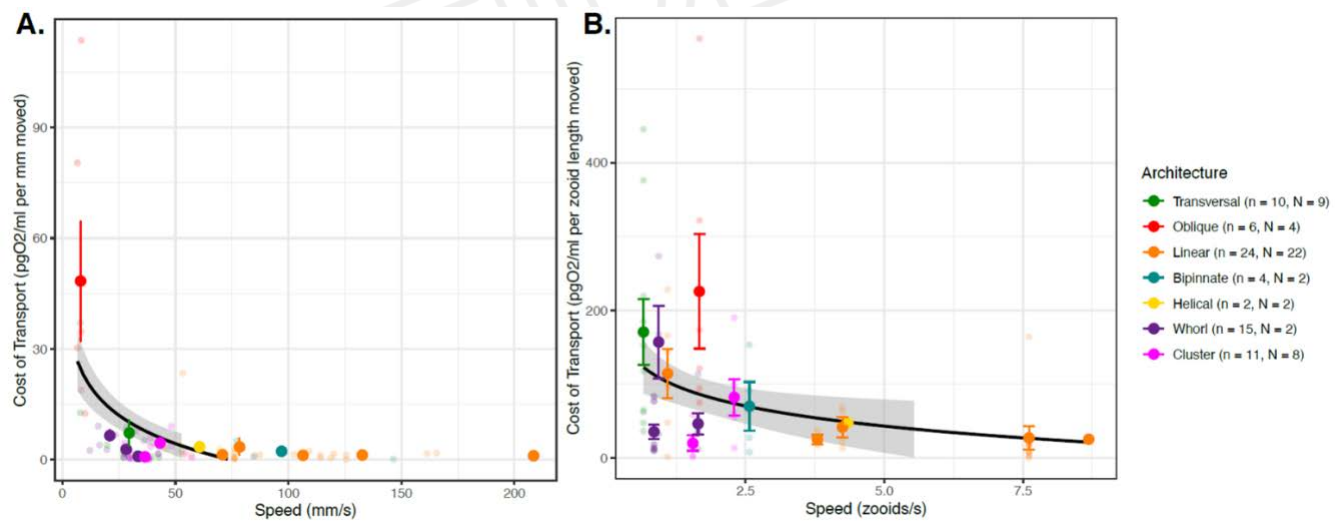
404 between architectures (Fig. 6, ANOVA  $F > 5.9$ ,  $p < 0.001$ , Table S2B). In terms of absolute COT  
 405 per mm traveled, all architectures except oblique chains had similar high transport efficiencies  
 406 under 13 pgO<sub>2</sub>/ml. Every one of these architectures was significantly more efficient per mm  
 407 traveled than oblique architectures (Tukey's  $p < 0.001$ ). In terms of relative COT per zooid length  
 408 traveled, linear chains, clusters, and whorls had similar transport efficiencies that are significantly  
 409 faster than transversal and oblique chains (Tukey's  $p < 0.05$ ). Some of the differences between  
 410 COT per mm and COT per zooid length are likely due to scaling with body size, as can be  
 411 observed with the relative shift in the minuscule *Thalia* sp. (5.2 mm zooids) and the massive *Salpa*  
 412 *maxima* (93.4 mm zooids).



413  
 414 Figure 6. Mean cost-of-transport per mm (A) and per zooid length (B) moved for each salp  
 415 species, and for each colonial architecture (C, D) with standard errors. Bar colors indicate colonial  
 416 architecture. Sample sizes and Tukey's post-hoc pairwise comparisons across architecture types  
 417 are listed in Dataset 1B and Table S2B, respectively.

418  
 419 When comparing the proportion of investment of metabolic costs into swimming  
 420 (compared to the species mean baseline) across salp species (Fig. S2B), eight species had  
 421 locomotion budgets under 50%, and the other seven have budgets above 50%. We then

422 compared the proportion of energetic investment in swimming to the COT values across species  
 423 (Fig. S3A,B). We found no relationship with absolute COT ( $N = 74$ , 14 species,  $p = 0.24$ ). We  
 424 found a positive relationship with zooid-length scaled COT ( $N = 74$ , 14 species, Swimming % =  
 425  $0.11 \times \text{COT per zooid length} + 34.4$ , adjusted  $R^2 = 0.22$ ,  $p < 0.001$ ), indicating that species with  
 426 more costly locomotion per zooid length invest a larger proportion of their energy budget in  
 427 swimming. Finally, we compared the proportion of energetic investment in swimming with speed  
 428 (Fig. S3C,D). We found no relationship (neither in mm/s nor in zooids/s), indicating that faster  
 429 swimmers do not invest more of their energy budget into their locomotion efforts. We found that  
 430 regardless of whether we consider transport in terms of absolute distances (Fig. 7A,  $N = 64$ , 14  
 431 species, linear regression: COT per mm =  $-0.12 \times \text{Speed mm/s} + 13.46$ , adjusted  $R^2 = 0.09$ ,  $p <$   
 432 0.005; exponential regression:  $\log\text{COT per mm} = -0.015 \times \text{Speed mm/s} + 1.39$ , adjusted  $R^2 = 0.14$ ,  
 433  $p < 0.001$ ) or relative to body lengths (Fig. 7B, 64 specimens, 14 species, linear regression COT  
 434 per zooid length =  $-12.9 \times \text{Speed zooid lengths/s} + 116.1$ , adjusted  $R^2 = 0.07$ ,  $p < 0.01$ , exponential  
 435 regression  $\log\text{COT per zooid length} = -0.24 \times \text{Speed zooid lengths/s} + 4.28$ , adjusted  $R^2 = 0.14$   $p$   
 436  $< 0.001$ ), the COT decreases in species with faster swimming speeds.  
 437  
 438



439  
 440 Figure 7. COT (specimen mean with standard error,  $n=75$ ) per mm (A) and zooid length (B) moved  
 441 across the specimen mean absolute (A) or relative (B) swimming speeds. The dot color indicates  
 442 colonial architecture. Gray areas represent the 95% confidence intervals of the exponential  
 443 regressions (black lines).

444

## 445 Discussion

446 We compared the swimming speeds and costs of transport of salp colonies across the  
447 most comprehensive representation of salp species diversity. Our results show a wide range of  
448 colonial swimming speeds across salp species and architectures with linear species swimming  
449 fastest (Fig. 3). Moreover, this study shows for the first time how salp colonial swimming speed  
450 scales with the number of zooids in the colony (Fig. 5), suggesting that incremental propulsive  
451 power from additional zooids does can produce higher swimming speeds for species with a  
452 constant frontal area. Across species, salps have a low COT (Fig. 6) and as speed increases,  
453 COT decreases (Fig. 7), which may be a unique advantage of multi-jet swimmers.

454 *Architectural determinants of salp swimming speed*

455 Colonial architecture was the strongest predictor of swimming speed, though there is a  
456 large amount of unexplained variation which may relate to species-specific differences,  
457 behavioral, or environmental factors (see global GLM results). We expected that swimming speed  
458 in colonial salps would be predicted by pulsation rate as a measure of swimming effort. Our results  
459 indicate that this relationship only exists when accounting for zooid size (Fig. S1B), suggesting  
460 an underlying relationship between pulsation rate and zooid length that may be masking its  
461 predictive power over absolute speeds. This is consistent with the distribution of our data and our  
462 observations in the field where larger salps pulsate at a slower rate than smaller ones. We find a  
463 significant increase in speed with larger zooid sizes (Fig. S1C,D), consistent with previous findings  
464 of jet propelled invertebrates (Gemmell et al 2021; Bone and Trueman 1983) and more broadly  
465 across aquatic swimmers (Andersen et al. 2016).

466 The relationship between the number of zooids and speed in linear chains is complicated  
467 by shifts in zooid orientation during development. Salp colonies start their free-living phase when  
468 the developing buds detach from the solitary oozooid. The newly released colony has the  
469 maximum number of zooids since the zooid number only gets reduced as the colony splits or  
470 loses zooids to turbulence, disease, or predation. Therefore, colonies with higher numbers of  
471 zooids are typically composed of smaller, younger zooids. In linear architectures, these younger  
472 colonies could still be developing their dorsoventral rotation (Damian-Serrano & Sutherland 2023),  
473 thus effectively being more like oblique architecture. A less acute dorsoventral rotation angle  
474 would explain why these more numerous linear chains are not as fast as we would expect, given  
475 that our results support a significant relationship between this angle and swimming speed (Fig.  
476 4). Finding a strong relationship between zooid number and speed in whorls was surprising given  
477 their less streamlined configuration (Fig. 5). This could be due to the smaller range of slow speeds  
478 and few zooids in the data we obtained for these species. Our regression results on pooled  
479 architectures, as well as finding a significant relationship between number of zooids and speed

480 for linear and bipinnate chains but not for clusters nor transversal chains, support our primary  
481 hypothesis that the different frontal area scaling relationships across architectures has an impact  
482 on swimming speed.

483 Linear chains swam faster than all other architectures, including those that share a  
484 constant frontal area feature like bipinnate chains (Fig. 3, Table S2). One potential explanation  
485 for this difference could come from the relative thrust provided by the jets. Linear chains eject  
486 their jet plumes at very small angles (near parallel) to the axis of locomotion (Sutherland et al.  
487 2024), just wide enough to avoid interaction between jet plumes (Sutherland & Weihs 2017).  
488 Bipinnate and helical chains (both with constant frontal area) have the atrial siphons (point of jet  
489 ejection) of their constituent blastozooids oriented at a wider angle (Madin 1990), which may lead  
490 to wider angles of their jets relative to the axis of locomotion. This in turn would result in a larger  
491 proportion of the force exerted by the jet to be applied as torque rather than thrust onto the colony.  
492 This hypothesis could be tested by measuring the 3D angles of the actual jets instead of the  
493 angles of the zooids since salps can use their atrial muscles and siphon morphology to direct the  
494 angle of their jets.

495 Finding that clusters can swim at speeds comparable to those of bipinnate and helical  
496 chains, even faster than whorls, defies our intuitive understanding of the mechanical properties  
497 of these colonies and thus warrants further investigation into how these species coordinate their  
498 jets to produce forward thrust. While oblique chains are architectural intermediates between  
499 transversal and linear chains (Damian-Serrano & Sutherland 2023), our data indicate that oblique  
500 chains may be the slowest swimmers among salps. This incongruence may be explained by the  
501 fact that we only had speed data from one oblique specimen (of *Thalia* sp.) with very small zooid  
502 sizes. Small salps might operate at notably lower Reynolds numbers than large ones, which may  
503 require a non-linear size correction for meaningful speed comparisons. Swimming speed data  
504 from the much larger oblique chains of *Thetys vagina* may provide a more comparable example  
505 of the locomotory performance of this oblique colonial configuration.

506 The questions addressed in this study focus on the effect of frontal area of colonial  
507 architectures on swimming speed. This effect may be associated with form and pressure drag  
508 differences between more and less streamlined colony shapes. To test whether these are the  
509 forces responsible for differences in swimming speed, drag would have to be measured or  
510 calculated, which is beyond the scope of this study. Other unaccounted forces may be significant  
511 energetic contributors to the system that explain the remainder of the observed variation. Chain  
512 length for the streamlined forms (helical, linear, and bipinnate chains) could have negative effects  
513 on swimming speeds that may partially counteract the positive effect of increased propeller thrust.

514 For example, skin drag increases proportionally to the surface area of the system, and the  
515 smoothness of the chain may increase pressure drag through vortex shredding (Vogel 1981).  
516 While added (virtual) mass could also be an issue, asynchronously swimming colonies do not  
517 suffer as much from these acceleration-related costs, since their speed is maintained near  
518 constant while cruising (Bone & Trueman 1983). Chain length could also lead to reduced stability  
519 and efficiency, though some linear species capitalize on this by swimming in corkscrew orbital  
520 spirals (Sutherland et al. 2024). However, if friction drag, chain stability, or vortex shredding were  
521 indeed more important contributors than frontal form drag, we would predict that linear chains  
522 would appear slower than other more stable and compact architectures. Future studies may  
523 unravel these potential confounding effects on the biomechanics of colonial salp swimming.

524 *Salp swimming speed and diel vertical migration*

525 Salps are important players in the oceanic carbon cycle, grazing upon both phytoplankton  
526 and bacteria (Henschke et al. 2016). Their carcasses and fecal pellets export large quantities of  
527 fixed carbon into the deep sea, accelerating carbon sequestration in the biological carbon pump  
528 (Wiebe et al. 1979, Décima et al. 2023). Part of this process is enhanced by the diel vertical  
529 migrations by some salp species though the distribution of this behavior across species diversity  
530 is poorly known. Off Bermuda, Madin et al. (1996) reported *Pegea* spp., *B. rostrata*, and *C. polae*  
531 as non-migratory, all of which we found to have slow swimming speeds. Other slow-swimmer  
532 species like *C. affinis* were found to only migrate a few meters through the diel cycle. The species  
533 *S. aspera*, *S. fusiformis*, *S. zonaria*, *I. punctata*, and *R. retracta* have been observed vertically  
534 migrating off Bermuda (Madin et al 1996, Stone & Steinberg 2014), which is congruent with our  
535 observations during fieldwork. These species all have constant frontal area and fast swimming  
536 speeds.

537 Vertical migrators need to be fast enough to follow the dark isolumes as they shift during  
538 dawn and dusk in time to maximize their exploitation of the food resources near the surface. Thus,  
539 absolute speed is important to the autoecology of these animals. Other *Salpa* species have also  
540 been reported as strong vertical migrators throughout the literature (Henschke et al. 2021, Madin  
541 et al. 2006, Pascual et al. 2017). A species that does not fit this pattern is *I. cylindrica*, a fast-  
542 swimming non-migratory species that spends night and day near the surface (Madin et al 1996;  
543 and pers. obs.). However, other studies do report moderate diel vertical migration for this species  
544 (Stone & Steinberg 2014), so it may be adapted for facultative vertical migration under specific  
545 oceanographic conditions. Some migratory species, such as *S. aspera*, are known to travel  
546 distances of over 800m at dawn and dusk, at rates predicted to require 5-10 m/min (83-166 mm/s)

547 based on MOCNESS trawl intervals (Wiebe et al. 1979). These predictions are consistent with  
548 the speeds we recorded for this species (88-145 mm/s) and similar congeners.

549 *Ecophysiological implications*

550 While the importance of a few well-studied linear chain salp species in the biological  
551 carbon pump has been delineated, the question of whether this ecological role is generalizable to  
552 other salp species remains unanswered. In addition to vertical migration behavior, another likely  
553 important factor in their carbon flow is their respiration rate. The higher their respiration rate, the  
554 larger the proportion of assimilated carbon that will be released back into the water as dissolved  
555 carbon dioxide. This study provides the broadest taxonomic perspective on respiration rates (18  
556 species, Fig. S2A) and swimming cost of transport (14 species), finding 17-fold differences in their  
557 respiration rates and over 77-fold differences in their mean COT. Except for a few species with  
558 extremely high and low values, most respiration rates are centered between 0.2 and 1  
559  $\mu\text{mol/g/hour}$ , assuming a salp tissue density of 1.025 g/ml. In general, the respiration rates we  
560 estimated for salps are within the range of those reported in the literature (Trueblood 2019, Iguchi  
561 and Ikeda 2004). Compared to the metabolic rates estimated for the broader diversity of marine  
562 pelagic animals (Seibel & Drazen 2007), the rates that we measured for salps are in a similar  
563 range to those measured for *Salpa thompsoni* (Iguchi and Ikeda 2004). Our values are also similar  
564 to those measured by Seibel & Drazen (2007) in nemerteans, chaetognaths, and most fishes (0.1-  
565 1  $\mu\text{molO}_2/\text{g/h}$ ), which are generally higher than other gelatinous animals like ctenophores or  
566 scyphomedusae (0.01-0.1  $\mu\text{molO}_2/\text{g/h}$ ), but generally lower than those of cephalopods,  
567 crustaceans, or large fish (1-10  $\mu\text{molO}_2/\text{g/h}$ ). Salp species known to have strong vertical migration  
568 behaviors (*Salpa* spp., *S. zonaria*, *I. punctata*, and *R. retracta*) have low basal metabolic rates  
569 (Fig. S2A) and low costs of transport. These results indicate that many non-migratory species,  
570 while likely still being important players in the biological carbon pump via their fecal pellet  
571 production, are releasing more of the consumed carbon as carbon dioxide near the surface than  
572 their more metabolically efficient relatives. The ultimate ecological outcome of each species  
573 needs to be assessed holistically, considering their microbial filtration and pellet deposition rate  
574 as well as their relative abundance in the water column.

575 Our metabolically calculated costs of transport range between 5-50 J/kg/m when  
576 converting the mg of oxygen to J via aerobic respiration free energy equations at 23°C. These  
577 values are higher than the highly efficient 1-2 J/kg/m reported for salps in the literature (Bone &  
578 Trueman 1983, Gemmell et al. 2021), and approach the less-efficient values found in single jet-  
579 propelled invertebrates like scallops or squids. We suspect that COT calculated from mechanical  
580 parameters such as the displacement of water mass is not directly comparable to the COT

581 calculated from respiration rates. Furthermore, the standard aerobic respiration free-energy  
582 equation based on glucose may not fully represent the metabolic energy-conversion processes  
583 in salps, which could rely on a combination of sugars and fatty acids derived from their  
584 microscopic prey.

585 While COT increases with swimming speed fishes (Rubio-Gracia et al. 2020) and jet-  
586 propelled squid (Bi & Zhu 2019), multi-jet swimmers may circumvent this tradeoff by having  
587 multiple swimming units. In colonial siphonophores, as zooid number increases swimming speed  
588 increases together with a decrease in COT (Du Clos et al. 2022). Our results show that faster  
589 swimming species have lower COT (Fig. 6), which suggests that faster speeds and higher  
590 locomotory efficiency have a common cause, where both speed and efficiency depend on frontal  
591 area which may partly drive form and pressure drag forces. However, this hypothesis is not  
592 supported by the distribution of COT across architectures (Fig 6C, D), where except for oblique  
593 and transversal chains, all architectures present similarly efficient COT values. Perhaps there are  
594 other underlying explanatory factors linking swimming speed and swimming efficiency, such as  
595 shared ancestry, muscle content, jet coordination, or jetting angles (thrust-to-torque ratios).

#### 596 *Evolutionary implications*

597 Across the evolutionary history of salps, linear chains have evolved multiple times  
598 independently from oblique ancestors (Damian-Serrano et al. 2023), suggesting the adaptive role  
599 of this architecture as a functional trait. Linear chain architectures evolved independently in *M.*  
600 *hexagona*, *S. zonaria*, *I. punctata*, and before the common ancestor of *Iasis* and *Salpa*. Our results  
601 show that going from an oblique form to a linear one may confer significant advantages in  
602 locomotory speed and energetic efficiency. However, multiple colonial architectures, which we  
603 find to be slower swimmers (such as transversal chains, helical chains, whorls, and clusters in  
604 the genus *Pegea* and the Cyclosalpidae family) had also evolved from oblique and linear  
605 ancestors. This is incongruent with a scenario where natural selection strongly favors locomotion  
606 efficiency across all ecological niches of salps. Therefore, the evolution of colonial architecture  
607 may be driven by ecological trade-offs with other non-locomotory functions. Alternatively, in some  
608 of these lineages, locomotion at the colonial stage may not be important enough for selection to  
609 maintain these highly streamlined forms, allowing for neutral evolutionary processes to produce  
610 a diversity of non-adaptive forms. In the current study, we did not use phylogenetic comparative  
611 methods in our analysis because like other investigators comparing biomechanical properties  
612 across species (e.g. Dabiri et al. 2010, DiSanto et al. 2021) we were interested in inherent  
613 mechanical relationships dictated by the colony architectures. For instance, a linear arrangement  
614 of zooids inherently reduces drag due to a cluster arrangement, leading to faster swimming

615 speeds and potentially higher efficiency regardless of phylogenetic history. In other words, any  
616 phylogenetic inertia is irrelevant in instantaneous relationships between traits (Felsenstein 1985).  
617 Moreover, independence of data is often incorrectly assumed to be an assumption of standard  
618 (nonphylogenetic) regressions (Uyeda et al. 2018), when in reality the assumptions relate to the  
619 independence and distribution of the error terms. Thus, when all the phylogenetic signal is present  
620 in the predictor, as it is in the case with colonial architecture (Damian-Serrano et al. 2022) and its  
621 associated characteristics, there is no need for any “phylogenetic correction” (Uyeda et al. 2018).  
622 However, there may be unaccounted factors explaining the residual variation in our analyses that  
623 may bear phylogenetic signal. For example, tunic stiffness, tunic smoothness, muscle band  
624 number, muscle fiber density, swimming behavior, as well as metabolic and physiological  
625 baselines may be more similar between more closely related species, potentially erasing some of  
626 the architecture-specific signal. Future studies could address the role of phylogeny and heritable  
627 factors in salp swimming speed and cost of transport using phylogenetic comparative methods.  
628 These analyses could reveal whether these factors have co-evolved with each other and/or with  
629 respiration rate or colonial architecture.

### 630 *Insights for bioinspired underwater vehicle design*

631 Pulsatile jet propulsion is a promising avenue for bioinspired aquatic vehicles and robots  
632 (Mohensi 2006, Gohardini 2014, Yue et al. 2015). Multijet propulsion systems with multiple  
633 propellers akin to salp colonies have been explored in an engineering context (Chao et al. 2017,  
634 Costello et al. 2015) with direct inspiration from gelatinous animals (Marut 2014, Krummel 2019,  
635 Bi et al 2022, Du Clos et al. 2022). Salp diversity provides a natural laboratory to explore the  
636 hydrodynamic implications of different multijet arrangement designs. Our findings underscore the  
637 importance of considering the scaling hydrodynamic properties of propeller arrangements to  
638 optimize speed and energy efficiency in bioinspired underwater vehicle design. While linear chain  
639 arrangements were the fastest and among the most energy efficient, robot (or vehicle)  
640 configurations such as a cluster form may confer unique object manipulation or maneuverability  
641 advantages. Our results show that these seemingly inefficient propeller configurations do not  
642 impose large disadvantages in terms of speed and fuel efficiency.

### 643 **Acknowledgments:**

644 We are grateful to the crew of Aquatic Life Divers, Kona Honu Divers for their assistance  
645 and support in hosting our offshore diving operations. We also wish to thank Marc Hughes, Jeff  
646 Milisen, Rebecca Gordon, Matt Connelly, Clint Collins, Paul Richardson, and Anne Thompson for  
647 their assistance during diving, collections, and filming operations in the field. We would like to

648 thank Tiffany Bachtel for her valuable advice on the respirometry experiment design. We thank  
649 the associate editor and two anonymous reviewers for their helpful comments.

650 **Funding**

651 This research was supported by the Gordon and Betty Moore Foundation [grant number  
652 8835] and the Office of Naval Research [grant number N00014-23-1-2171].

653 **Data availability**

654 Data used to generate the results presented in this paper are available in the supplementary  
655 information. Any other datasets used directly or indirectly for this study are available from the  
656 authors upon reasonable request.

657 **Competing interests**

658 No competing interests declared.

659 **Literature cited**

660 Alexander, A. J. (1968). Forward Speed Effects on Annular Jet Cushions. *The Aeronautical  
661 Journal*, 72(689), 438-441.

662 Andersen, K. H., Berge, T., Gonçalves, R. J., Hartvig, M., Heuschele, J., Hylander, S., ... &  
663 Kiørboe, T. (2016). Characteristic sizes of life in the oceans, from bacteria to whales.  
664 *Annual review of marine science*, 8(1), 217-241.

665 Bi, X., & Zhu, Q. (2019). Dynamics of a squid-inspired swimmer in free swimming. *Bioinspiration  
666 & Biomimetics*, 15(1), 016005.

667 Bi, X., Tang, H., & Zhu, Q., 2022. Feasibility of hydrodynamically activated valves for 416 salp-  
668 like propulsion. *Physics of Fluids*, 34(10), 101903.

669 Biggs, D. C. (1977). Respiration and ammonium excretion by open ocean gelatinous zooplankton  
670 1. *Limnology and Oceanography*, 22(1), 108-117.

671 Bone, Q., Anderson, P. A. V., & Pulsford, A. (1980). Morphology of salp chain communication.  
672 *Proceedings of the Royal Society of London. Series B. Biological Sciences*, 210(1181),  
673 549-558.

674 Bone, Q., & Trueman, E. R. (1983). Jet propulsion in salps (Tunicata: Thaliacea). *Journal of  
675 Zoology*, 201(4), 481-506.

676 Cetta, C. M., Madin, L. P., & Kremer, P. (1986). Respiration and excretion by oceanic salps.  
677 *Marine Biology*, 91, 529-537.

678 Chao, S., Guan, G., & Hong, G. S., 2017, September. Design of a finless torpedo-shaped micro  
679 AUV with high maneuverability. In OCEANS 2017-Anchorage (pp. 425 1-6). IEEE.

680 Colin, S. P., Gemmell, B. J., Costello, J. H., & Sutherland, K. R. (2022). In situ high-speed  
681 brightfield imaging for studies of aquatic organisms. *Protocols.io*.

- 682 Costello, J. H., Colin, S. P., Gemmell, B. J., Dabiri, J. O., & Sutherland, K. R., 2015. 429 Multi-jet  
683 propulsion organized by clonal development in a colonial siphonophore. 430 *Nature*  
684 communications, 6(1), 8158.
- 685 Dabiri, J. O., Colin, S. P., Katija, K., & Costello, J. H. (2010). A wake-based correlate of  
686 swimming performance and foraging behavior in seven co-occurring jellyfish species.  
687 *Journal of experimental biology*, 213(8), 1217-1225.
- 688 Damian-Serrano, A., & Sutherland, K. R. (2023). A developmental ontology for the colonial  
689 architecture of salps. *The Biological Bulletin*, 245(1), 9-18..
- 690 Damian-Serrano, A., Hughes, M., & Sutherland, K. R. (2023). A new molecular phylogeny of salps  
691 (Tunicata: thalicea: salpida) and the evolutionary history of their colonial architecture.  
692 *Integrative Organismal Biology*, 5(1), obad037.
- 693 Décima, M., Stukel, M. R., Nodder, S. D., Gutiérrez-Rodríguez, A., Selph, K. E., Dos Santos, A.  
694 L., ... & Pinkerton, M. (2023). Salp blooms drive strong increases in passive carbon export  
695 in the Southern Ocean. *Nature communications*, 14(1), 425.
- 696 Di Santo, V., Goerig, E., Wainwright, D. K., Akanyeti, O., Liao, J. C., Castro-Santos, T., & Lauder,  
697 G. V. (2021). Convergence of undulatory swimming kinematics across a diversity of fishes.  
698 *Proceedings of the National Academy of Sciences*, 118(49), e2113206118.
- 699 Du Clos, K. T., Gemmell, B. J., Colin, S. P., Costello, J. H., Dabiri, J. O., and Sutherland, K. R.  
700 2022. Distributed propulsion enables fast and efficient swimming modes in physonect  
701 siphonophores. *Proceedings of the National Academy of Sciences*. 119:e2202494119.
- 702 Felsenstein, J. (1985). Phylogenies and the comparative method. *The American  
703 Naturalist*, 125(1), 1-15.
- 704 Gemmell, B. J., Dabiri, J. O., Colin, S. P., Costello, J. H., Townsend, J. P., & Sutherland, K. R.  
705 (2021). Cool your jets: biological jet propulsion in marine invertebrates. *Journal of  
706 Experimental Biology*, 224(12), jeb222083.
- 707 Gohardani, A. S. *Distributed Propulsion Technology* Nova Science Publishers (2014).
- 708 Haddock, S. H. (2004). A golden age of gelata: past and future research on planktonic  
709 ctenophores and cnidarians. *Hydrobiologia*, 530, 549-556.
- 710 Haddock, S. H., & Heine, J. N. (2005). Scientific blue-water diving.
- 711 Hamner, W. M., Madin, L. P., Alldredge, A. L., Gilmer, R. W., & Hamner, P. P. (1975). Underwater  
712 observations of gelatinous zooplankton: Sampling problems, feeding biology, and  
713 behavior 1. *Limnology and Oceanography*, 20(6), 907-917.

- 714 Henschke, N., Cherel, Y., Cotté, C., Espinasse, B., Hunt, B.P. and Pakhomov, E.A., 2021. Size  
715 and stage specific patterns in *Salpa thompsoni* vertical migration. *Journal of Marine*  
716 *Systems*, 222, p.103587.
- 717 Krummel, G. M. (2019). Locomotion and Control of Cnidarian-Inspired Robots (Doctoral  
718 dissertation, Virginia Tech).
- 719 Mackie, G. O. (1986). From aggregates to integrates: physiological aspects of modularity in  
720 colonial animals. *Philosophical Transactions of the Royal Society of London. B, Biological*  
721 *Sciences*, 313(1159), 175-196.
- 722 Madin, L. P. (1990). Aspects of jet propulsion in salps. *Canadian Journal of Zoology*, 68(4), 765-  
723 777.
- 724 Madin, L. P., & Deibel, D. (1998). Feeding and energetics of Thaliacea. *The biology of pelagic*  
725 *tunicates*, 81-104.
- 726 Madin, L. P., Kremer, P., & Hacker, S. (1996). Distribution and vertical migration of salps  
727 (Tunicata, Thaliacea) near Bermuda. *Journal of Plankton Research*, 18(5), 747-755.
- 728 Madin, L.P., Kremer, P., Wiebe, P.H., Purcell, J.E., Horgan, E.H. and Nemazie, D.A., 2006.  
729 Periodic swarms of the salp *Salpa aspera* in the Slope Water off the NE United States:  
730 Biovolume, vertical migration, grazing, and vertical flux. *Deep Sea Research Part I:*  
731 *Oceanographic Research Papers*, 53(5), pp.804-819.
- 732 Marut, K. J. (2014). Underwater Robotic Propulsors Inspired by Jetting Jellyfish (Doctoral  
733 dissertation, Virginia Tech).
- 734 Mayzaud, P., Boutoute, M., Gasparini, S., Mousseau, L., & Lefevre, D. (2005). Respiration in  
735 marine zooplankton—the other side of the coin: CO<sub>2</sub> production. *Limnology and*  
736 *Oceanography*, 50(1), 291-298.
- 737 Mohensi, K., 2006. Pulsatile vortex generators for low-speed maneuvering of small 482  
738 underwater vehicles. *Ocean Eng.* 33, 2209–2223.
- 739 Pascual, M., Acuña, J.L., Sabatés, A., Raya, V. and Fuentes, V., 2017. Contrasting diel vertical  
740 migration patterns in *Salpa fusiformis* populations. *Journal of Plankton Research*, 39(5),  
741 pp.836-842.
- 742 R Core Team, R. (2021). R: A language and environment for statistical computing.
- 743 Rubio-Gracia, F., García-Berthou, E., Guasch, H., Zamora, L., & Vila-Gispert, A. (2020). Size-  
744 related effects and the influence of metabolic traits and morphology on swimming  
745 performance in fish. *Current Zoology*, 66(5), 493-503.

- 746 Schneider, G. (1992). A comparison of carbon-specific respiration rates in gelatinous and non-  
747 gelatinous zooplankton: a search for general rules in zooplankton metabolism.  
748 *Helgoländer Meeresuntersuchungen*, 46, 377-388.
- 749 Seibel, B. A., & Drazen, J. C. (2007). The rate of metabolism in marine animals: environmental  
750 constraints, ecological demands and energetic opportunities. *Philosophical Transactions  
751 of the Royal Society B: Biological Sciences*, 362(1487), 2061-2078.
- 752 Stone, J. P., & Steinberg, D. K. (2014). Long-term time-series study of salp population dynamics  
753 in the Sargasso Sea. *Marine Ecology Progress Series*, 510, 111-127.
- 754 Sutherland, K. R., & Weihs, D. (2017). Hydrodynamic advantages of swimming by salp chains.  
755 *Journal of The Royal Society Interface*, 14(133), 20170298.
- 756 Sutherland, K. R., Damian-Serrano, A., Du Clos, K. T., Gemmell, B. J., Colin, S. P., Costello, J.  
757 H. (2024). Spinning and corkscrewing of oceanic macroplankton revealed through in situ  
758 imaging. *Science Advances* 10(20).
- 759 Sutherland, K. R., & Madin, L. P. (2010). Comparative jet wake structure and swimming  
760 performance of salps. *Journal of Experimental Biology*, 213(17), 2967-2975.
- 761 Trueblood, L. A. (2019). Salp metabolism: temperature and oxygen partial pressure effect on the  
762 physiology of *Salpa fusiformis* from the California Current. *Journal of Plankton Research*,  
763 41(3), 281-291.
- 764 Trueman, E. R., Bone, Q., & Braconnor, J. C. (1984). Oxygen consumption in swimming salps  
765 (Tunicata: Thaliacea). *Journal of Experimental Biology*, 110(1), 323-327.
- 766 Uyeda, J. C., Zenil-Ferguson, R., & Pennell, M. W. (2018). Rethinking phylogenetic comparative  
767 methods. *Systematic Biology*, 67(6), 1091-1109.
- 768 Vogel, S. (1981). Life in moving fluids. *Princeton University Press*, Princeton, NJ.
- 769 Vogel, S. (2008). Modes and scaling in aquatic locomotion. *Integrative and Comparative Biology*,  
770 48(6), 702-712.
- 771 Wiebe, P. H., Madin, L. P., Haury, L. R., Harbison, G. R., & Philbin, L. M. (1979). Diel vertical  
772 migration by *Salpa aspera* and its potential for large-scale particulate organic matter  
773 transport to the deep-sea. *Marine Biology*, 53, 249-255.
- 774 World Register of Marine Species (WoRMS). (2024). WoRMS Editorial Board. Accessed January  
775 30, 2024. Available online at <http://www.marinespecies.org>
- 776 Yue, C. et al., 2015. Mechantronic system and experiments of a spherical underwater 510 robot:  
777 SUR-II. *J. Intell. Robot Syst.* Doi:10.1007/s10846-015-0177-3.